STUDIES ON PREPARATIONS AND ELECTROCHEMICAL PROPERTIES OF POLYMER-COATED ELECTRODES

1990

SUSUMU KUWABATA

Department of Applied Chemistry
Faculty of Engineering
Osaka University

STUDIES ON PREPARATIONS AND ELECTROCHEMICAL PROPERTIES OF POLYMER-COATED ELECTRODES

(高分子被覆電極の調製と電気化学特性に関する研究)

1990

SUSUMU KUWABATA

Department of Applied Chemistry
Faculty of Engineering
Osaka University

Preface

The work of this thesis was done under the guidance of Professor Hiroshi Yoneyama and many other members of Yoneyama Laboratory at Department of Applied Chemistry, Faculty of Engineering, Osaka University.

The objective of this thesis is preparation of several kinds of polymer-coated electrodes and electrochemical study of them. The author hopes that the findings obtained in the work would give some suggestions for construction of practical electrodes having useful functions.

Susumu Kuwabata

Department of Applied Chemistry
Faculty of Engineering
Osaka University
Yamada-oka 2-1, Suita, Osaka 565
Japan

Contents

General Introduction

Electrochemical properties of polymer-coated electrodes have been studied intensively by many investigators since early of 1980s. The polymer-coated electrode is roughly divided into two types; one is electrodes coated with conducting polymers, and the other is electrodes coated with ion-exchange polymers.

The conducting polymers such as polypyrrole [1-11], polythiophene [12-16], and polyaniline [17-22] have received much attention as new functional materials, and researches on them have been done not only in the field of electrochemistry but also in physics and polymer chemistry. In the field of electrochemistry, intensive studies have been done regarding the electrochemical preparation of the conducting polymers on electrode substrates and the electrochemical properties of the resulting polymer films on the electrodes. As for the electrochemical properties, redox properties of the polymers have attracted much attention [4-6,9-11,13-19,23]. In general, the conducting polymer films possess redox activities, and electrolyte anions are inserted into the polymer films on their oxidation, while the inserted electrolyte anions are dissolved out into the electrolyte solution on their reduction to maintain the electrical neutrality of the film. Such compositional change in the redox reaction accompanies changes in the color and electrical conductivity of the polymer films. The films in oxidized state show high conductivities, while those in reduced state show insulating properties. These properties are feasible for practical applications; the redox properties can be utilized in active materials of secondary batteries [24-26], and the color change can be utilized in electrochromic display devices [27-29]. Researches regarding

these applications have been done actively. Another interesting property of the conducting polymers is that electrolyte anions are incorporated into the conducting polymers during the course of their electrochemical preparation. This property has successfully been utilized as the means of attaching special functions such as electrocatalysis to the electrodes by using the functional molecules as electrolyte anions in the deposition bath of the conducting polymers [31-34]. Besides the conducting polymer-coated electrodes, electrodes coated with ion-exchange polymers such as polyvinylpyridine [35-38] and Nafion [39-41] are also useful in preparing electrodes having desired functions. The polymer layers on the electrodes electrostatically bind cationic or anionic functional molecules. Most studies on this kind of electrodes have been devoted to elucidation of charge transfer properties in the polymer layers, because the rate of the electrode reaction in this case are primarily controlled by the charge transfer in the polymer layers.

Although intensive studies have been carried out regarding the polymer-coated electrodes as mentioned above, there still remain many important subjects to be investigated. The present study has been conducted focusing to the following four subjects which have not intensively been studied.

(1) To accomplish electrochemical copolymerization of different kinds of monomers having different oxidation potentials.

(2) To clarify the effect of electrochemical preparation conditions on the conductivity of the resulting polymer films.

(3) To establish techniques which allows incorporation of cationic electrolyte species into conducting polymer films.

(4) To devise new simple techniques for the attachment of electroactive

species having special functions to the electrode substrate.

The first subject has important significance in opening new routes for the preparation of new conducting polymers. The second subject is very important in clarifying how greatly the conductivity of the conducting polymers is controlled by the electrolysis conditions in the preparation of the polymers. The third subject is of significance in widening functionalization routes of conducting polymers, and the fourth subject is of scientific significance in allowing the preparation of various kinds of electroactive electrodes.

Chapter 1 describes electrochemical properties of polypyrrole and copolymers of pyrrole and thiophene. The utility of electrochemical technique for copolymerization of pyrrole and thiophene will be demonstrated, and differences of electrochemical properties between the prepared copolymers and polypyrrole will be presented. Chapter 2 mainly deals with the effect of electrolyte anions incorporated in the polypyrrole film on the film conductivity. It will be shown that the conductivity of the polypyrrole film is decreased with increasing the valence number and the basicity of the incorporated anions. These results can be quantitatively interpreted in terms of interaction between the incorporated anions and positive charge carriers in the polymer chains. In chapter 3, the preparation and electrochemical properties of polyaniline with incorporated methylene blue as a cationic redox dye will be described. The cationic methylene blue can be incorporated in the polyaniline film using methylene blue-bound Nafion as an electrolyte anions in the preparation bath. The incorporation behaviors of methylene blue in polyaniline will be discussed based on those of methylene blue in Nafion. Chapter 4 describes electrochemical properties of electrodes coated with

polystyrene film containing ionic surface-active agents. It will be shown that the electrode described in this chapter is useful for attaching functions to the electrodes.

List of Publications

1. Redox Behavior and Electrochromic Properties of Polypyrrole Films in Aqueous Solutions.
   S. Kuwabata, H. Yoneyama, and H. Tamura
   Bull. Chem. Soc. Jpn., 57, 2247 (1984).
2. Effect of Organic Dopants on Electrical Conductivity of Polypyrrole Films.
   S. Kuwabata, K. Okamoto, O. Ikeda, and H. Yoneyama
   Synth. Met., 18, 101 (1987).
3. Conductivity of Polypyrrole Films Doped with Aromatic Sulphonate Derivatives.
   S. Kuwabata, K. Okamoto, and H. Yoneyama
   J. Chem. Soc., Faraday Trans. 1, 84, 2317 (1988).
4. Copolymerization of Pyrrole and Thiophene by Electrochemical Oxidation and Electrochemical Behavior of the Resulting Copolymers.
   S. Kuwabata, S. Ito, and H. Yoneyama
   J. Electrochem. Soc., 135, 1691 (1988).
5. Electrodes Coated with Polystyrene Films Containing Surface-active Agents: Attachment of Screening Capabilities for Electrode Reactions of Electroactive Ionic Species.
   S. Kuwabata, Y. Maida, and H. Yoneyama
   J. Electroanal. Chem., 242, 143 (1988).

6. The Effect of Basicity of Dopant Anions on the Conductivity of Polypyrrole Films.

   S. Kuwabata, J. Nakamura, and H. Yoneyama

   J. Chem. Soc., Chem. Comm., 779 (1988).

7. Dimerization Kinetics of Methylene Blue Incorporated in a Nafion Film.

   S. Kuwabata, J. Nakamura, and H. Yoneyama

   J. Electroanal. Chem., 261, 363 (1989).

8. Preparation of Polyaniline Films Doped with Methylene Blue-bound Nafion and the Electrochromic Properties of the Resulting Films.

   S. Kuwabata, K. Mitsui, and H. Yoneyama

   J. Electroanal. Chem., 281, 97 (1990).

9. Electrical Conductivity of Polypyrrole films Doped with Carboxylate Anions.

   S. Kuwabata, J. Nakamura, and H. Yoneyama

   J. Electrochem. Soc., 137, 1788 (1990).

10. Dependence of Conductivity of Polypyrrole Film Doped with p-Phenol Sulfonate on Solution pH.

    S. Kuwabata, J. Nakamura, and H. Yoneyama

    J. Electrochem. Soc., 137, 2147 (1990).

11. Kinetics of Glassy Carbon Electrodes Coated with Polystyrene Films Containing Ferrocene and Ionic Surface-active Agents.

    S. Kuwabata, T. Hamamoto, and H. Yoneyama

    J. Electroanal. Chem., in contribution.

Chapter 1

Electrochemical Properties of Polypyrrole and Copolymers of Pyrrole and Thiophene

1-1

Redox Behavior and Electrochromic Properties of Polypyrrole Films in Aqueous Solutions

1-1-1 Introduction

Recently many reports have been published concerning electrochemical properties of electroconductive polymers. Among them, polypyrrole has been studied most extensively. Except for earlier reports by Weiss et al., [42-44] most of electrochemical studies have been conducted on films prepared by anodic polymerization of pyrrole in an acetonitrile medium. According to Diaz et al. [4,10,11,23,45,46] polypyrrole coated Pt electrodes show redox behavior in acetonitrile solution: Insertion of anionic species into films and elimination of inserted anions from films occur in the oxidation and reduction of films, respectively. The oxidized film contains 0.25 mol of anions in 1 mol of pyrrole rings and exhibits high conductivity. This property was used for stabilization of unstable semiconductor electrodes such as n-Si and n-GaAs in aqueous solutions by coating electrode surface with thin polypyrrole films [47-52].

Concerning electrochemical properties of polypyrrole films in aqueous solutions, redox behavior of several electroactive species such as $[Fe(CN)_6]^{3-/4-}$ and ferrocene/ferricinium has been investigated by using Pt

or Ta as the electrode substrates and it has been found that the polymer films serve as inert electrodes like Pt electrodes [23,53-55]. Their photoelectrochemical properties were also investigated in relation to the conduction mechanisms [55]. In this section, electrochemical properties of polypyrrole in aqueous solutions containing a supporting electrolyte alone will be described. The results obtained in that study will be shown with particular reference to their redox behavior. Furthermore, it will be shown that the color of polypyrrole films changes with the redox behavior, as have been obtained with stable inorganic oxides such as WO_3 [56-60] and organic materials such as phthalocyanines [61]. The color change of polymer-coated electrodes during the course of their polarization has been described with several polymers [16,45,62], but no systematic study with focusing on the application to electrochromic display seems to have been conducted.

1-1-2 Experimental

Preparation of Polypyrrole. Redox reactions of polypyrrole were investigated with its film prepared on a Pt substrate. For this purpose, a flat Pt plate was mounted on a Teflon electrode holder having an exposed electrode area of 1 cm^2. An anodic polymerization of pyrrole was carried out in an N_2 atmosphere in acetonitrile containing 0.1 mol dm^{-3} pyrrole and 0.3 mol dm^{-3} $LiClO_4$ at 0.3 mA cm^{-2} for 2 min. By this procedure polypyrrole of ca. 90 nm thickness was deposited on the Pt as determined with a multi-reflection interferometer (Mizojiri Kogaku, Model 2). The electrode Prepared in this manner is denoted here by PPy/Pt. For the purpose of elemental analysis the film was prepared on a Pt electrode

having a large area of ca. 20 cm^2 under the same conditions as described above except for the electrolysis time which was 20 min, and was teared away from the substrate. The film thickness in this case was ca. 220 nm.

Measurements of electrochromic properties of polypyrrole were carried out with a film prepared on a SnO_2-coated glass electrode. The SnO_2-coated glass electrode was prepared in this laboratory by pyrolysis of a spray mixture of 3 mol dm^{-3} $SnCl_4$, 0.15 mol dm^{-3} $SbCl_5$, and 1.5 mol dm^{-3} HCl [63], and its area was 3.5 cm^2. An electrical lead wire was attached to its round rim with silver-epoxy by coating it first with epoxy resin and then with silicone rubber adhesive. The SnO_2-coated glass electrode prepared in this manner had an exposed area of ca. 3 cm^2, which was used as the substrate for the deposition of polypyrrole. The deposition was performed under the same conditions as in the case of PPy/Pt and the prepared electrode will be denoted here by PPy/OTE.

Electrochemical Measurements. Measurements were carried out in a Pyrex beaker type cell. A saturated calomel electrode (SCE) served as a reference electrode. Cyclic voltammograms were obtained by use of a potentiostat (Hokuto Denko HA-104), a function-generator (Hokuto Denko HB-104), and an X-Y recorder (Yokogawa Electric Inc. 3077). An electronic coulometer (Hokuto Denko HF-201) was used as required. For measurements of resistivity of polypyrrole films the four-probe method [64] was applied to a film sample which had been teared away from PPy/Pt by use of an adhesive tape.

Electron Probe X-ray Microanalysis of Polypyrrole Films. A qualitative analysis of anions contained in polypyrrole films was performed

to obtain direct information on the anion transfer into and from films which occur in the course of redox reaction of PPy/Pt electrodes. An energy dispersive electron probe X-ray microanalyzer (EPMA) (Horiba EMAX-1500E) connected to a scanning electron microscope (Hitachi S-450) served for this purpose.

Measurements of Electrochromic Properties. A PPy/OTE working electrode and a counter electrode (ca. 1 cm^2 Pt plate) were set in a quartz cell (20 x 10 x 40 mm). The cell was connected to a reference electrode (SCE) with a salt bridge and set in an UV-visible spectrophotometer (SHimadzu MPS-5000). The absorbance of polypyrrole films was measured in situ in the course of polarization measurements.

1-1-3 Results and Discussion

Redox Behavior of Polypyrrole in Aqueous Solutions. Cyclic voltammograms of PPy/Pt electrodes in 0.5 mol dm^{-3} KCl or 0.5 mol dm^{-3} Na_2SO_4 are shown in Fig. 1. Well-defined peaks are seen both in the anodic and cathodic potential scans. Peak currents increase linearly with increasing sweep rate from 20 to 100 mV s^{-1}, suggesting that these peaks are due to electrochemical reactions of the film itself [65]. In the KCl solution the anodic and cathodic peaks appear at -0.35 and -0.15 V, respectively, and the peak potentials are eventually invariant with sweep rate. On the other hand, two anodic peaks appear in the Na_2SO_4 solution, though the cathodic behavior is almost the same as in the KCl solution. The first peak like a shoulder appears at -0.44 V, whereas the more marked

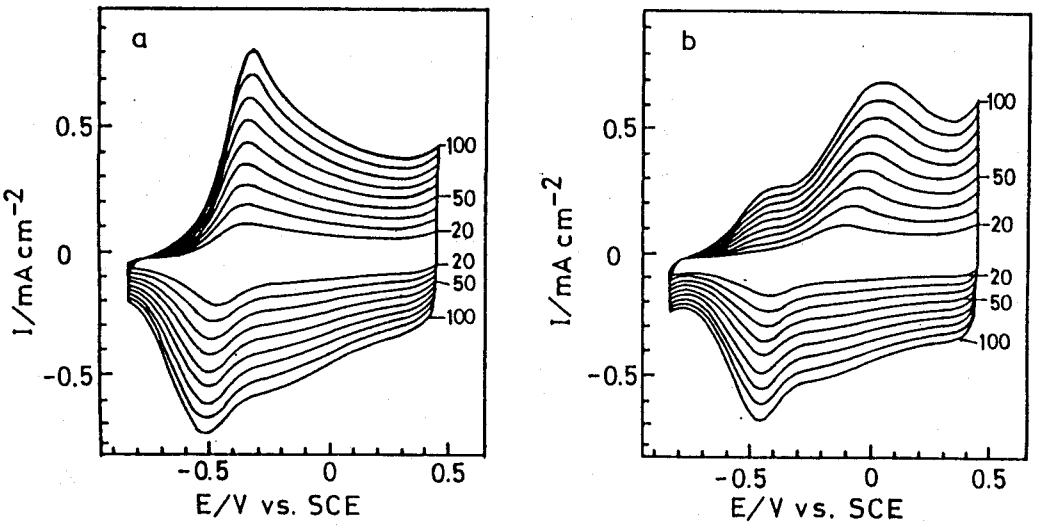

Fig. 1. Cyclic voltammograms of PPy/Pt electrodes taken in 0.5 mol dm^{-3} KCl (a) and 0.5 mol dm^{-3} Na_2SO_4 (b) at various sweep rates in an interval of dE/dt = 10 mV s^{-1}. The number denotes the sweep rate in mV s^{-1}.

second peak shows a tendency to shift its potential towards the positive direction with increasing sweep rate.

Cyclic voltammograms were obtained in other kinds of electrolytes. The peak potential and current of the cyclic voltammograms obtained at the sweep rate of 50 mV s^{-1} are shown in Table 1. In the case of appearance of two anodic peaks, the peak potential and current at the lower potential are given with the subscript pa-1 and those at the higher potential with pa-2. When only one anodic peak appears the values are given in the column of pa-1. As recognized from this Table, monovalent anions give one anodic peak, while divalent anions give two peaks. The peak potential and current of cathodic waves are little influenced by the kind of electrolyte anions, whereas different situations can be seen in the anodic waves.

The E_{pa-1} observed in divalent anions is more negative than E_{pa-1}

Table 1. Peak potentials and currents of cyclic voltammograms of PPy/Pt electrodes obtained at dE/dt = 50 mV s^{-1} in a variety of electrolytes

Electrolyte[a)]	E_{pa-1}/V	E_{pa-2}/V	E_{pc}/V	i_{pa-1}/mA	i_{pa-2}/mA	i_{pc}/mA
0.5 M KCl	-0.31		-0.47	0.36		-0.41
0.5 M KBr	-0.32		-0.46	0.34		-0.38
0.5 M KI	-0.29		-0.56	0.41		-0.36
0.5 M $LiClO_4$	-0.31		-0.48	0.39		-0.30
0.5 M Na_2SO_4	-0.44	0.04	-0.46	0.12	0.35	-0.34
0.5 M K_2SO_4	-0.45	0.02	-0.48	0.09	0.36	-0.35
0.5 M Li_2SO_4	-0.42	0.21	-0.44	0.07	0.38	-0.41
0.5 M Na_2HPO_4	-0.42	0.02	-0.36	0.13	0.41	-0.45
0.5 M Na_2WO_4	-0.42	0.45	-0.49	0.13	0.40	-0.43

a) M = mol dm^{-3}.

observed in monovalent anions, but E_{pa-2} is more positive than the latter. Voltammograms obtained in individual solution were not remarkably varied in the temperature range 0 - 80 ℃. It is suggested from cyclic voltammograms obtained in the presence of divalent anions that the oxidation in this case occurs in two steps: In the first step, the surface of polypyrrole film may be oxidized weakly by attaching anions onto the polymer surface; in the following step, anions may be inserted into the film and an oxidation of the film occurs simultaneously. It is seen in Table 1 that E_{pa-2} depends on the kind of anions; sulfate and hydrophosphate ions give nearly the same E_{pa-2} except for Li_2SO_4, whereas WO_4^{2-} gives more anodic E_{pa-2}. The discrepancy in the values of E_{pa-2} seems to be closely related to diameter of the hydrated anions [66] to be incorporated into the film. The diameter of hydrated HPO_4^{2-} and SO_4^{2-} are ca. 4 Å, while that of WO_4^{2-} is ca. 5 Å. If this difference is serious, it is then suggested that the larger the diameter of anions, the more anodic potentials are needed for the incorporation of anions into the film. As to the monovalent anions given in Table 1, the diameter of hydrated Cl^-, Br^-, and I^- are ca. 3 Å and that

of ClO_4^{2-} is 3.5 Å, which are smaller than those of the divalent ions used, and the smaller size of monovalent anions may make the peak potential less negative than the E_{pa-2} obtained for the divalent anions. In connection to this hypothesis, it seems important to notice that the onset potential of film oxidation is eventually the same between the monovalent and divalent ions.

Effects of the electrolyte concentration on cyclic voltammograms were investigated in KCl solutions. According to the results obtained, the peak potentials and currents were not appreciably varied with the concentration of electrolytes as long as it was higher than 10^{-3} mol dm^{-3}. In more dilute solutions, however, the voltammograms were deformed owing to IR drop in the electrolyte.

Figure 2 shows effects of pH on the redox behavior of polypyrrole. The concentration of Cl^- anions was kept constant in this case. As noticed from Fig. 2, the redox behavior appears in solutions having pH values higher than 2.0. In solutions of lower pH, hydrogen evolution becomes predominant, resulting in shadowing the redox behavior of polypyrrole itself.

It was reported in acetonitrile solution [45] that the redox behavior is due to anion insertion into polypyrrole films and elimination of inserted anion from the film. In order to confirm whether or not this is true in aqueous solutions, anionic species in the film were analyzed by EPMA. The results are shown in Fig. 3. Figure 3-(a) is the spectrum of a PPy/Pt electrode prepared in the acetonitrile solution. A peak assignable to chlorine is seen, which gives the evidence that ClO_4^- inserted into the film in the course of anodic polymerization. This electrode was kept in 0.5 mol dm^{-3} KI aqueous solution for 2 min at -0.85 V which is enough to cause the

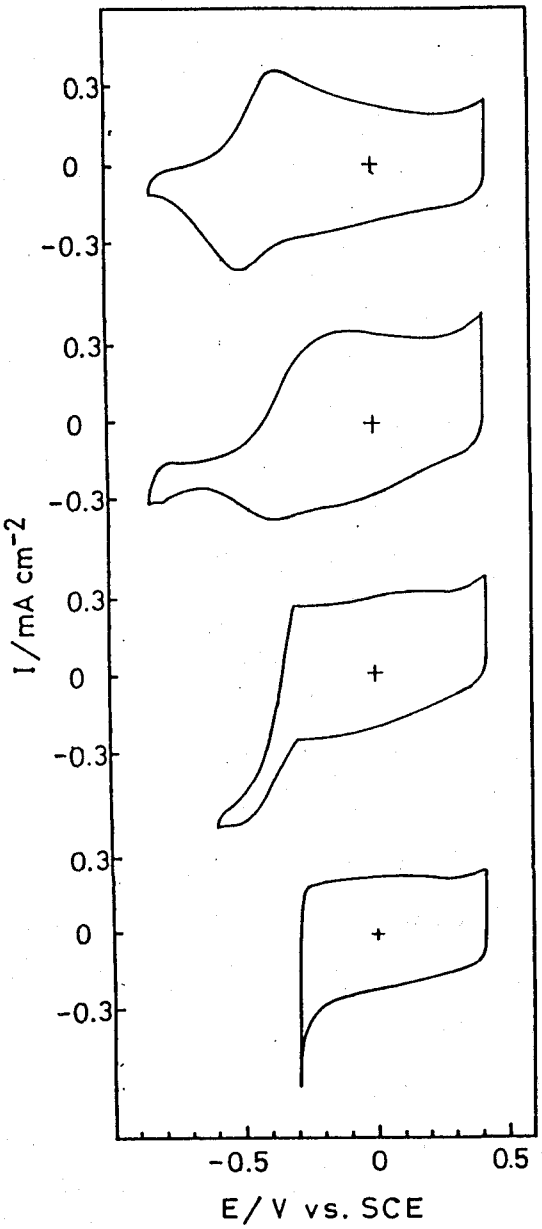

Fig. 2. Effects of solution pH on cyclic voltammograms of PPy/Pt electrodes in 1 mol dm^{-3} chloride solutions. pH = (a) 5.5, (b) 2.0, (c) 1.5, (d) 0.6. dE/dt = 50 mV s^{-1}.

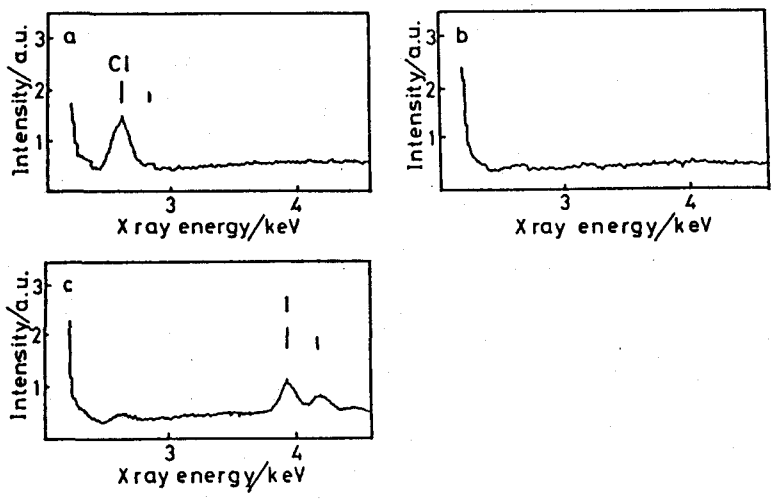

Fig. 3. EPMA spectra of PPy/Pt electrodes. (a) Original electrode prepared in 0.1 mol dm^{-3} $LiClO_4$/acetonitrile. (b) Reduced at -0.85 V vs. SCE in a 0.5 mol dm^{-3} KI aqueous solution for 2 min. (c) Successively oxidized at 0.45 V vs. SCE in the same solution for 2 min.

cathodic process of redox reaction, and then washed with water. Then the chlorine peak disappeared, as shown in fig. 3-(b). When this sample was again kept for 2 min in the same solution at 0.45 V vs. SCE to cause the anodic process of redox reaction, peaks of iodine appeared as shown in Fig. 3-(c). Similar results of the occurrence of replacement of anionic species were obtained in other electrolytes such as KBr, Na_2SO_4, and Na_2HPO_4. Thus, it is evident that the redox reaction is accompanied with the anion transfer into and from the film.

Resistivity measurements and elemental analyses on polypyrrole films were carried out both for the as-grown film prepared in the acetonitrile solution and for films polarized afterwards in 0.5 mol dm^{-3} KCl aqueous solution for 2 min at -0.85, 0, or 0.45 V vs. SCE. Prior to the measurements and analyses films were washed thoroughly with twice distilled water. The

Table 2. Elemental analysis and resistivity of polypyrrole films polarized at different potentials in 0.5 mol dm^{-3} KCl aqueous solution

E vs. SCE/V	Molar ratio to nitrogen				Resistivity/ohm cm
	C	H	N	Cl	
-0.85	4.06	3.33	1.00	0.03	3.9×10^{4}
0.00	4.03	3.28	1.00	0.15	1.2×10^{-2}
0.45	4.04	3.30	1.00	0.30	3.2×10^{-3}
as-grown	4.02	3.29	1.00	0.20	3.8×10^{-3}

value of resistivity was found to be invariable for a few days in air. The observed results are shown in Table 2. In this table, the results of elemental analyses are given in relative molar ratio of each element to nitrogen. As expected, the as-grown film has a low resistivity. When this film was polarized at -0.85 V in 0.5 mol dm^{-3} KCl aqueous solution, an elimination of a large part of the inserted ClO_4^- occurs and the resistivity is enhanced. With an increase in anodic polarization, the incorporation of Cl^- anions into the film becomes appreciable as expected. Simultaneously, the resistivity becomes lowered. Judging from the results from the elemental analyses, the insertion of Cl^- is not completed at 0 V vs. SCE which is enough positive to the peak potential of voltammogram (see Fig. 1-(a)). It is noticed in the voltammogram that relatively large anodic currents flow in the potential region between 0 and 0.45 V. At a glance, they seem to be attributable to capacitive currents [46], but according to the results obtained that the content of Cl^- was increased by changing the polarization potential from 0 to 0.45 V vs. SCE, anodic oxidation of polypyrrole with insertion of anions still occurs in this potential region.

Another interesting point to be noticed is that the molar ratio of Cl^- was higher for the film polarized at 0.45 V in 0.5 mol dm^{-3} KCl than for the as-grwon film which contained the incorporated ClO_4^-. This result suggests that the charge involved in the redox process in 0.5 mol dm^{-3} KCl is higher than the excess charge retained in the film in the course of anodic polymerization of pyrrole. According to a literature [45], 2.25 mol of electrons are involved in the electropolymerization of 1 mol of pyrrole, and 2 mol of electrons are consumed in the polymer chain formation. The extra amount of electrons is consumed in the ionization of film and the equivalent amount of anions is incorporated at that time. Judging from the results given in Table 2, these sample had an excess charge of 0.2 mol per mol of pyrrole when prepared in the acetonitrile solution, but more than 0.3 mol of electrons were found to be involved in the aqueous redox processes, as described below.

According to the results with the as-grown film given in Table 2, 2.2 mol of electrons per mol of pyrrole are involved in the deposition of polypyrrole, whereas the results with the film polarized at 0.45 V suggest that 0.3 mol of electrons can be used in the aqueous redox processes. The amount of charge consumed in the preparation of the PPy/Pt electrode was 36 mC cm^{-2}. When this sample was subjected to an anodic potential sweep from -0.8 to 0.4 V under the same conditions as chosen in the experiment shown in Fig. 1-(a), the charge of 4.8 mC cm^{-2} was consumed. Therefore, if such an assumption is made that 0.3 mol of electrons is involved in the aqueous redox processes, the charge capable of participating in the redox processes will be 36 mC cm^{-2} x 0.3/2.2 = 4.9 mC cm^{-2}, which is in fair agreement with the charge obtained in the course of anodic sweep.

These results undoubtedly support the validity of the reactions

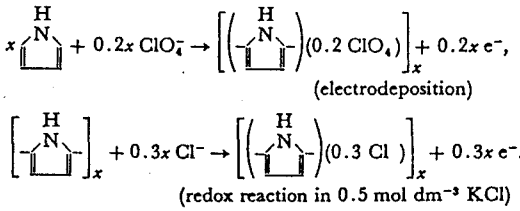

(electrodeposition)

(redox reaction in 0.5 mol dm^{-3} KCl)

Resistivity measurements were carried out for polypyrrole films prepared in the presence of other kinds of anions and almost the same values as shown in Table 2 were obtained. Judging from these results, electrical properties are primarily determined by charged conditions of polypyrrole, which are controlled not by the kind but by the amount of incorporated anions.

Electrochromic Properties of Polypyrrole. It was reported [16,45] that the color of polypyrrole is variable with redox behavior in acetonitrile solutions. It was found that the same was true in aqueous solutions. The color change is reproducible and seems to be applicable to electrochromic display devices.

Visible absorption spectra of a PPy/OTE electrode, obtained under steady states at several different potentials, are shown in Fig. 4. Polymer films with incorporated Cl^- exhibit a brown-black color and show no appreciable absorption peaks. However, when the film is reduced, it turns yellow as recognized from an increase in absorption at wavelengths shorter than 500 nm. The absorption is thought to be assignable to the π-π^* transition of polypyrrole [55]. The coloring occurs noticeable at -0.1 V vs. SCE and is enhanced with an increase in cathodic potential up to -0.7 V, beyond which no appreciable increase in absorbance appears.

The change in the absorbance of polypyrrole films with electrolysis charge was pursued in situ in 0.5 mol dm^{-3} KCl. The films used were those

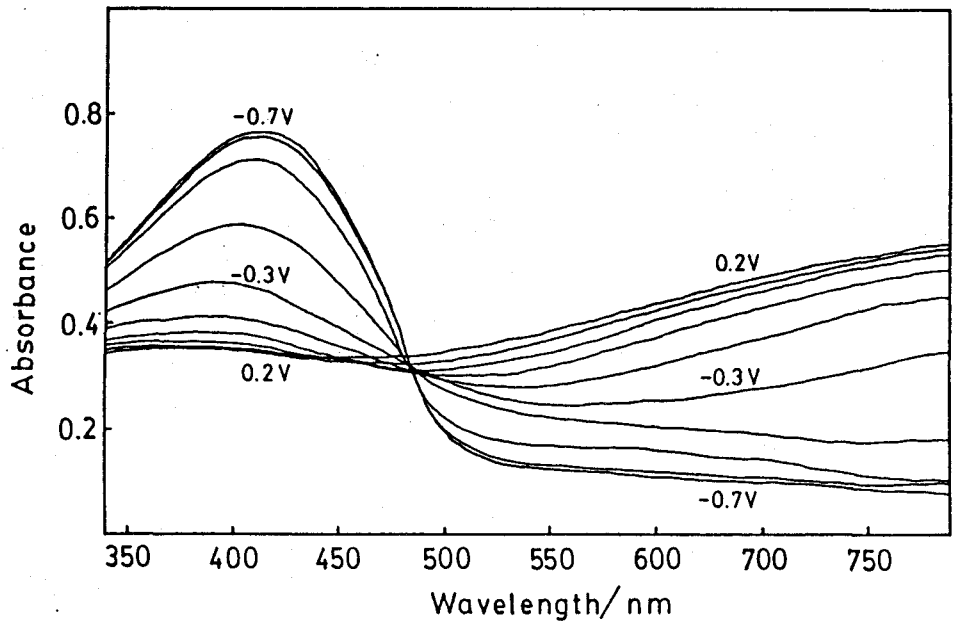

Fig. 4. Absorption spectra of a PPy/OTE electrode obtained in situ at different potentials in a 0.1 V interval in 0.5 mol dm^{-3} KCl.

prepared by anodic oxidation at 0.3 mA cm^{-2} for 2, 4, or 6 min in acetonitrile containing 0.1 mol dm^{-3} pyrrole and 0.3 mol dm^{-3} $LiClO_4$ and were initially reduced at -0.7 V in the solution for the measurement. The absorbance of these films was then measured in situ during the course of anodic oxidation at 0.3 mA cm^{-2}. Results are given in Fig. 5-(a) as a function of the quantity of electricity consumed in the oxidation. The electrode potential values of the film in the initial and final stages (-0.7 and 0.4 V) and an intermediate stage (-0.2 V) are also given in the figure. In the final stage almost all the charges capable of being retained must have been accumulated in the film, as judged from the results given in Table 2. Figure. 5-(b) shows absorbances at these potentials as a function of the quantity of electricity consumed in the film preparation (Q_d) which

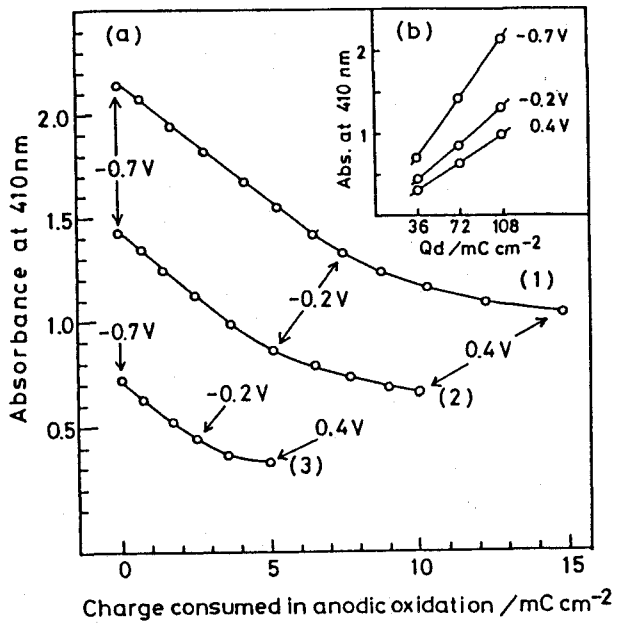

Fig. 5. (a) Absorbance at 410 nm of PPy/OTE having different film thickness as a function of the charge consumed in anodic oxidation at 0.3 mA cm^{-2} in 0.5 mol dm^{-3} KCl. (b) Absorbance at 410 nm of PPy/OTE at -0.7 V, -0.2 V, and -0.4 V in 0.5 mol dm^{-3} as a function of charge consumed for film preparation (Q_d). The film preparation was carried out in acetonitrile containing 0.1 mol dm^{-3} pyrrole and 0.3 mol dm^{-3} $LiClO_4$ at 0.3 mA cm^{-2} for 2 min (Q = 36 mC cm^{-2}) (1), for 4 min (Q_d = 72 mC cm^{-2}) (2), and for 6 min (Q_d = 108 mC cm^{-2}) (3).

is a measure of the film thickness. It is seen from this figure that the absorbance is proportional to the film thickness.

According to Fig. 5-(a), for the films having different thickness, linear relations with the same gradient are established between the absorbance and the charge consumed in the anodic oxidation of film in 0.5 mol dm^{-3} KCl as long as the electrode potential is more negative than -0.2 V. However, the rate of absorbance change becomes declined at potentials positive to -0.2 V. This behavior is in qualitatively agreement with the

results shown in Fig. 4. The quantity of electricity consumed in the linear part is half the total charge capable of being stored, although with this amount of charges the absorbance at 410 nm changes by ca. 80% of the total change.

Relations for the linear part in Fig. 5-(a) are formulated as follows:

$$Abs = -0.119Q_c + 0.72 \quad (\text{for } Q_d = 36 \text{ mC cm}^{-2}) \tag{1}$$

$$Abs = -0.121Q_c + 1.44 \quad (\text{for } Q_d = 72 \text{ mC cm}^{-2}) \tag{2}$$

$$Abs = -0.120Q_c + 2.16 \quad (\text{for } Q_d = 108 \text{ mC cm}^{-2}) \tag{3}$$

where Abs and Q_c denote the absorbance at 410 nm and the charge consumed in the anodic oxidation, respectively. Since the absorbance is proportional to the quantity of electricity consumed in the film preparation, these equations may reduce to one equation

$$Abs = -0.12Q_c + 0.02Q_d \tag{4}$$

Since the total amount of charge capable of being stored is $0.3/2.2 \times Q_d$ as stated above and half the charge is involved in the linear portion of the absorbance change (from -0.7 to -0.2 V), the upper limit of Q_c in the above equation is then $0.07\ Q_d$.

Cyclic voltammograms and absorbances at 410 nm of a PPy/OTE electrode are shown in Fig. 6 for the cases of 0.5 mol dm^{-3} KCl and 0.5 mol dm^{-3} Na_2SO_4. In the KCl solution the absorbance changes quite smoothly with variation in electrode potentials and the change in absorbance shows a hysteresis in the direction of potential sweep. A similar trend of change in absorbance appears also in the Na_2SO_4 solution. In both

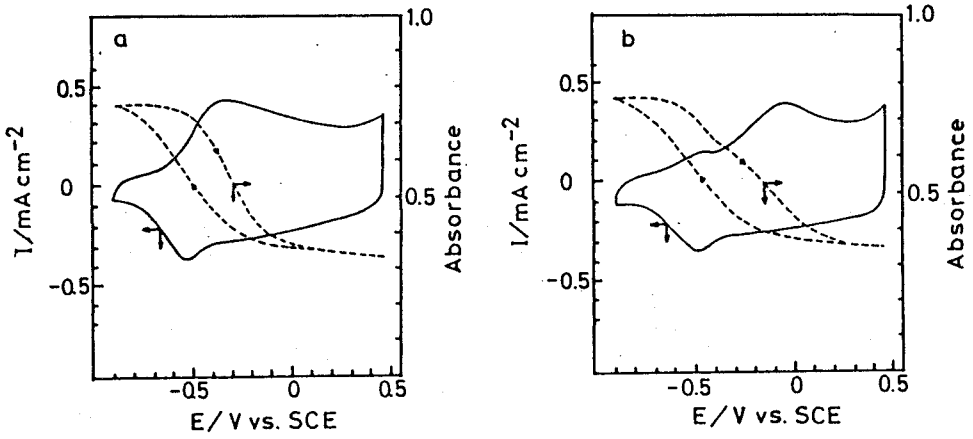

Fig. 6. Change in absorbance at 410 nm obtained in situ in the measurements of cyclic voltammograms. (a) in 0.5 mol dm^{-3} KCl (b) in 0.5 mol dm^{-3} Na_2SO_4. dE/dt = 50 mV s^{-1}.

solutions the absorbance vs. potential relations show inflections at the potentials where the voltammograms show their peaks. Thus, two inflections are noticed in the voltammograms obtained on the anodic potential scan in 0.5 mol dm^{-3} Na_2SO_4. These results are closely related to the fact that the change in absorbance is brought about by the redox processes of polypyrrole.

Response behavior of absorbance to pulsed potential were investigated in 0.5 mol dm^{-3} KCl at 410 nm with a potential pulse of -0.85 or 0.45 V. Results are shown in Fig. 7. The response to the anodic pulse is faster than that to the cathodic one. The slowness of the cathodic response must be related to the fact that the polymer becomes resistive on application of -0.85 V. However, improvement of the response will be possible by appropriate choice of the film thickness, electrode area, and conductive substrate. Stability tests on the redox processes of polypyrrole were investigated in 0.5 mol dm^{-3} KCl with the PPy/Pt electrode. Results are

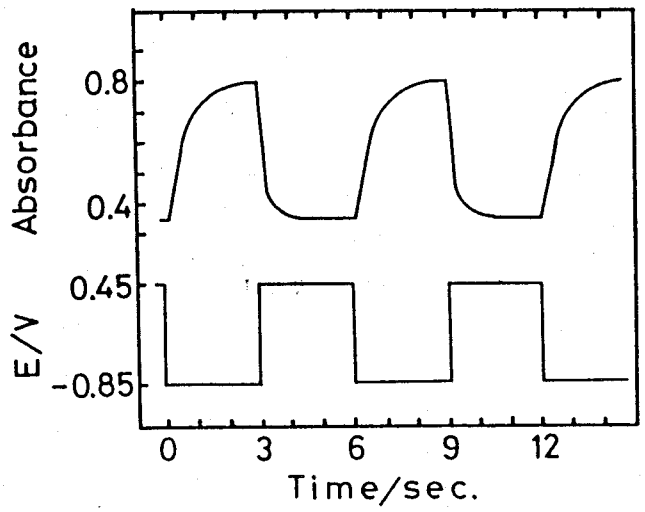

Fig. 7. Response behaviors of the absorbance change of the PPy/OTE electrode to repeated potential pulses of -0.85 V and 0.45 V vs. SCE in 0.5 mol dm^{-3} KCl. Absorbance was measured at 410 nm.

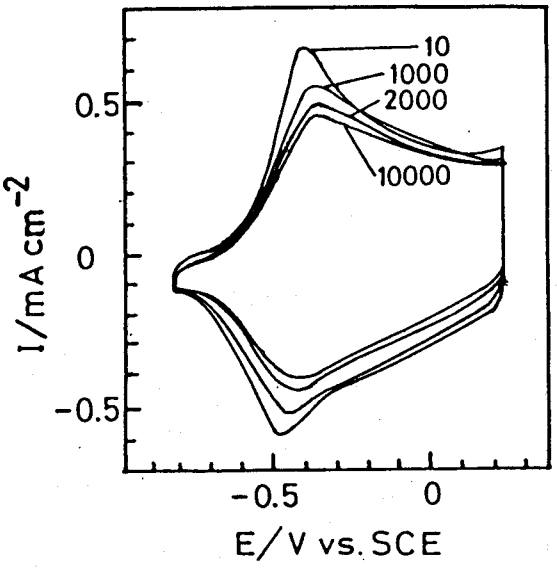

Fig. 8. Change in cyclic voltammograms of PPy/Pt electrode with the number of potential sweep cycles in 0.5 mol dm^{-3} KCl. The number in the figure denotes the cycle number. $dE/dt = 50$ mV s^{-1}.

shown in Fig. 8. The shape of voltammograms taken at the sweep rate of 100 mV s^{-1} becomes ill-defined with an increase in potential sweep cycles, but no appreciable change in film color is noticed to the naked eye during 10000 potential sweeps. These results suggest that polypyrrole is a promising candidate as a material for electrochromic display devices.

1-2

Copolymerization of Pyrrole and Thiophene by Electrochemical Oxidation and Electrochemical Behavior of the Resulting Copolymers

1-2-1 INTRODUCTION

The conducting polymers of five-membered heterocyclic compounds such as polypyrrole and polythiophene have extensively been studied and the utility of these polymers in electrochromic devices and polymer batteries [24-26] have been investigated. In these studies electrochemical properties of copolymers of different kind of the heterocyclic compounds have also been investigated [67-71]. So far copolymers of pyrrole and N-methyl pyrrole [68], pyrrole and phenol [69], and of pyrrole and terthienyl [70] have been prepared by electrolytic oxidation of mixtures of the monomers. The electrochemical oxidation of mixed monomers successfully produced the copolymer in these cases mainly due to the fact that oxidation potentials of the monomers used were close to each other. Electrochemical copolymerization by another means has also been reported: a pyrrole and thiophene copolymer [67] and a thiophene and benzene copolymer [71] were prepared by electrochemical polymerizations of 2,2'-thienylpyrrole and 1,4-di-(2-thienyl)benzene, respectively. In these cases, the monomers used as the starting materials contained the component units of the copolymer in the molecule.

In the present section, the achievement of electrochemical copolymerization of pyrrole and thiophene from a mixture of each monomer is shown. The oxidation potentials of these monomers are greatly

different, and to my knowledge electrochemical preparation of a copolymer using two kinds of monomers whose oxidation potentials are greatly different has not yet been reported. Thus, the technique which will be described in this section has scientific implication in giving a new route for copolymerizing two kinds of simple monomers whose oxidation potentials are far apart and is believed to be widely applicable to preparation of a variety of copolymers.

1-2-2 Experimental

Electropolymerization of polypyrrole, polythiophene, and polypyrrole-polythiophene copolymers was carried out potentiostatically under conditions which will be described in the Results and Discussion section. The quantity of electricity used was 100 mC cm^{-2} for all cases. As the electrode substrate, a Pt plate (ca. 3 cm^2) was used except for spectroelectrochemical measurements where an ITO was used. Film preparations and all electrochemical measurements were carried out in a glove box (Miwa Seisakusyo SDB-1A) saturated with N_2. The techniques for polymerization, electrochemical study, and photoelectrochemical study were essentially the same as those described in the previous section, except for the reference electrode, which was a silver-silver chloride electrode (Ag/AgCl) in an acetonitrile containing 0.1 M tetraethylammonium chloride.

IR measurements of the copolymers were carried out by using KBr discs dispersed with powder of polythiophene, polypyrrole, a mixture of polythiophene and polypyrrole (1:1), and of prepared copolymers. The polymer powders were prepared by grinding the polymer films prepared

electrochemically on a large Pt plate (ca. 6 cm^2). The IR spectra were obtained with FT-IR spectrophotometer (Japan Spectroscopic Co., Ltd. FT/IR-3). ESCA analyses of the prepared copolymers were carried out using a Shimadzu ESCA 650B X-ray photoelectron spectrophotometer (XPS).

1-2-3 RESULTS AND DISCUSSION

Preparation of Copolymers of Pyrrole and Thiophene. According to the literature [15], electropolymerization of pyrrole occurs at potentials positive of 0.6 V vs. SCE and that of thiophene at potential positive of 1.6 V vs. SCE, the oxidation potentials being quite different between the two. The copolymerization strategy employed in the present study was to oxidize pyrrole under diffusion limiting conditions at potentials where thiophene oxidation takes place. For this purpose a concentration of pyrrole was arbitrarily set at as low as 2.0×10^{-3} M, while that of thiophene was set at 0.1 M. Acetonitrile was used as a solvent and 0.1 M $LiClO_4$ was used as a supporting electrolyte.

Current-potential curves taken in quiet solutions at a potential sweep rate of 10 mV s^{-1} are given in Fig. 9. The measurements were carried out with ascending anodic potentials. The curve (a) concerns a current-potential curve (I-E curve) for electropolymerization of 2.0×10^{-3} M pyrrole. A diffusion limiting current which was distinctly influenced by stirring the electrolyte solution was seen at potentials positive of 1.5 V vs. Ag/AgCl. The diffusion limiting current shown in the figure does not parallel to the potential axis but varies a little, due probably to some change in the electrode environments such as electrode roughness caused

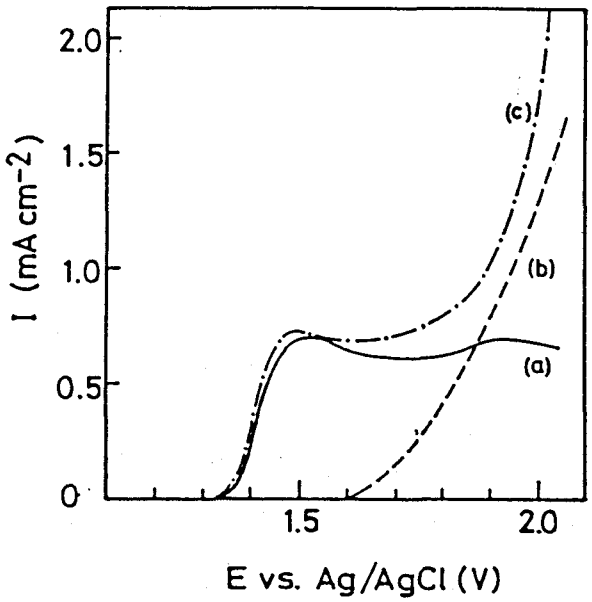

Fig. 9. I-E curves of Pt electrodes in the presence of 2.0 x 10^{-3} M pyrrole (a), 0.1 M thiophene (b), and a mixture of both species in the above described concentration (c) in acetonitrile containing 0.1 M $LiClO_4$. dE/dt = 10 mV s^{-1}.

by successive deposition of polypyrrole. When the polypyrrole films were prepared in this solution at 2.05 V vs. Ag/AgCl and at 1.5 V vs. Ag/AgCl, the resulting polymer films gave almost the same cyclic voltammograms, suggesting that the electrochemical properties of polypyrrole films are not appreciably influenced by the potentials chosen for polymerization of pyrrole. On the other hand, an I-E curve taken in a 0.1 M thiophene solution (curve (b) in Fig. 9) under the same conditions shows that anodic currents concerning the polymerization monotonically increase with increasing anodic potentials from 1.60 V vs. Ag/AgCl. The anodic currents in that case also became diffusion limited at 2.4 V vs. Ag/AgCl, although not shown here. When an I-E curve was taken in an acetonitrile solution containing 2.0 x 10^{-3} M pyrrole and 0.1 M thiophene, curve (c) was obtained,

which is regarded as superposition of the curve (a) on the curve (b). However, the curves (a) and (b) do not strictly add up to make the curve (c). This may be partly due to some change in the electrode environment caused during the course of I-E curve measurements as described above, and partly due to contribution of IR drop which is expected to be greater at copolymer films as will be shown later.

The surfaces of polymer films prepared at 1.37, 1.67, 1.87, and 2.07 V vs. Ag/AgCl in the acetonitrile solution containing 2.0 x 10^{-3} M pyrrole and 0.1 M thiophene were analyzed with XPS, and results on the signal intensity of C, N, S, and Cl in the films are given in Table 3. Apparently XPS intensities of N and Cl decrease and that of S increases with an anodic shift of the polymerization potentials (E_{dep}). If it is assumed from these results that pyrrole and thiophene are copolymerized, the ratio of each component involved in the prepared films could be changed with changing E_{dep}. Also shown in this table is the ratio of pyrrole to thiophene ring in the prepared polymers which was determined by the elemental analyses;

Table 3. XPS intensity (in C.P.S.)[a] of surface and elemental analysis of the copolymer prepared at various potentials in an acetonitrile solution containing 2.0 x 10^{-3} M pyrrole, 0.1 M thiophene, and 0.1 M $LiClO_4$

E_{dep} vs. Ag/AgCl/V	XPS intensity				Elemental analysis		
	C(1S)	N(1S)	S($2P_{3/2}$)	Cl($2P_{3/2}$)	C	H	N
1.37	10200	2080	0	580	4.00	3.16	0.93
1.67	10100	1740	260	520	4.00	3.02	0.73
1.87	11500	1260	740	320	4.00	2.58	0.47
2.07	10500	1010	1660	200	4.00	2.06	0.19

a) The unmonochromatized AlK_{α} radiation was used under the condition of V = 7 KV, I = 36 mA, and scanning speed = 0.05 V/S.

the relative ratio of H and N is given to the number of C of a pyrrole or thiophene rings to make it possible to determine the ratio of the occupation of pyrrole rings in the prepared polymers directly from the value of N. It is found that the ratio of pyrrole to thiophene rings in the film essentially follows the I-E behaviors shown in Fig. 9. For example, almost the same quantity of pyrrole as that of thiophene is found in the film prepared at 1.87 V vs. Ag/AgCl where the oxidation current of thiophene intersects with that of pyrrole. Pyrrole becomes the major component of the prepared polymer films, if electropolymerization is conducted at potentials negative of this boundary potential. Thus, it is concluded that the component of the film can easily be changed by changing E_{dep} without any change in the concentration of each monomer in the electrolyte solution. It seems that the strategy used here can be applied to other concentrations of pyrrole and thiophene, but the pyrrole concentration should be low enough to give diffusion limiting currents at potentials where thiophene oxidation occurs under activation-controlled conditions.

As will be shown below, the prepared polymers are not mixtures of polypyrrole and polythiophene, but copolymers. Accordingly, the term "copolymer" will be used below.

IR and Optical Absorption Spectra of Copolymers. FT-IR spectra of polythiophene, polypyrrole, a mixture of polythiophene and polypyrrole, an as-grown copolymer prepared at 1.87 V vs. Ag/AgCl, and of the same copolymer which was later reduced at -0.5 V vs. Ag/AgCl are shown in Fig. 10, and positions of absorption bands in each spectrum are listed in Table 4. As expected, the shapes and positions of the absorption bands of the

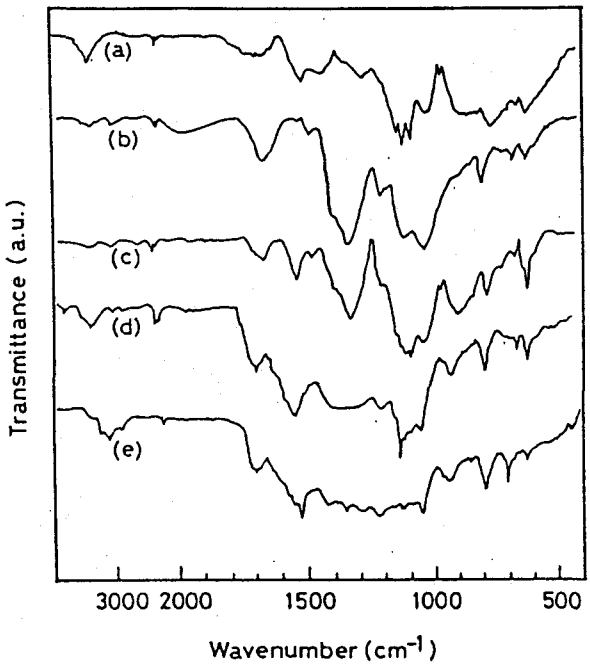

Fig. 10. IR spectra of polypyrrole (a), polythiophene (b), mixture of polypyrrole and polythiophene(1:1) (c), as-grown copolymer (d) and the copolymer reduced at -0.5 V vs. Ag/AgCl (e). The copolymers were prepared at 1.85 V vs. Ag/AgCl.

Table 4. The band position of IR spectra shown in Fig. 10

Sample	Band position of IR spectra (cm^{-1})												
PPy		1520	1470		1275	1144	1121	1089	1030	964	890	768	711	626
PTh	1672		1477	1333		1205	1118		1036			792	672	620
mixture of PPy and PTh	1674	1528	1475	1333		1202	1120	1089	1039	965	899	789	673	625
as-grown copolymer	1701	1550				1210	1122	1109	1048		931	796	668	623
reduced copolymer	1680	1520		1412		1208			1040		942	792		626

mixture of polythiophene and polypyrrole are constituted by those observed from polypyrrole and polythiophene, whereas the spectrum of the as-grown copolymer is different from that of the mixture. The most characteristic difference in the copolymer is the lack of a large bant at 1333 cm^{-1} which is characteristic of oxidized polythiophene [12], although the absorption band at 1100 cm^{-1} which is known to appear at both oxidized polypyrrole [72] and polythiophene [12] is seen for the as-grown copolymer. The latter band disappeared with reduction of the copolymer, as in the case of polypyrrole and polythiophene [12,72]. Another noticeable feature in the spectrum is that an absorption band around 790 cm^{-1}, which is characteristic of α-substituted five membered heterocyclic compounds [12], appears in the copolymer, suggesting that α-positions of each monomer are involved in copolymerization.

The lack of the band around 1333 cm^{-1} at the copolymer strongly suggests that isolated polythiophene chains do not eventually exist in the copolymer, and that pyrrole and thiophene monomers are bonded effectively during the polymerization. The appearance of the band at 1100 cm^{-1} is then judged to be associated with the pyrrole rings of the copolymer rather than the thiophene rings. It is then said that polarons and/or bipolarons seem to be localized on pyrrole ring units of the copolymer.

Optical absorption spectra of copolymers reduced at -0.5 V vs. Ag/AgCl are shown in Fig. 11 for polymerization potentials of 1.37, 1.67, 1.77, 1.87, and 2.07 V vs. Ag/AgCl, together with that of reduced polythiophene. The absorption peak shown in the figure represent the band gap transitions of the prepared polymer films. The spectrum of the polymer film prepared at 1.37 V vs. Ag/AgCl having absorption maximum at 420 nm (2.96 eV) is essentially the same as that of reduced polypyrrole

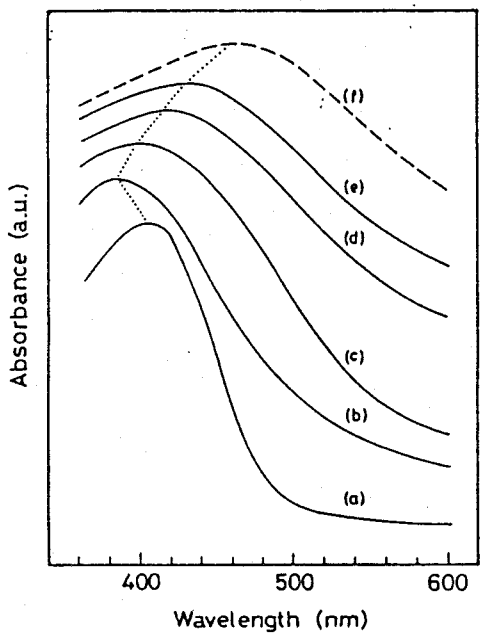

Fig. 11, Optical absorption spectra of the copolymers prepared at 1.37 (a), 1.67 (b), 1.77 (c), 1.87 (d), and 2.07 (e) V vs. Ag/AgCl and of polythiophene (f) prepared at 2.07 V vs. Ag/AgCl, all of which were reduced at -0.5 V vs. Ag/AgCl.

which is shown in Fig. 4 of the previous section and by some other investigators [16,62,73]. The results on XPS and elemental analyses already shown in Table 3 also show that the polymer films prepared at 1.37 V vs. Ag/AgCl were purely polypyrrole. According to other authors [74,75], however, the bandgap transition of reduced polypyrrole appears at 3.2 eV (388 nm), and with increasing a doping level a blue shift in the transition up to 3.6 eV (345 nm) is seen. Presently it is not known why such discrepancies in the bandgap value of reduced polypyrrole have been obtained.

When the polymerization potential was increased to 1.67 V, the resulting copolymer contained ca. 25% of the thiophene ring as shown in

Table 3, and exhibited an absorption maximum at 390 nm. If 420 nm is taken as the bandgap transition of reduced polypyrrole, it is then said that a blue shift occurs with incorporation of thiophene rings into the polypyrrole chain by ca. 25% in the monomer unit. A plausible explanation for the observed blue shift is that the incorporation of thiophene rings causes some instability in the ground state geometry of polypyrrole. Anyway, further increase in the ratio of thiophene to pyrrole rings in the copolymer with increasing E_{dep} does not bring about further blue shifts in the absorption spectra. Rather it causes systematic red shifts, as shown in the figure, in such a manner that the band structure of the copolymer changes gradually from that of polypyrrole to polythiophene as the ratio of thiophene to pyrrole rings in the copolymer increase from ca. 25 mole%.

Cyclic Voltammograms and Conductivities of Copolymers. Cyclic voltammograms (CV) of the copolymers obtained in an acetonitrile solution containing 0.1 M $LiClO_4$ are shown in Fig. 12 for films prepared at 1.37, 1.67, 1.87, and 2.07 V vs. Ag/AgCl. An anodic/cathodic peak current couple appears in each copolymer film as in the case of a copolymer of pyrrole and N-methyl pyrrole [68]. If the prepared polymers were mixtures of polypyrrole and polythiophene, two couples of anodic/cathodic peak currents due to the redox reactions of polypyrrole and polythiophene should have appeared at different potentials. Thus, the cyclic voltammograms support again that these polymers are copolymers of pyrrole and thiophene. Moreover it is noteworthy that the copolymer prepared at 1.87 V vs. Ag/AgCl, in which the ratio of pyrrole and thiophene ring is almost 1:1, shows almost the same CV shape as that of the copolymer of pyrrole and thiophene prepared by the polymerization of 2,2'-thienylpyrrole

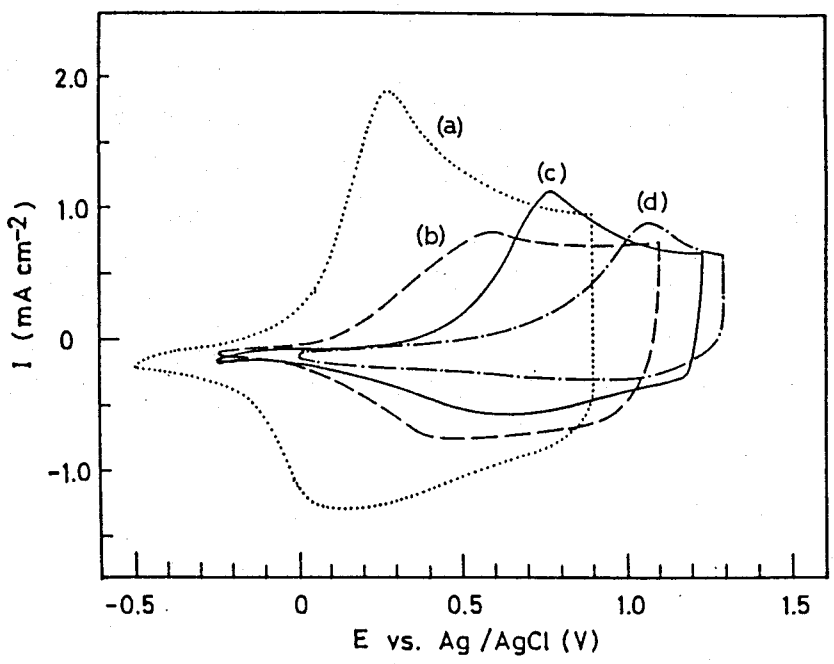

Fig. 12. Cyclic voltammograms of the copolymers in an acetonitrile solution containing 0.1 M $LiClO_4$. Preparation potential of copolymers: at (a) 1.37, (b) 1.67, (c) 1.87, (d) 2.17 V vs. Ag/AgCl. dE/dT = 100 mV s^{-1}.

(E_{pa} = 0.81 V vs. Ag/AgCl) [67]. It is suggested from the dependence of E_{pa} on E_{dep} that voltammetric behaviors of copolymers are systematically changed from those of polypyrrole (E_{pa} = 0.26 V vs. Ag/AgCl) [45] to those of polythiophene (E_{pa} = 1.33 V vs. Ag/AgCl) [13] by increasing E_{dep}.

The conductivities of polymer films prepared at 1.37, 1.67, 1.87, and 2.07 V vs. Ag/AgCl were 44, 40, 0.16, and 0.15 S cm^{-1}, respectively. These values were highly reproducible. The value obtained for the film prepared at 1.37 V vs. Ag/AgCl is close to that reported for polypyrrole [45] and that for the film prepared at 2.07 V vs. Ag/AgCl is close to that for polythiophene films prepared in acetonitrile solutions containing Bu_4NBF_4

[13] and $LiClO_4$ [14] as supporting electrolytes, though at polythiophene much greater conductivities have also been reported [15,16]. It is noticed by combining these conductivity values with the film compositions which are given in Table 3 that the conductivity does not systematically change with variation of the film composition. A large change in the film conductivity by two orders of magnitude is observed between the copolymers prepared at 1.67 and 1.87 V vs. Ag/AgCl in which the relative occupation of the pyrrole rings is 73% and 47%, respectively. The observed behavior of the film conductivity for the present copolymers are quite different from that for copolymers of pyrrole and N-methyl pyrrole [68], where the film conductivity systematically changes depending on the relative ratio of these two components. As discussed in the results of IR measurements of the copolymers, polarons or bipolarons seem to be populated on pyrrole rings rather than on thiophene rings of the copolymer due probably to lower oxidation potentials of the former than the latter. If this is valid, a rapid decrease in conductivities with an increase in thiophene rings would occur when distribution of thiophene rings in the polypyrrole chains becomes such that it causes isolation of polarons and/or bipolarons on pyrrole rings.

Chapter 2

Control of Conductivity of Polypyrrole Films by Anions Incorporated in the Films

2-1

Conductivity of Polypyrrole Films Doped with Aromatic Sulfonate Derivatives

2-1-1 Introduction

As described in the previous chapter, polypyrrole films prepared by electrolytic polymerization of pyrrole show high electric conductivities. The mechanism of the appearance of the high conductivity has been widely investigated, and it has been clarified from optical and ESR studies [1-3] that polarons and bipolarons in the polymer films serve as positive charge carriers. In addition, strong attention has been paid to a variety of factors which control the conductivity of polypyrrole films. The conductivity of polypyrrole films is primarily controlled by adjusting its potential in an electrolytic system [4-9], but it is also influenced by another factors such as the concentration of a supporting electrolyte [7], and the kinds of electrolyte anions in a preparation bath [76-78]. Furthermore, it was reported that the stretching of the prepared polymer films increased their conductivities [79]. The effect of dopant anions on the polypyrrole film properties has recently become of importance, since the use of aqueous electrolytes allows the preparation of polypyrrole films doped with a variety of anions having special functions such as electrocatalysis and electrochromic behaviors, as demonstrated, for example,

in the polypyrrole films doped with phthalocyanines and porphyrins [30-32]. However, there are few systematic investigations with regards to the effect of the kinds of dopant anions on the conductivity of polypyrrole films.

In this section, it will be described that the conductivity of polypyrrole films doped with organic sulfonate derivatives decreases with increasing the number of sulfonate groups of a dopant molecule, and that the current density used for the film preparation strongly influences the conductivity of the resulting polymer films. In addition, discussion will be focused to how such events appear, based on X-ray diffraction patterns, visible absorption spectra, and electrochemical behaviors of the prepared films.

2-1-1 Experimental

Pyrrole was purified by distillation under N_2. Sodium salts of naphthalene-2-sulfonate (N-1), naphthalene-1,5-disulfonate (N-2), and naphthalene-1,3,6-trisulfonate (N-3) were purified first by dissolving in hot water, followed by filtration, then by extracting the filtrate with benzene for several times, and finally by evaporating water. Sodium salts of anthraquinone-2-sulfonate (A-1), anthraquinone-2,6-disulfonate (A-2), and copper phthalocyanine-3,4',4'',4'''-tetrasulfonate (P-4) were of reagent grade and used without further purification.

The polypyrrole films were prepared by anodic polymerization of 0.1 mol dm^{-3} pyrrole dissolved in water containing one of the above-described aromatic sulfonate derivatives in 0.01 mol dm^{-3} as a supporting electrolyte which served as a dopant. The quantity of electricity chosen for the

polymerizations was 1.2 C cm^{-2} for X-ray diffraction analyses and 200 mC cm^{-2} for the other measurements.

The conductivity of the prepared polypyrrole films was determined by the four probe method. For this purpose, the prepared polypyrrole film was teared off from the electrode substrate and its thickness was determined by observations with a scanning electron microscope (SEM) (HITACHI S-450). X-ray diffraction analyses of the polypyrrole films were carried out using a Shimadzu XD-3A X-ray diffractometer.

2-1-3 Results

Concentration of dopant anions and conductivity of polypyrrole films. The molar concentrations of sulfonate anions doped in the polypyrrole films prepared at 0.005, 0.2, and 10 mA cm^{-2} were determined by the elemental analyses. The results were listed in Table 5 as the molar ratio of sulfonate groups to pyrrole rings. Except for the case of P-4, the molar concentrations of sulfonate groups of the prepared polymer films are almost the same as those reported for univalent inorganic dopants such as ClO_4^- and Cl^- [6], and are independent of the number of sulfonate groups of a dopant molecule and the preparation current density. These results show that the degree of ionization of polypyrrole films prepared by the electropolymerization is the same even if multivalent anions are used as a dopant material. In the case of the polypyrrole films doped with P-4, the molar concentration was lower than that of the other polymers. This should be attributable to the molecular size of P-4 which may be too large to be doped completely in the polymer films.

Table 5. The molar concentration of sulfonate anions doped in PPy films prepared at various current density

Dopant	Concentration[a)]		
	0.005[b)]	0.2[b)]	10[b)]
A-1	0.29	0.34	0.32
A-2	0.32	0.33	0.33
N-1	0.33	0.32	0.31
N-2	0.32	0.31	0.33
N-3	0.33	0.33	0.34
P-4	0.24	0.26	0.26

a) Molar ratio of sulfonate anions to pyrrole rings.
b) Current density for preparation of the polymer (mA cm^{-2}).

Plots of the conductivity of all kinds of the polypyrrole films prepared in the present study against the current density used in the film preparation are shown in Fig. 13, and those of the conductivity against the number of sulfonate groups of naphthalene sulfonate derivatives are shown in Fig. 14. It is noticed from these figures that even with excluding the polypyrrole films doped with P-4 the conductivity of polypyrrole films is different by more than one order of magnitude between A-1 and N-3 dopants when the films were prepared at 0.005 mA cm^{-2}.

Rearrangements of Fig. 13 for the cases of naphthalene sulfonate dopants give Fig. 14. The curves (a) and (b) in Fig. 14 which depict the case of the film preparation at 0.005 and 0.02 mA cm^{-2}, respectively, show that an increase in the number of sulfonate groups of a dopant molecule

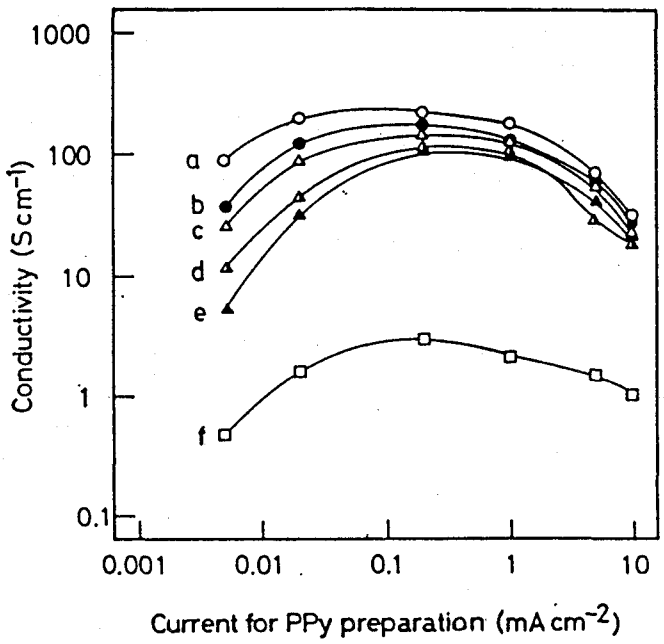

Fig. 13. The relationship between the current density used for polymer film preparation and the conductivity of polypyrrole films doped with A-1 (a), A-2 (b), N-1 (c), N-2 (d), N-3 (e), and P-4 (f).

definitely reduces the conductivity of the polymer films when the film preparation is made at relatively low current densities. However, the difference in the conductivity due to the number of sulfonate groups of a dopant becomes small with an increase in the current density chosen in the preparation of polypyrrole films, as the curves (c) and (d) show. Although not shown here, the same was true in the case of anthraquinone sulfonate derivatives as dopants. Furthermore, it is noticed from Fig. 13 that the conductivity reaches its maximum at an optimum current density of the film preparation (0.2 mA cm^{-2}) for all the polypyrrole films having a variety of dopants. The extremely low conductivities of the polypyrrole films doped with P-4 as shown in Fig. 13 may be caused partly by a large number of

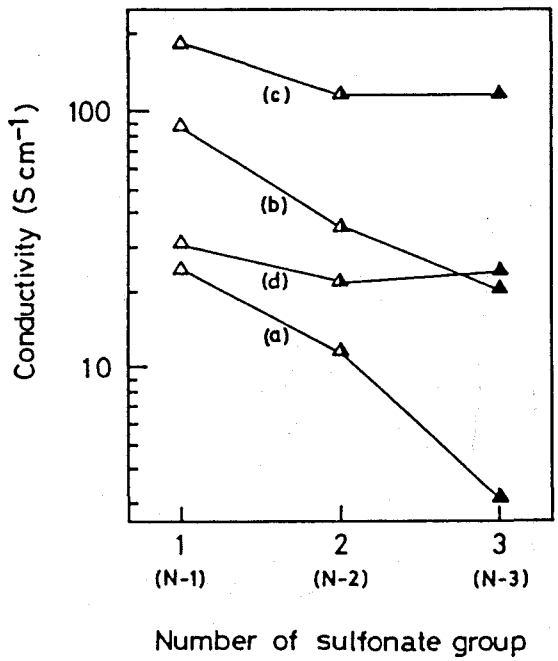

Fig. 14. The relationship between the conductivity of polypyrrole films prepared at 0.005 (a), 0.02 (b), 0.2 (c), and 10 (d) mA cm^{-2} and the number of sulfonate groups of a dopant molecule.

sulfonate groups of a dopant molecule and partly by shortage of the anion concentration in the polymer films as described above.

X-ray diffraction analyses of polypyrrole films. It has been reported that polypyrrole films doped with n-alkylsulfates or n-alkylsulfonates showed an intense X-ray diffraction peak below 2θ = 5° [80] which is indicative of a layered structure of polypyrrole films doped with the organic anions. The polypyrrole films doped with aromatic sulfonate derivatives used in the present study also showed similar X-ray diffraction peaks. Typical examples are shown in Fig. 15. The intensity of the peak observed around 2θ = 3° was varied depending on the kind of dopants and

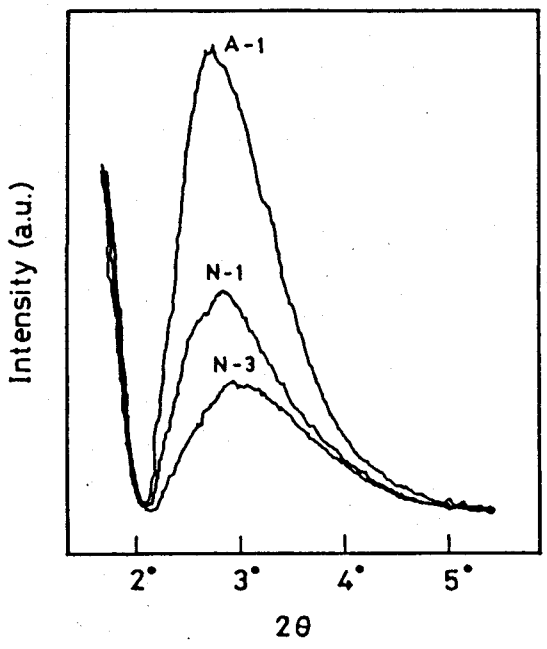

Fig. 15. X-ray diffraction patterns of polypyrrole films doped with A-1, N-1, and N-3. The polymer film preparation was made at 0.005 mA cm^{-2}.

the current density of the polymer film preparation. It is well known that the intensity of X-ray diffraction peak is a measure of crystallinity of polymers [81]. Then the crystallinity of the polypyrrole films prepared in various electrolyte solutions at a variety of current densities was evaluated by comparing the intensity of the diffraction peak of each sample. The polypyrrole films prepared at 0.005 mA cm^{-2} in the A-1 electrolyte solution gave the highest diffraction peak, and then the ratio of the peak height of each sample to that of this sample was adopted as a relative measure of the crystallinity. The relationship of the crystallinity and the conductivity of polypyrrole films prepared at 0.005 mA cm^{-2} and 0.2 mA cm^{-2} are shown in Fig. 16. As for the polymer films prepared at 0.005 mA cm^{-2}, the film having a high crystallinity shows a high conductivity, as

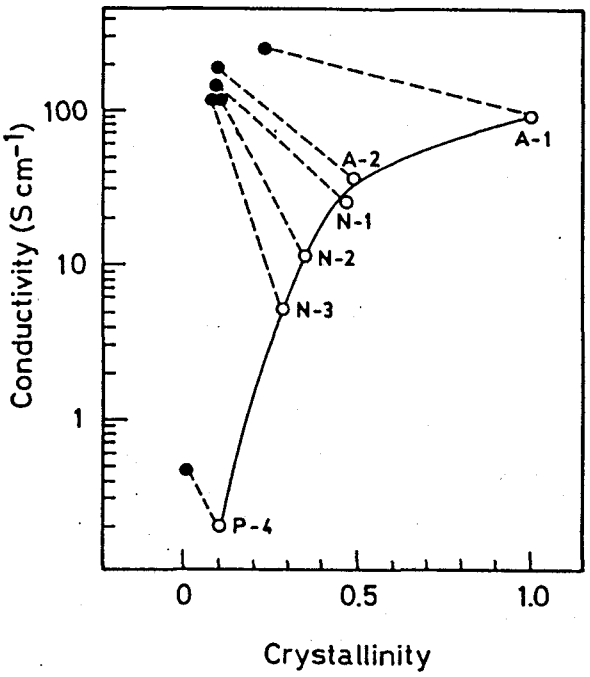

Fig. 16. The relationship between the conductivity and the crystallinity of polypyrrole films prepared at 0.005 (○) and 0.2 (●) mA cm^{-2}.

already suggested by other investigators [792,82]. In contrast, the polymer films prepared at 0.2 mA cm^{-2} have lower crystallinities than those prepared at 0.005 mA cm^{-2} but they possess higher conductivities. These results suggest that the conductivity of polypyrrole films is not governed by the crystallinity of the polymer films alone. Furthermore, the polymer films prepared at 0.2 mA cm^{-2} have the conductivities of almost the same order of magnitude regardless of the kinds of dopants except for the case of P-4. It is then suggested that the effects of dopant anions on the film conductivity which are observed in the film prepared at 0.005 mA cm^{-2} (see Fig. 13) are obscured in those prepared at 0.2 mA cm^{-2} by disordering of the polymer structure.

Visible absorption spectra of polypyrrole films. The visible absorption spectra of polypyrrole films prepared could be measured without dopant interference for the films doped with naphthalene sulfonate derivatives, since these dopants have no absorption band in a visible region. The as-grown films exhibit absorption bands due to the transition between bonding and antibonding bipolaron bands [1,2]. According to the results shown in Fig. 17 for the polymers prepared at 0.005 mA cm^{-2}, a decrease in the number of sulfonate groups of the dopant causes a red shift and broading of the absorption band. This result may reflect a situation where the overlaps between the bipolaron states [1,2] are weakened by increasing the number of sulfonate groups of dopants, thereby narrowing their resonant area in the polymer chains. Similar red shifts of the absorption maximum were observed with increasing the current density

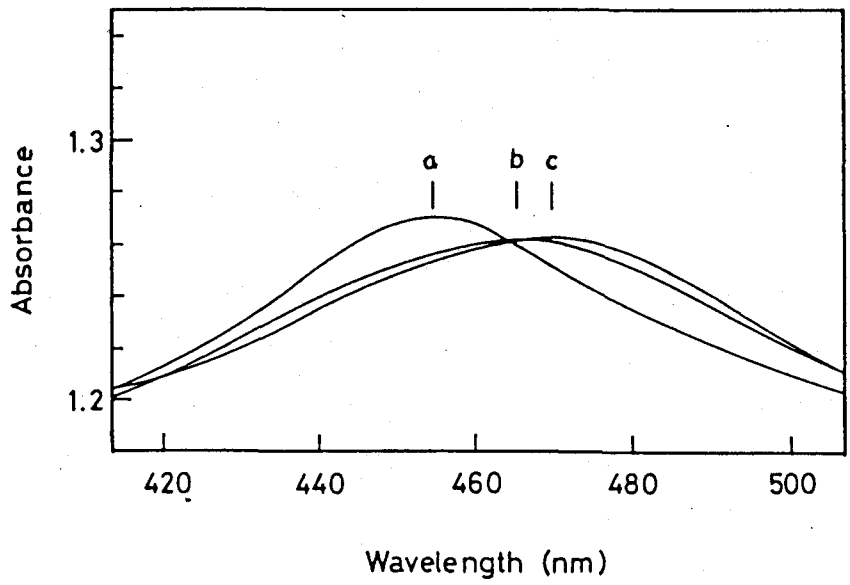

Fig. 17. Visible absorption of polypyrrole films doped with N-3 (a), N-2 (b), and N-1 (c). The polymer films were prepared at 0.005 mA cm^{-2}.

Table 6. The peak position of visible absorption bands for PPy films doped with N-1, N-2, and N-3

Preparation Current /mA cm^{-2}	Peak position (nm) N-1	N-2	N-3
0.005	472	464	457
0.2	483	478	477
10	485	481	479

of the film preparation, as shown in Table 6. As long as the results on the polymer films prepared at 0.005 and 0.2 mA cm^{-2} are concerned, the red shift in the absorption maximum is accompanied by the increase in the conductivity.

The electrochemical behaviors of polypyrrole films Cyclic voltammograms of N-2-doped polypyrrole films prepared at 0.005, 0.2, and 10 mA cm^{-2} are shown in Fig. 18. The redox behaviors of these polymers are different from those of polypyrrole films doped with inorganic anions, which shows well-defined anodic and cathodic waves in KCl solution, as shown in Fig. 1 of the section 1-1. Concerning the N-2-doped films, a cathodic current peak shifts anodically with increasing the current density used for the film preparation. Similar shifts of the cathodic wave are observed for N-1 and N-3-doped films as listed in Table 7. It has been reported [83] that when polypyrrole films doped with large anions such as polyvinylsulfates were reduced, the doped anions were not eliminated but electrolyte cations are incorporated into the films to keep their electrical neutrality. Similar situations were also observed at the present polymer

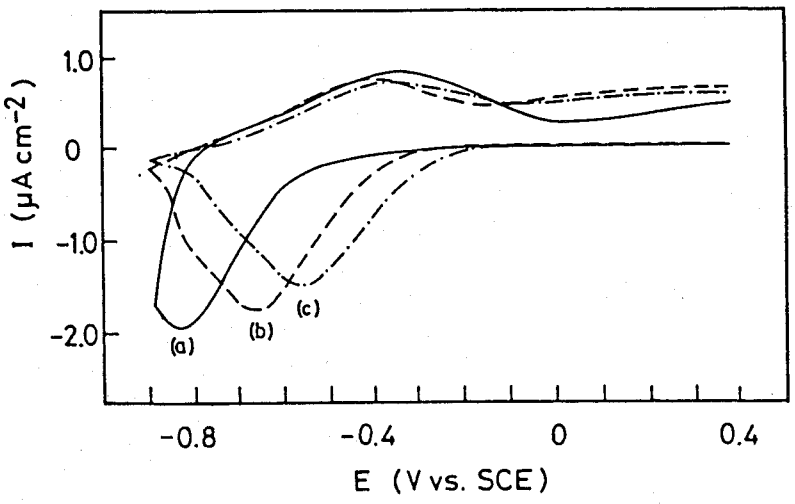

Fig. 18. Cyclic voltammograms of N-2-doped polypyrrole films prepared at 0.005 (a), 0.2 (b), 10 (c) mA cm^{-2} in 1M KCl aqueous solution. dE/dt = 50 mV s^{-1}.

Table 7. Peak potentials of cathodic waves of cyclic voltammograms for PPy films doped with N-1, N-2, and N-3

Preparation Current /mA cm^{-2}	Peak position/V vs. SCE N-1	N-2	N-3
0.005	-0.80	-0.82	-0.80
0.2	-0.77	-0.67	-0.76
10	-0.67	-0.56	-0.60

films doped with the aromatic sulfonate derivatives; these dopants were not eliminated in the polymer films by the reduction, as judged from the results by elemental analyses of the reduced polymers, and furthermore potassium was detected by EPMA only in the reduced polymer films as shown in Fig. 19. The cathodic waves in Fig 18 are then judged to be due to the insertion of potassium cations into the films. In this respect, the finding

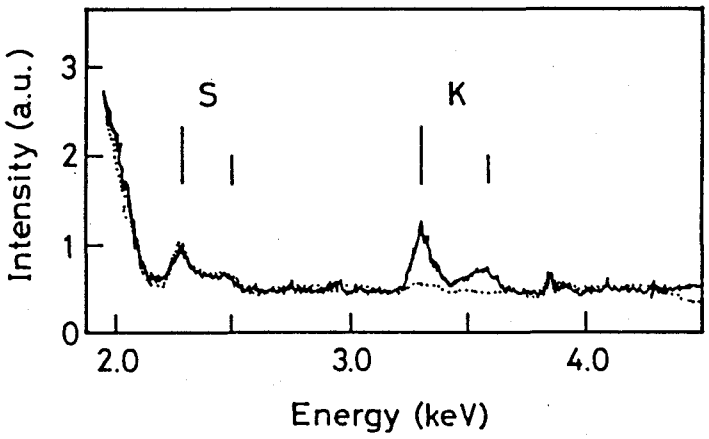

Fig. 19. EPMA spectra of oxidized (---) and reduced (——) polypyrrole films doped with N-1.

shown in Fig. 18 that the cathodic current peak of the voltammograms shifts anodically with increasing the current density of the film preparation may be said to reflect that the polymer films prepared at higher current densities must be so much porous as to allow easier penetration of K^+ into the film on its reduction.

2-1-4 Discussion

polypyrrole films prepared at low current densities such as 0.005 mA cm^{-2} shows high crystallinities, reflecting a general rule observed, for example, in metal plating that a lower deposition rate of a crystalline materials results in higher crystallinities. However, in the polypyrrole films prepared in the present study the conductivity and the crystallinity of the films are affected greatly by the number of sulfonate groups of a

dopant as Fig. 16 shows. The decrease in the conductivity with increasing the number of sulfonate groups of a dopant may be explained in terms of the degree of charge localization in the doped polypyrrole films. The larger the number of negative charges of a dopant, the more strong the attraction of positive charges in the polymer chain. The decrease in the crystallinity with increasing the number of sulfonate groups of a dopant may also be explained by the interaction between the concentrated negative charges of a dopant with the positive charges in the polymer chains, as schematically illustrated in Fig. 20.

The X-ray diffraction analyses show that an increase in the current densities of the film preparation causes a decrease in the crystallinity of the resulting films, whereas the results shown in Table 6 on the visible absorption spectra suggest that resonance of bipolarons in the polymer chains becomes spread with losing the crystallinity. These phenomena can be explained by assuming that with increasing the current density for the film preparation, cross-linking of the polymer chains becomes more enhanced, thereby the interaction between the positive charge carriers and the dopant anions decreases as illustrated in Fig. 21. The increase in the density of cross-linking makes the conductivity of polymer films increase, and the decrease in the interaction between the positive charge carriers and the dopant anions should weaken the charge localization in the doped polypyrrole chains and then the film conductivity becomes not affected by the number of sulfonate groups of dopants.

Although the X-ray diffraction patterns and the visible absorption spectra are not remarkably different among the polymer films prepared at current densities above 0.2 mA cm^{-2}, the conductivities decrease with increasing the current density as shown in Fig. 13. The principal cause

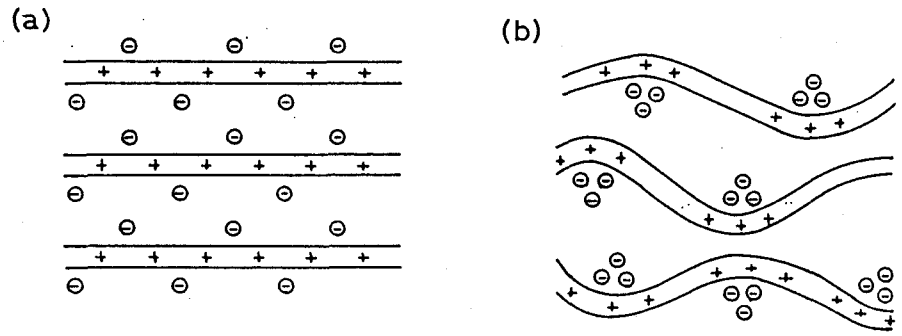

Fig. 20. Hypothetical illustration of polymer structures of polypyrrole films doped with mono (a) and multi (b) valent anions.

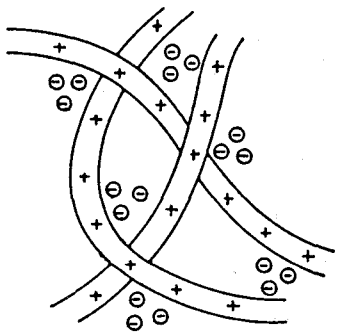

Fig. 21. As in Fig. 20, but for at a higher current density.

for bringing about such phenomenon may be related to the increase in the porosity of the polymer films with increasing the current density for the film preparation, as already described based on the voltammetric behaviors of the polypyrrole films prepared at different current densities. The degree of the contact of the cross-linked polymer chains will be low at a polymer film of high porosity and hence the conductivity is low at such polymer films.

2-2

The Effect of Basicity of Incorporated Carboxylate Ions on Conductivity of Polypyrrole Films

2-2-1 Introduction

As described in the previous section, the conductivity of polypyrrole films doped with organic sulphonate derivatives decreases with an increase in the number of sulphonate groups of a dopant molecule. These results are qualitatively interpreted in terms of interaction between the doped anions and the positive charge carriers such as polarons and/or bipolarons in the polymer chains. Later it was found that the basicity of the doped anions also influences the interaction, resulting in the changes in the conductivity of the polypyrrole films.

In this section, these findings obtained by using several kinds of carboxylate anions will be described in detail. Furthermore, it will be shown that the conductivity of polypyrrole films doped with monoanions of dicarboxylic acids decreases systematically with increasing pH of aqueous solutions in which the polymer films are immersed as a result of dissociation of the doped monoanions into the corresponding dianions.

2-2-2 Experimental

Carboxylic acids which are listed in Table 8 were used in the present study. They were reagent grade chemicals and used without further purification. Electropolymerization of pyrrole was carried out

Table 8. Carboxylic acid used in this study and their pK_a values

Acid	pK_a	
trifluoroacetic acid	-0.3	
trichloroacetic acid	0.64	
dichloroacetic acid	1.26	
oxalic acid	1.27[a]	4.28[b]
2,4-dinitrobenzoic acid	1.42	
maleic acid	1.93[a]	6.59[b]
o-nitrobenzoic acid	2.18	
cyanoacetic acid	2.43	
monofluoroacetic acid	2.59	
malonic acid	2.76[a]	5.77[b]
3,5-dinitrobenzoic acid	2.80	
p-nitrobenzoic acid	3.40	
acetic acid	4.75	

a) The first stage dissociation constant pK_{a1} values.
b) The second stage dissociation constant pK_{a2} values.

galvanostatically at 0.2 mA cm^{-2} in 0.1 M pyrrole dissolved in water containing one of the above mentioned carboxylic acid in 0.01 M. The electrolyte solutions containing a monocarboxylic acid were adjusted to pH 6 with 0.1 M KOH solution to ionize the monocarboxylic acid. For cases of dicarboxylic acids such as oxalic acid, maleic acid, and malonic acid, the solution pH was adjusted to pH 3 which gave monoanions only of the dicarboxylic acids used.

The changing conductance of polypyrrole films in aqueous solutions caused by changing the pH of solutions was measured in-situ by using the electrode assembly as shown in Fig. 22 A polypyrrole film of 5 mm x 8 mm

was stripped from the electrode substrate and was sandwiched between two ITO glass slides (50 mm x 10 mm x 2 mm) in two ends of the film. The distance between two polypyrrole sandwiched ITO glass slides was 2 mm, and the film in the area was exposed to solutions. After immersing the electrode assembly in 0.1 M KCl solution, DC voltages less than 0.5 V were applied to the Au lead wires and resulting currents were monitored. By plotting current-voltage relations, the apparent resistance of the polypyrrole film was obtained. Since the apparent resistance determined in this way contained the resistance of the ITO glass slides of the electrode assembly, the contribution of the latter to the former must be eliminated to obtain the conductance of the polypyrrole film sandwiched between the two ITO glass slides. The resistance of the ITO glass slides of the

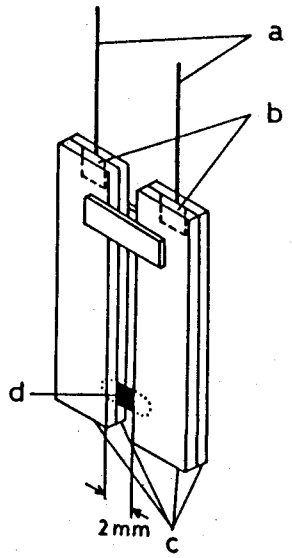

Fig. 22. In-situ measurements of changes in the conductance of polypyrrole films caused by changing pH of solutions. a: Au wire (0.3 mmϕ), b: Au foil (8 mm x 8 mm x 50 μm), c: ITO plate (50 mm x 10 mm x 2 mm), d: polypyrrole film (5 mm x 8 mm).

electrode assembly was determined in a similar manner as in the determination of the apparent resistance of the polypyrrole films by replacing the polypyrrole film with an Au plate of 5 mm x 8 mm x 50 μm thickness. The KCl solution in which the film was immersed was magnetically stirred, and its pH was changed to desired values by adding appropriate amount of 0.1 M HCl or 0.1 M KOH using a burette.

2-2-3 Results and Discussion

Electropolymerization of pyrrole in the presence of carboxylate anions. It was found that the pK_a value of carboxylic acids plays a decisive role in the growth of polypyrrole films. If carboxylates whose conjugated acids have pK_a values greater than that of p-nitrobenzoic acid (pK_a = 3.40) was used as dopants, no appreciable film growth of polypyrrole was observed. Soon after beginning of the constant current electrolysis of pyrrole solutions, the electrode potential rose up to 2 V vs. SCE or more, and simultaneously the polypyrrole film growth apparently ceased. The polypyrrole films obtained in those cases were too thin to be stripped from the substrate, and cyclic voltammetry of the film-coated electrode in 0.01 mol dm^{-3} $K_3Fe(CN)_6$ and 0.1 mol dm^{-3} Na_2SO_4 did not result in any appreciable redox waves. In the case of maleic, malonic, and oxalic acid, similar phenomena were observed when attempts were made to prepare polypyrrole films in a solution of pH 7, but not so in a solution of pH 3.

When carboxylic acids having pK_a values smaller than 3,5-dinitrobenzoic acid (pK_a = 2.50) were used, polypyrrole films could be prepared with electrolysis charge of 200 mC cm^{-2}. Elemental analyses of

polypyrrole films prepared in these cases showed that the carboxylate anions were doped in the films in the molar concentration of 0.3 $\pm$ 0.02 to pyrrole rings and that maleic, malic, and oxalic acid were doped in the form of monoanion. It is then said that the degree of ionization of polypyrrole films prepared in this study were almost the same as those prepared in electrolyte solutions containing aromatic sulfonate derivatives as described in the section 2-1.

Conductivity of polypyrrole films doped with carboxylate anions. Plots of the conductivity of the polypyrrole films (σ) against pK_a values of the conjugated acids of carboxylate anions doped in the films are shown in Fig. 23. A polypyrrole film doped with CF_3COO^- exhibits the highest conductivity (60 S cm^{-1}) among the films prepared in the present study, and the film conductivity distinctly decreases by almost three orders of magnitude with increasing the pK_a of conjugated acid. These results indicate that an increase in the basicity of dopant anions reduces the conductivity of polypyrrole films. A linear relationship is established between pK_a and log σ for pK_a values greater than 1, which can be formulated by log σ = $-1.22pK_a$ + 2.50. On the other hand, the dependence of the conductivity on pK_a is weak when pK_a values of the conjugated acids of dopant anions are smaller than 1.

The observed effects of the basicity of dopant anions on the conductivity of polypyrrole films may be explained in terms of an interaction between positive charges in the polymer chains and the doped anions in the film. The interaction is thought to become stronger for carboxylic acids of higher pK_a, because when the conjugated anions are doped in polypyrrole films, they must have affinities to positive charges in

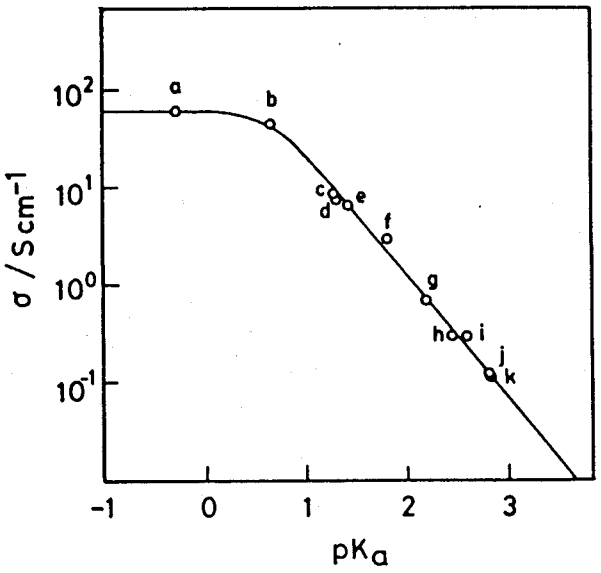

Fig. 23. Relationship between the conductivity of polypyrrole films and pK_a values of conjugated acids of carboxylates doped in the films. The carboxylate anions doped in polypyrrole films are trifluoroacetate (a), trichloroacetate (b), dichloroacetate (c), oxalic acid monoanion (d), 2,4-dinitrobenzoate (e), maleic acid monoanion (f), o-nitrobenzoate (g), cyanoacetate (h), monofluoroacetate (i), malonic acid monoanion (j), and 3,5-dinitrobenzoate (k).

the polymer chains in such a manner that they show affinities to positively charged protons in water the degree being dependent on their pK_a values. The finding that polypyrrole film did not grow in the presence of carboxylate whose conjugated pK_a are greater than that of p-nitrobenzoic acid can be explained by assuming that the electrostatic interaction between the dopant and positive charges of polypyrrole is too strong in these cased to possess any appreciable conductivities in the deposited films. The finding that the very thin films prepared under such environments did not show any redox activities provides further indirect supports to insulating properties of the polypyrrole film prepared in those

cases. The deviation from the linear relationship between log σ and pK_a observed at pK_a values less than 1 seems to reflect that the interaction of positive charges with dopant anions is very weak below pK_a = 1, and that another factors determine the conductivity of polypyrrole films.

Quantitative interpretations of the interaction between the doped carboxylate ions and positive charges in the polypyrrole films. The strength of the electrostatic interaction of ion pairs such as carboxylate ions and organic cations is usually controlled by charge densities of both kinds of ions, distance between them, and the dielectric constant of medium in which these ions are present [84]. The basicity of organic anions does not have marked effect in determining the strength of the interaction, being different from the case of anion-doped polypyrrole films, where it is believed that the positive charge carriers behave like Lewis acid such as protons and metal chlorides [85]. Then the positive charge concentration in the polymer chains must be controlled by the following mass action law

$$P^+ + A^- \rightleftharpoons PA \qquad (5)$$

$$K_p = \frac{[P^+][A^-]}{[PA]} \qquad (6)$$

where P^+, A^-, and PA denote a free positive charge, a free dopant anion, and a positive charge bound with a dopant anion, respectively, and K_p is the dissociation constant of PA. If it assumed that the conductivity of polypyrrole film is proportional to the concentration of free positive charges, the degree of dissociation (α) of PA should determine the

conductivity

$$\sigma = \alpha \sigma_o \quad (7)$$

where σ_o denotes the conductivity that is obtained when there is no association of positive charges with dopant anions ($\alpha = 1$). A situation giving σ_o will be seen for dopants whose conjugated acids have pK_a <1, because the highest and almost constant conductivity is obtained there independently of pK_a (see Fig. 23). As the value of σ_o, the conductivity value of CF_3COO^- - doped polypyrrole film (60 S cm^{-1}) is adopted. By using α, eq. (6) is transformed into eq. (8)

$$K_p = \frac{\alpha^2}{1 - \alpha} [P^+]_o \quad (8)$$

where $[P^+]_o$ is the sum of the concentration of positive charges with and without the association with doped anions and should be equal to the concentration of the dopant anions in the film. Since the concentration of dopant anions was almost the same for all polypyrrole films prepared in this study as described above, $K_p/[P^+]_o$ is proportional to K_p, which is denoted here as K_p'. Then eq. (9) is obtained

$$K_p' = \frac{\alpha^2}{1 - \alpha} \quad (9)$$

One can deduce α values for each dopant from eq. (7) and then K_p' is estimated. The -log K_p' values obtained in this way are plotted against pK_a values of the conjugated acids of the dopant anions, as shown in Fig.

24. Apparently a linear relationship is observed between the two, which is formulated as

$$-\log K_p = 2.56pK_a - 1.78 \qquad (10)$$

It has been shown that in reactions of a Lewis acid with several kinds of Lewis bases a linear relation establishes between equilibrium constants (K) and pK_a of protonated bases, which is formulated by pK (= -log K) = A pK_a + B, where A and B are constants [85-88]. It is suggested from the establishment of eq. (10) in anion-doped polypyrrole films that the dissociation of positive charges bound to carboxylate anions in polypyrrole

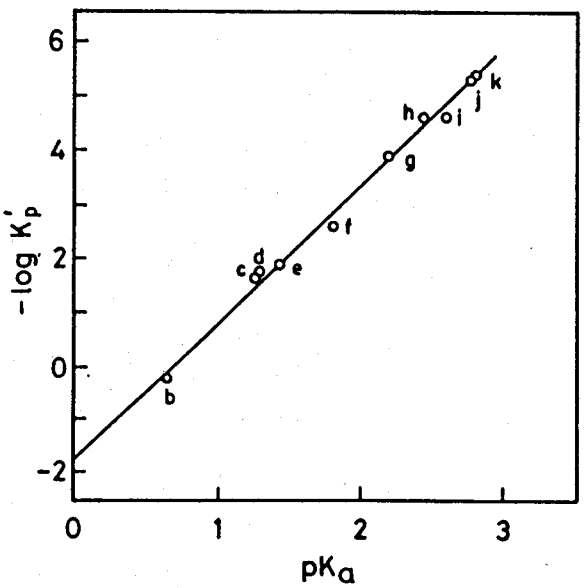

Fig. 24. The relationship between -log K_p' values for polypyrrole films estimated by using eq. (9) and pK_a values of conjugated acids of carboxylates used as dopant anions.

is primarily determined by standard Gibbs energy changes for deprotonations of the conjugated carboxylic acids.

Conductivity of polypyrrole films doped with monoanions of dicarboxylic acids in aqueous solutions. The conductivities of polypyrrole films doped with oxalic acid monoanions were determined by applying the four probe method to the films which were stripped from the electrode substrate. After immersion for one hour of the films in 0.1 M KCl aqueous solutions adjusted to various pH with use of either HCl or KOH, they were washed with acetonitrile in an ultrasonic bath for 30 min, followed by drying in vacuo for conductivity measurements. The conductivities determined are shown in Fig. 25 as a function of pH of

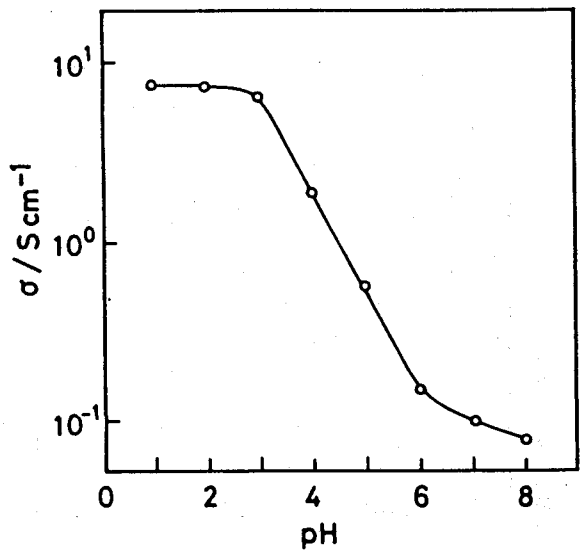

Fig. 25. Effect of pH on conductivity of polypyrrole films doped with oxalic acid monoanion. The electrolyte solutions used were 0.1 mol dm^{-3} KCl. The pH adjustment was made by adding either HCl or KOH to the KCl solution.

solutions in which the polypyrrole films were immersed. As this figure shows, the film conductivity was not varied by immersing the film in solutions of pH < 3, and was essentially the same as that of the as-grown film, while when the polypyrrole film was immersed in solutions of pH > 3, the conductivity of the film was distinctly decreased depending on pH of the solution.

To obtain information on the effect of immersion on the compositional changes of the polypyrrole film, the films immersed for one hour in KCl solutions of pHs 3 and 8 were analyzed by EPMA. In the measurements of EPMA, the polypyrrole films were subjected to the same pretreatments as those employed in the conductivity measurements which have been described above. The results are shown in Fig. 26. The spectrum of the polypyrrole

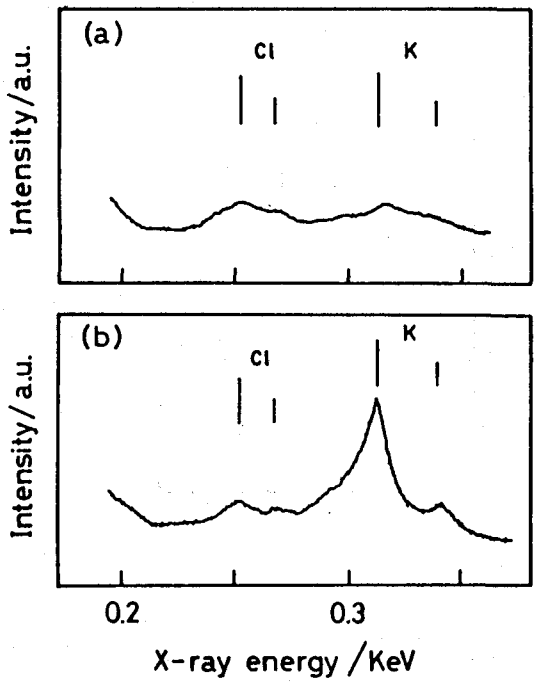

Fig. 26. EPMA spectra of polypyrrole films doped with oxalic acid monoanion after immersing in 0.1 mol dm^{-3} KCl aqueous solutions adjusted to pH = 3 (a) and 8 (b).

film immersed in the solution of pH 3 showed weak peaks assigned to chlorine and potassium which were not observed in an EPMA spectrum of the as-grown film, indicating that KCl was incorporated into the film. The incorporation of KCl must result from the incorporation of electrolyte solution into polypyrrole films. Physically adsorbed KCl must have remained in the film after washing the film with acetonitrile. The film immersed in the solution of pH 8 also showed chlorine signals whose intensity was comparable to that obtained in the film immersed in solution of pH 3. In contrast potassium signals were greatly enhanced by immersion in the solution of pH 8. The unbalancing of the signal intensities observed in this case between Cl^- and K^+ cannot be attributed to the KCl incorporation. Rather the enhancement of K^+ signals must result from its incorporation into polypyrrole films. The occurrence of such event is rationalized if it is assumed that oxalic acid monoanions as the dopant anions are dissociated into dianions, and K^+ ions are incorporated into polypyrrole films to compensate the generated negative charges. The mode of the composition changes in such cases is illustrated as shown in Fig. 27. The dissociation of oxalic acid monoanions could also be confirmed by FT-IR spectra of the films. The band at 1720 cm^{-1} which is characteristics of COOH of oxalic acid was seen at the as-grown film and the film immersed in the solution of pH 3, whereas this band disappeared if the as-grown film was immersed in the solution of pH 8. It has been reported by quartz microbalance measurements of conducting polymers such as polypyrrole and polyaniline [89-92] that electrolyte salt and/or solvent are incorporated into the polymers in the course of their redox reactions. However, such findings are not necessarily applicable to the present studies, because it is believed that no redox reactions are involved in the conductance change.

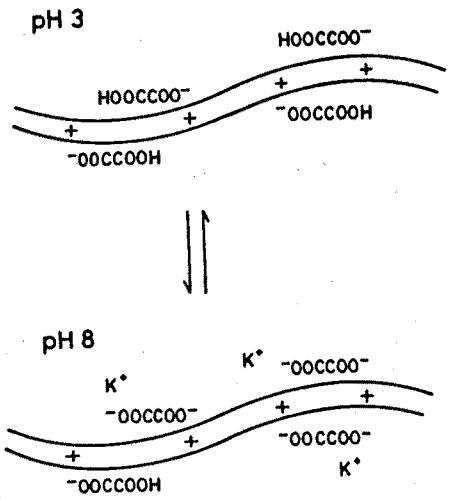

Fig. 27. Hypothetical illustration of the mode of composition change in polypyrrole film on dissociation of oxalic acid monoanion.

The observed decrease in the film conductivity with increasing pH of the solution as shown in Fig. 25 must result from a decrease in the concentration of free positive charges in the polypyrrole film caused by the enhancement of the electrostatic bindings of positive charges with newly generated dianions.

Changes in conductance of polypyrrole films doped with monoanions of dicarboxylic acids, caused by changing the pH of solutions in which polypyrrole films were immersed, were measured in-situ using the electrode assembly shown in Fig. 22. Typical results obtained for a polypyrrole film doped with oxalic acid monoanions are shown in Fig. 28. As shown in this figure, few minutes were needed to complete the conductance change. Since the change in solution pH was made by adding appropriate amounts of HCl or KOH under magnetically stirring KCl solution, the pH change must be

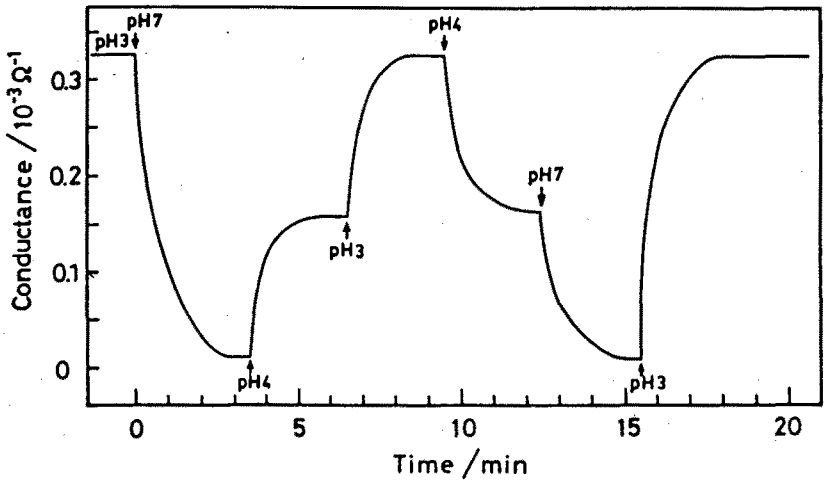

Fig. 28. Response of conductance changes of polypyrrole film caused by pH changes of solution in which the film doped with oxalic acid monoanion was immersed.

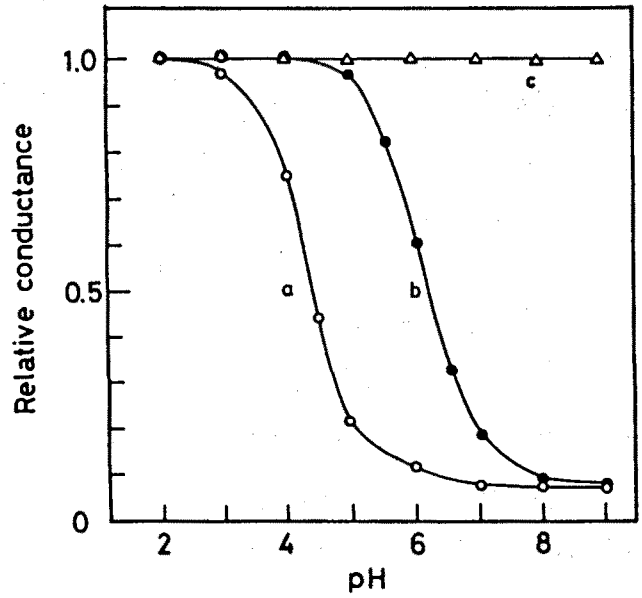

Fig. 29. Conductance of polypyrrole films doped with monoanions of oxalic acid (a), maleic acid (b), and doped with trichloroacetate anion (c) in 0.1 mol dm^{-3} aqueous solutions as a function of the pH.

completed rapidly. It is, therefore, suggested that the rate of diffusion of K^+ in the film must determine the rate of the conductance changes caused by the pH changes. It is noteworthy that the response as shown in Fig. 28 was reproducible with the repetition of changes in the pH of solution.

The conductance of polypyrrole films doped with monoanions of oxalic aid and maleic acid was measured in-situ in aqueous solutions at several pHs. In Fig. 29 steady values are given in a relative scale to that obtained in the solution at pH 2, together with results for polypyrrole films doped with CF_3COO^- for comparison. The conductance of the CF_3COO^- - doped polypyrrole film does not vary in a pH region shown in the figure, whereas those of the others decreased with increasing pH. CF_3COO^- ions do not further dissociate in pH > 2, but oxalic acid monoanions and maleic acid monoanions dissociate; pK_{a2} of the former is 4.28 and that of the latter 6.59. Evidently the pH region in which each polypyrrole film showed a large conductance change covers a pH region that includes the second stage ionization of the dopants. The conductance of the polypyrrole films decreased systematically with an increase in the degree of dissociation of the doped monoanions of dicarboxylic acids into dianions. Then the suggestions arises that pK_{a2} values of the dicarboxylic acids are not largely varied even if they are incorporated in polypyrrole films. It is concluded from results shown in Figs. 28 and 29 that pH sensitivity may be imparted to polypyrrole films by doping anions which have multiple dissociation stages.

2-3

Dependence of Conductivity of Polypyrrole Film Doped with p-Phenol Sulfonate on Solution pH

2-3-1 Introduction

In the present section, the investigation on the conductivity of polypyrrole films doped with p-phenol sulfonate as a functions of pH of solutions will be described. It will be shown that conductivity changes occur as a result of dissociation of hydroxyl groups of the dopant in the manner similar to the case of the polypyrrole film doped with monoanions of dicarboxylic acids which have been described in the previous section. The relationship between the conductivity changes and the degree of dissociation of hydroxyl groups of p-phenol sulfonate will be shown. In addition, the apparent diffusion coefficient of electrolyte cations in the polypyrrole film have been evaluated by analyzing the response of the conductivity changes caused by abrupt change in pH in the presence of several electrolyte cations.

2-3-2 Experimental

Electropolymerization of pyrrole was carried out galvanostatically in an aqueous solution containing 0.1 mol dm^{-3} pyrrole and 0.01 mol dm^{-3} p-phenol sulfonic acid under N_2 atmosphere by using a potentiostat/ galvanostat (Hokuto Denko HA-301). The current density chosen was 0.2 mA cm^{-2}, and the quantity of electricity used was 200, 500, and 800 mC cm^{-2}

with which polypyrrole films having 1.0, 2.5, and 3.8 μm thickness, respectively, were prepared.

The techniques used for in-situ measurements of the conductance changes of polypyrrole films in aqueous solutions have been described in the previous section.

2-3-3 Results and Discussion

Conductivity changes of polypyrrole film doped with p-phenol sulfonate. The conductivity of polypyrrole films was measured in solid state by the four-probe method after immersion of the films into 0.1 mol dm^{-3} KCl aqueous solutions adjusted to various pH using either HCl or KOH, followed by washing with acetonitrile and then by drying in vacuo. The obtained results are shown in Fig. 30. Almost the same and high conductivities of ca. 130 S cm^{-1} were obtained for polypyrrole films immersed in solutions of pH < 6, the values being comparable to the conductivities of polypyrrole films doped with other aromatic sulfonate derivatives as shown in the section 2-1. However, when the polypyrrole films were immersed in solutions of pH > 6, the film conductivity distinctly decreased with increasing pH of the solution. The lowest conductivity, which was obtained by immersion in a solution of pH 12, was 1.1 S cm^{-1}. Similar conductivity variations with solution pH have already been shown in the section 2-2 for polypyrrole films doped with monoanions of dicarboxylic acids such as oxalic acid and maleic acid. In the case of using p-phenol sulfonate as the dopant, the decrease in the film conductivity must result from dissociation of hydroxyl groups of the dopant because remarkable

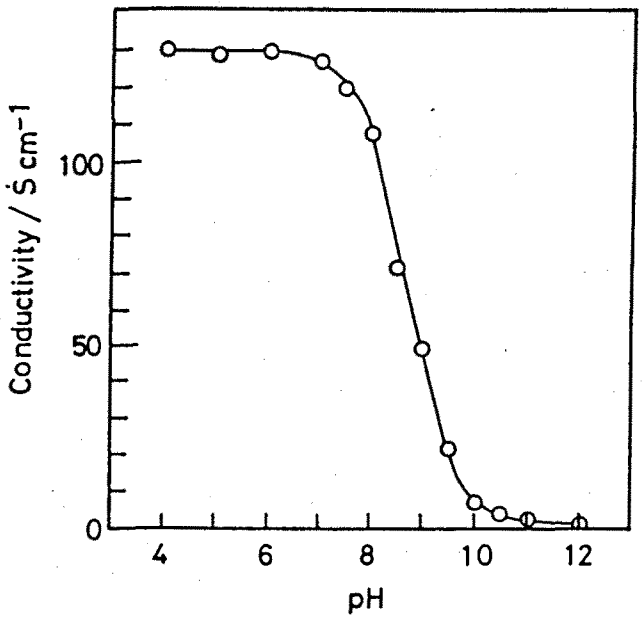

Fig. 30. The conductivity of polypyrrole films doped with p-phenol sulfonate as a function of the pH of solutions in which the films were immersed before the conductivity measurements.

conductivity changes occurred at pH where the pK_a value (8.7) of the hydroxyl group of p-phenol sulfonate predicts its dissociation.

This assumption was confirmed by qualitative analyses of the composition of the films by EPMA after immersion in solutions of pH 4, 8, and 11. As shown in Fig. 31, potassium signals which were not seen in the spectrum of the film immersed in the solution at pH 4 appeared at pH 8 and 11, and its intensity was greater at pH 11 than at pH 8, indicating that K^+ ions in solution were incorporated into the film to compensate negative charges generated by ionization of hydroxyl groups of the dopant, as schematically illustrated in Fig. 32. Since the produced phenoxide ions have relatively large basicity, they should bind positive charge carriers of polypyrrole, resulting in a decrease in the concentration of free positive charge carriers in the polypyrrole which contribute to the electrical conduction.

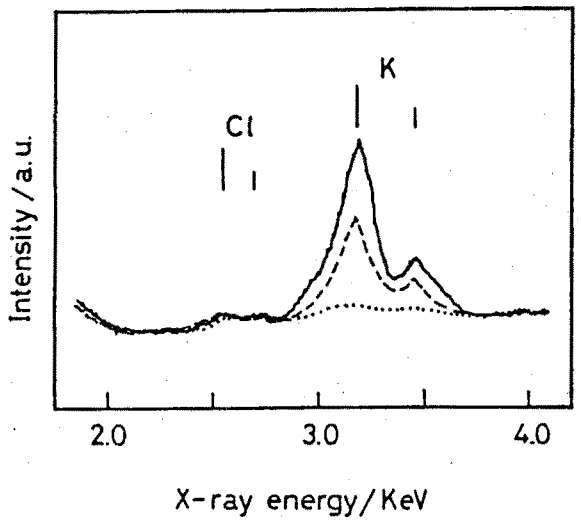

Fig. 31. EPMA spectra of polypyrrole films doped with p-phenol sulfonate, taken after immersing in 0.1 mol dm^{-3} KCl solutions adjusted to pH 4 (·····), 8 (---), and 11 (——) with either HCl or KOH.

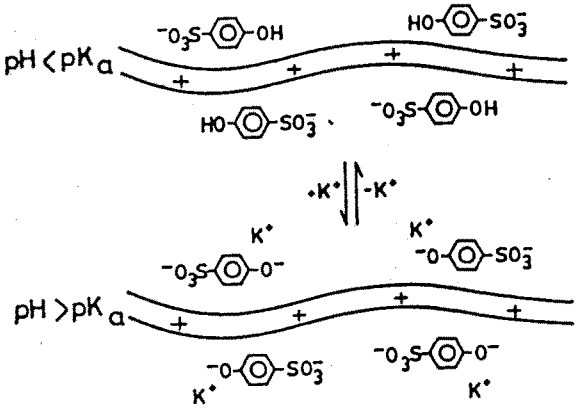

Fig. 32. Schematic illustration of compositional change in polypyrrole film upon dissociation of hydroxyl groups of doped p-phenol sulfonate.

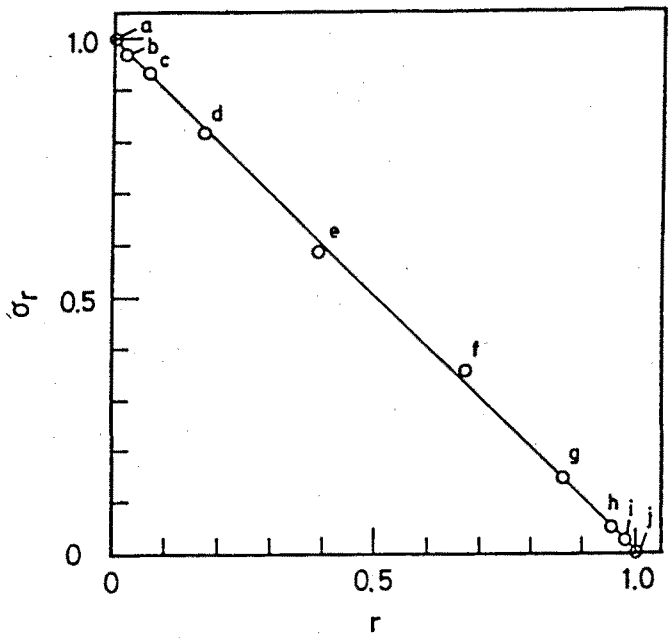

Fig. 33. The relationship between relative ratio of conductivity changes (σ_r) of polypyrrole films and the degree of dissociation of p-phenol sulfonate doped in the films. The pH of aqueous solutions in which the polypyrrole films were immersed were 6 (a), 7 (b), 7.5 (c), 8 (d), 8.5 (e), 9 (f), 9.5 (g), 10 (h), 10.5 (I), and 11 (j).

As described in the previous section, positive charge carriers of polypyrrole behave like Lewis acid such as protons and bind dopant anions, the degree depending on its basicity. The mode of the binding in this case is quite different from ion pair formations due to electrostatic interaction whose strength is not largely influenced by the basicity of the anions. This is the reason why the produced phenoxide ions make bindings with the positive charge carriers and not with the K^+ ions incorporated in the film.

Figure 33 shows the relative ratio of the conductivity changes as a function of the degree of the dissociation of the hydroxyl groups of the dopant. The relative ratio of the conductivity changes (σ_r) is defined by

eq. (11)

$$\sigma_r = \frac{\sigma - \sigma_{min}}{\sigma_{max} - \sigma_{min}} \qquad (11)$$

where σ is the conductivity at arbitrary pH, and σ_{max} and σ_{min} are the maximum conductivity (130 S cm^{-1}) which was observed at pH < 6 and the minimum conductivity (1.1 S cm^{-1}) which was observed at pH > 12. On the other hand, the degree of the dissociation (r) is given by

$$r = \frac{K_a}{[H^+] + K_a} \qquad (12)$$

According to Fig. 4, the conductivity of polypyrrole films decreases in proportion to an increase in the degree of dissociation of the hydroxyl groups of the dopant, and this relation can be formulated as

$$r = 1 - \sigma_r \qquad (13)$$

or

$$r = \frac{\sigma_{max} - \sigma}{\sigma_{max} - \sigma_{min}} \qquad (14)$$

When the conductance of a polypyrrole film doped with p-phenol sulfonate was measured in-situ in an aqueous solution by changing the solution pH from 3 to 12 at 0.5 intervals, the conductance decreased in a manner closely similar to the conductivity changes as shown in Fig. 30.

Since the film conductance obtained in this manner is directly proportional to the film conductivity because of invariance of the film geometry, it can be correlated to r in eq. (14) by replacing σ_{max}, σ_{min}, and σ with the maximum and minimum conductance, and conductance obtained at arbitrary pH, respectively. Accordingly, it is concluded that the conductivity or conductance of the polypyrrole films is entirely controlled by the degree of dissociation of p-phenol sulfonate used as the dopant.

Estimation of apparent diffusion constant of cations in polypyrrole films. Conductance changing behaviors of a polypyrrole film having 1.0 μm thickness are given in Fig. 34. Such changes in the film conductance occurred reversibly, but few minutes were needed to complete the conductance changes. Considering that the composition of polypyrrole film changes with the dissociation of the dopant as schematically shown in Fig. 32, the rate of the conductance changes must be determined by the rate of diffusion of electrolyte cations in the film. Truly, the rate of the conductance change was influenced by the kind of electrolyte cations as shown in Fig. 35. The results given in this figure were obtained by using electrolyte solutions prepared by mixing appropriate amounts of 0.1 mol dm^{-3} HCl and 0.1 mol dm^{-3} hydroxide of a variety of cations. The sudden pH change of the solutions was carried out by addition of the 0.1 mol dm^{-3} hydroxides. It is suggested from the results in this figure that the smaller the ion radius of the cations, the greater the rate of the conductance decrease. Then the diffusion rate of electrolyte cations seems to control the rate of the conductance changes observed.

To confirm the idea, the apparent diffusion coefficients of electrolyte cations were evaluated using eq. (15), which is applicable to diffusion

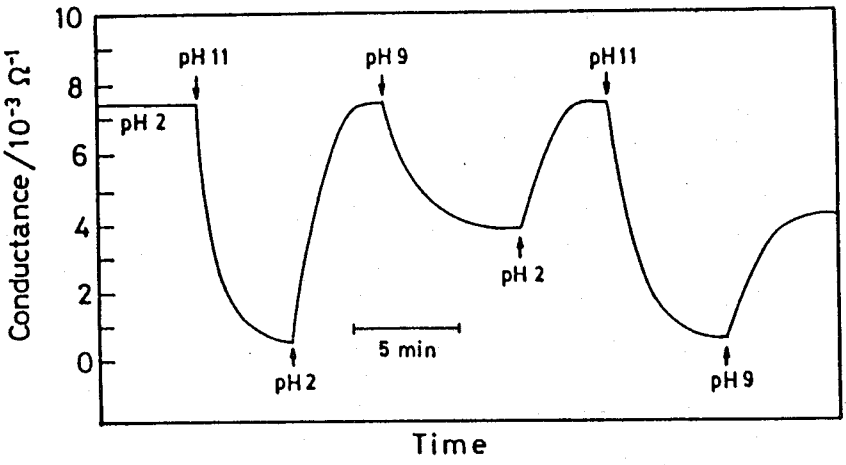

Fig. 34. Conductance changing behaviors of a polypyrrole film of 1.0 μm thickness caused by pH changes of solution in which the film was immersed.

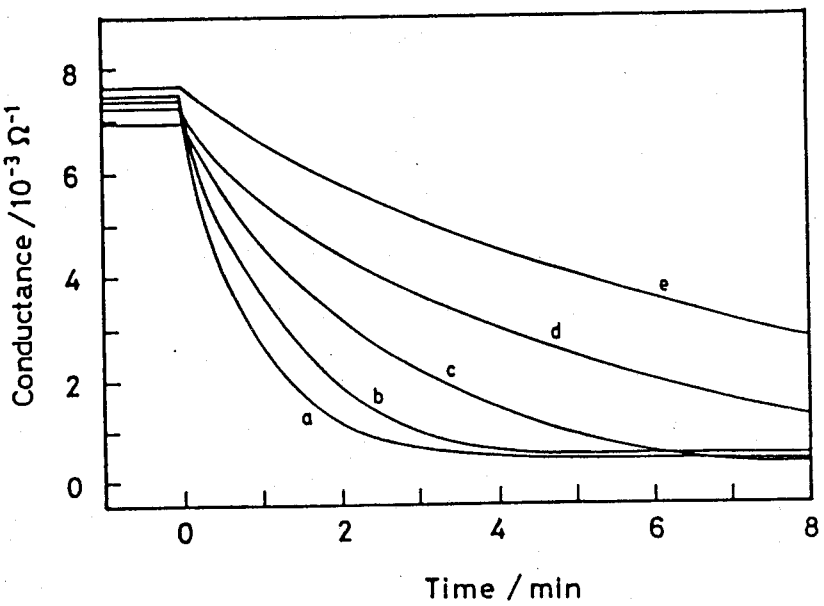

Fig. 35. Decrease in the conductance of polypyrrole films doped with p-phenol sulfonate of 1.0 μm thickness caused by sudden changes in pH from 4 to 12. The cations in solutions were Li^+ (a), Na^+ (b), K^+ (c), tetramethylammonium cation (TMA^+) (d), and tetrabuthylammonium cation (TBA^+) (e).

profiles which are governed by a semiinfinite planer diffusion model [93,94].

$$\frac{C}{C_s} = \frac{4}{L} \frac{D_{app}^{1/2}\ t^{1/2}}{\pi^{1/2}} \qquad (15)$$

In this equation, C and C_s respectively denote the concentration of a cation incorporated in the film and its saturated concentration, and D_{app}, L, and t are the apparent diffusion coefficient of the cation, thickness of the film, and the time elapsed after the sudden pH changes, respectively. Since the C/C_s must be equal to the degree of dissociation of p-phenol sulfonate (r), the C/C_s values in the polypyrrole films at arbitrary times was deduced by applying eq. (14) to Fig. 35. The obtained C/C_s values were plotted against $t^{1/2}$, as shown in Fig. 36. Table 9 gives values of D_{app} for the cations used in the present study, which were estimated using eq. (15) from the slopes of the linear relations shown in Fig. 36. Also given in this Table are the thickness of polypyrrole films determined under dry state which were used in the determination of D_{app} and the ion radius of cations. The D_{app} values obtained here seem to be a little smaller than those obtained in acetonitrile solutions for incorporation of electrolyte anions into polypyrrole films ($1 - 6 \times 10^{-10}$ cm^2 s^{-1}) [95]. Since polypyrrole films must swell at least a little in aqueous solutions, some errors must be contained in the D_{app} values obtained. Nevertheless, if it is assumed that the degree of the swelling is not greatly different among the electrolyte cations used, the results given in Table 9 indicate that the values of D_{app} decreases with an increase in the ion radius of cations. Similar things were noticed for the incorporation of electrolyte anions into polypyrrole films which occurs in the course of oxidation of the films

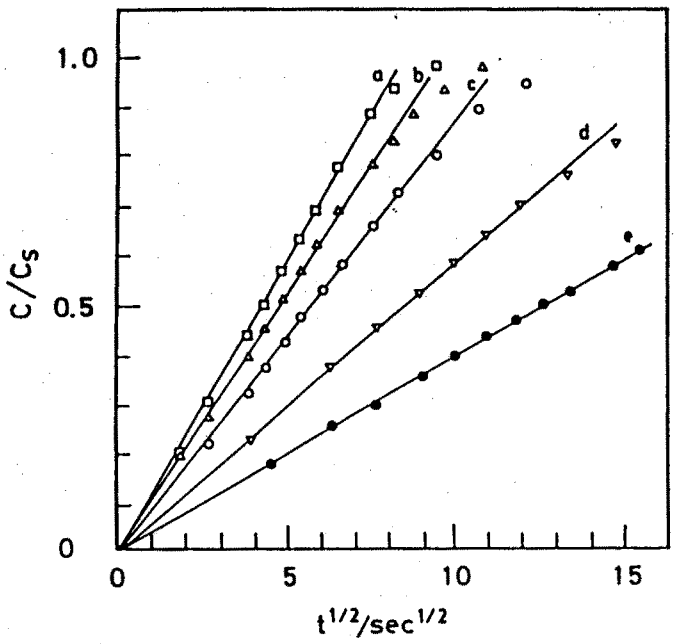

Fig. 36. Plots of C/C_s of cations incorporated in polypyrrole films as a function of square root of the time elapsed after the pH change. The cations in solutions were Li^+ (a), Na^+ (b), K^+ (c), tetramethylammonium cation (TMA^+) (d), and tetrabuthylammonium cation (TBA^+) (e).

Table 9. Apparent diffusion coefficients of cations in polypyrrole films doped with p-phenol sulfonate and thickness of the films measured in dry states

cation	ion radius/Å	$D_{app}/cm^{-2}\ s^{-1}$	film thickness/nm
Li^+	0.72	1.3×10^{-10}	1.0
Na^+	1.13	1.1×10^{-10}	1.1
K^+	1.65	5.5×10^{-11}	1.0
TMA^+	3.47	2.4×10^{-11}	1.0
TBA^+	4.52	1.3×10^{-11}	1.1
K^+	1.65	5.5×10^{-11}	2.5
K^+	1.65	5.4×10^{-11}	3.8

[96]; anions having the larger ion radius show the lower tendencies for the incorporation. An interesting finding shown in Table 9 is that the D_{app} values is determined by the size of unhydrated ions. If one uses the radius of hydrated ions, its size is in order of $TBA^+ > Li^+ > TMA^+ > Na^+ > K^+$, and there seems to be no definite correlation between these radius and the D_{app} values obtained.

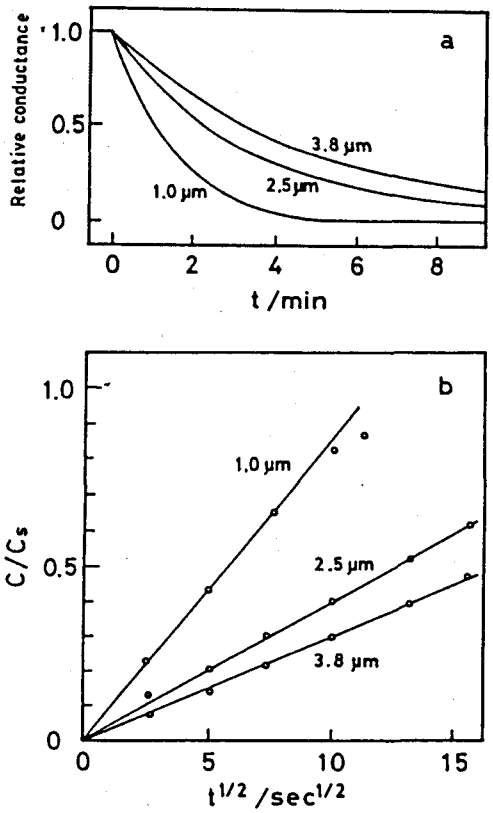

Fig. 37. Decrease in the conductance of polypyrrole films of 1.0, 2.5, and 3.8 μm thickness with changing pH of 0.1 mol dm^{-3} KCl from 4 to 12 (a) and the relationship between C/C_s and $t^{1/2}$ (b).

The dependence of the conductance changing behaviors on the film thickness of polypyrrole was investigated using K^+ as the cation for the films of 1.0, 2.5, and 3.8 μm thickness. As shown in Fig. 37 (a), the rate of decrease in the conductance became low with increasing the film thickness, but the value of D_{app} of K^+ ions, which were estimated from plots of C/C_S vs. $t^{1/2}$ shown in Fig. 37 (b), were found to be almost the same as the values shown in Table 9. These results confirm again that the conductance measured here is related not to the surface but to the bulk of polypyrrole films.

Chapter 3

Electrochemical Properties of electrodes coated with polymers containing redox dyes

3-1

Dimerization kinetics of methylene blue incorporated in Nafion Film

3-1-1 Introduction

Electrodes coated with polyelectrolytes, such as polyvinylpyridine [35,37,97-100] and Nafion perfluorosulfonic acid [39,101-104], are useful to confine electrostatically electroactive species to the electrode surfaces. The polyelectrolyte-coated electrodes have different features at least in the following two points as compared with naked electrodes. One is that electron mediation must take place in charge transfer processes between electroactive species incorporated in a polyelectrolyte layer. The other is that the concentration of electroactive species in the polyelectrolyte layer must be much higher than the concentration ordinary chosen in electrolyte solutions. The high concentration would result in different situations in the interaction between reactants, between reactants and products, and/or between products. The former subject of electron mediation have been intensively studied [36,105-111] but the latter subject has been little studied. To my knowledge only two reports have been published in which ligand substitution reactions of $Ru(NH_3)_5(H_2O)^{2+}$ incorporated in Nafion with pyridine derivatives were analyzed electrochemically [41,112]. These investigations have clarified that the

rate constants for the substitution of $Ru(NH_3)_5(H_2O)^{2+}$ with neutral and cationic pyridine derivatives obtained in Nafion are higher than those obtained in aqueous solutions by the reason that the pyridine species are concentrated in Nafion, but the substitution with anionic pyridine derivatives are depressed by electrostatic repulsion between the pyridine species and sulfonate groups of Nafion.

In this section, the redox reaction of methylene blue incorporated in Nafion film will be described. The redox reaction of methylene blue/leuco methylene blue has been studied fairly intensively in aqueous solutions [113-116], and the contribution of dimerized methylene blue to the redox reaction has also been clarified [115,116]. The main purpose of the present study is to investigate how greatly the redox reaction behaviors involving the dimerized methylene blue are affected by the presence of Nafion matrices. For this purpose, kinetic studies on the dimerization of the methylene blue have been carried out using in-situ spectroelectrochemical techniques. It will be shown that methylene blue is less likely to be dimerized in Nafion as compared with that in aqueous solution.

3-1-2 Experimental

Aldrich Nafion 117 (equivalent weight 1100, 5 wt% dissolved in a mixed solution of alcohol and water (9:1)) was applied onto a Pt electrode substrate, followed by allowing the solvent to evaporate in air. The amount of the Nafion solution applied to the substrate was 2.0 μl cm^{-2}. The thickness of the Nafion layer prepared in this manner was 0.50 μm. The incorporation of methylene blue (MB) in the Nafion layer was performed by immersing the Nafion-coated Pt electrodes into an aqueous solution

containing 1 mM MB.

3-1-3 Results and discussion

Cyclic voltammetry of methylene blue incorporated in Nafion. Methylene blue (MB) shows redox reactions in acidic and neutral solutions as shown in Scheme 1 [113,114,116]. It has positive charge and exhibits intense blue color which disappeared upon its reduction. When the Nafion-coated Pt electrode (Nafion/Pt) was immersed in an aqueous solution containing 1 mM chloride salt of methylene blue for a few minuets, the Nafion layer became blue, indicating that methylene blue was easily bound in the Nafion layer by electrostatic attraction with sulfonate groups of the Nafion. After immersion of the Nafion/Pt in the methylene blue solution for 30 min, followed by washing with distilled water, cyclic voltammetry of the electrode was taken in 0.5 M H_2SO_4. As shown in Fig. 38 (a), a couple of well-defined redox waves appeared, which were very stable to continued cyclic potential scans for several hours. The methylene blue

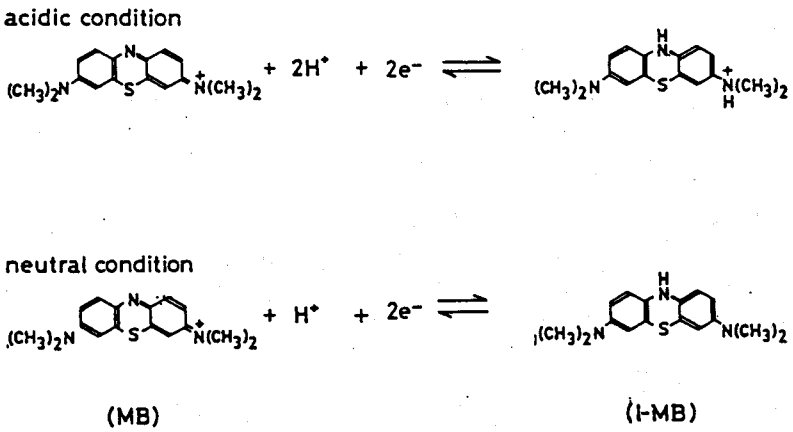

Scheme 1

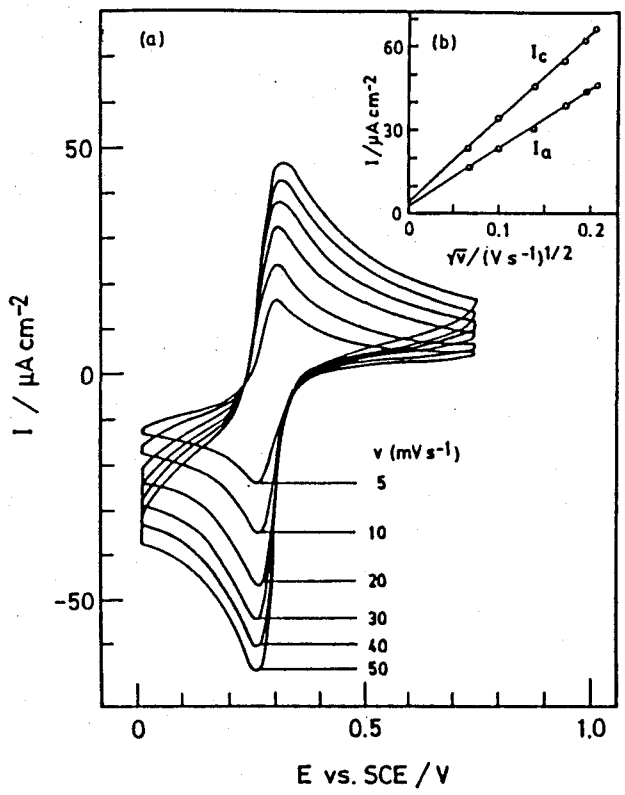

Fig. 38. Cyclic voltammograms of Nafion coated Pt electrode taken in 0.5 M H_2SO_4 at various potential scan rates (v) after being immersed in 1.0 x 10^{-3} M MB solution for 30 min (a), and plots of anodic (I_a) and cathodic (I_c) peak currents of the cyclic voltammograms against square root of the scan rates ($v^{1/2}$) (b).

was stably maintained in Nafion even when methylene blue-incorporated Nafion/Pt was immersed in 0.5 M Na_2SO_4, but if cyclic voltammetry of the electrode were carried out in the Na_2SO_4 solution, the peak currents decreased gradually with potential sweep cyclings and simultaneously the electrolyte solution was colored in light blue indicating the dissolution of methylene blue from the Nafion layer. This behavior seems to be related to that leuco methylene blue (l-MB) produced under neutral solution conditions does not have any positive charges as shown in scheme 1, resulting in the loss of interaction with sulfonate groups of the Nafion.

Figure 38 (b) shows plots of peak currents of cyclic voltammograms taken in 0.5 M H_2SO_4 against the square root of the potential scan rate. Since good linearities are seen between the two for both anodic and cathodic waves, it is thought that the redox reaction proceeds under diffusion controlled conditions when the peak currents appear. However, it is seen that the slope of the plots are different between the anodic and cathodic currents. Even if the diffusion constant of methylene blue is different from that of leuco methylene blue, the slope should be equal to each other between the oxidation and reduction processes. The most likely source for bringing about the different slopes may then be the occurrence of dimerization of methylene blue in the oxidation process. As will be shown below, the rate of dimerization is different from that of the release of the dimerization, so the contribution of dimerized methylene blue to the electron self-exchange reaction under diffusion controlled condition may be different, resulting in the different slopes as observed. The blue color of the Nafion layer disappeared completely when the electrode was maintained at 0 V vs. SCE for few minutes and recoloring occurred with almost the same time at 0.5 V vs. SCE, suggesting that all the methylene blue species incorporated in the Nafion layer were electrochemically active.

Dimerization of methylene blue incorporated in Nafion. Figure 39 shows absorption spectra of Nafion-coated ITO electrodes (Nafion/ITO) which were previously immersed in the methylene blue solution for 15 sec, 3 min, 10 min, and 30 min followed by washing with distilled water and by drying in vacuo. With the immersion for 15 sec, only one absorption peak appeared at 660 nm which is characteristic of monomeric methylene blue [117-120] but with increasing the immersion time, another absorption band

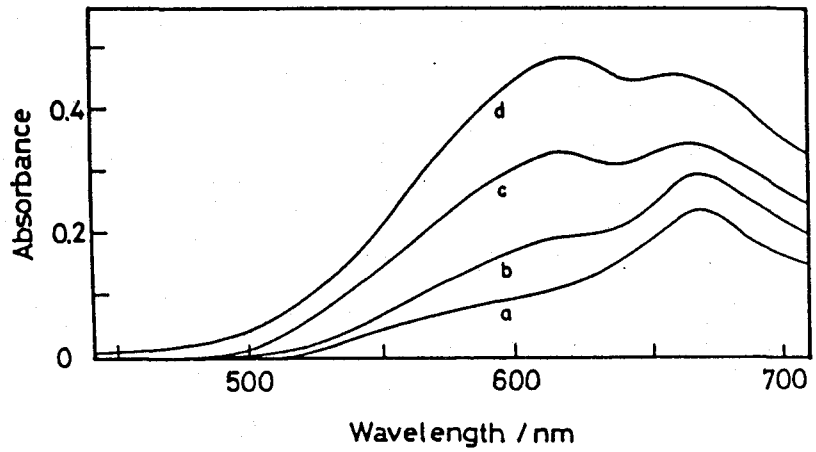

Fig. 39. Absorption spectra of MB incorporated in Nafion layer that was dried in vacuo. The MB incorporation was performed by immersing Nafion/ITO in 1.0 x 10^{-3} M MB solution for 15 sec (a), 3 min (b), 10 min (c), and 30 min (d).

which appeared at 610 nm became pronounced. This absorption is due to dimeric methylene blue which is denoted here as $(MB)_2$. It is, therefore, suggested from the observed absorption spectra that the dimerization of methylene blue takes place in the Nafion layer when the incorporation of methylene blue progresses.

The absorption spectra of MB-incorporated Nafion/ITO were measured under polarization at various potentials in 0.5 M H_2SO_4. The methylene blue incorporation was carried out by immersing in the methylene blue solution for 30 min. As shown in Fig. 40, the spectrum obtained at 0 V vs. SCE showed no appreciable absorption in a visible region, but with anodic shifts of the electrode potential from 0.1 V to 0.28 V vs. SCE, absorption due to methylene blue became steadily strong. With further increase in anodic potentials, absorption due to $(MB)_2$ was superposed in the absorption spectra, and its absorption intensity exceeded that of methylene blue at

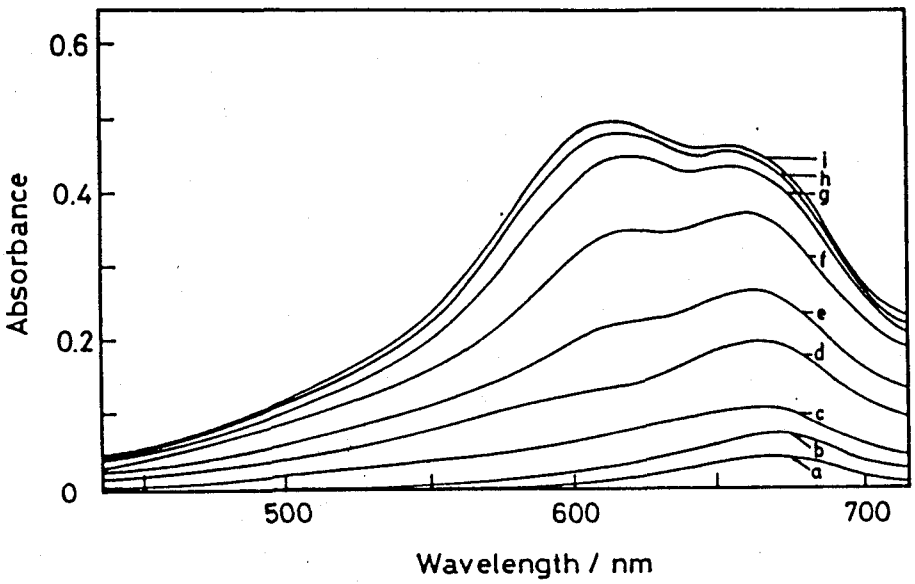

Fig. 40. Absorption spectra of MB-incorporated Nafion/ITO electrode polarized at 0.10 (a), 0.26 (b), 0.28 (c), 0.30 (d), 0.32 (e), 0.34 (f), 0.36 (g), 0.38 (h), and 0.5 (i) V vs. SCE in 0.5 M H_2SO_4. The MB incorporation was performed by immersing Nafion/ITO in 1.0×10^{-3} M MB solution for 30 min.

potentials positive of 0.36 V vs. SCE. It is recognized from this behavior that the only oxidized form of methylene blue is dimerized in the Nafion as in water [116].

By considering that the absorption bands are composed of those of methylene blue and $(MB)_2$ which have the absorption maximum at 660 and 610 nm, respectively, the absorbance at 660 nm and 610 nm is given by [120]

$$A^{660} = (\varepsilon_m^{660} C_m + \varepsilon_d^{660} C_d) \times D \qquad (16)$$

$$A^{610} = (\varepsilon_m^{610} C_m + \varepsilon_d^{610} C_d) \times D \qquad (17)$$

where D is the thickness of the Nafion layer, C_m, ε_m^{660}, and ε_m^{610} are the

concentration and the molar extinction coefficient at 660 and 610 nm of methylene blue, respectively, and C_d, ε_d^{660}, and ε_d^{610} are those of $(MB)_2$. Using eqs. (16) and (17), C_m and C_d are given by

$$C_m = \frac{\varepsilon_d^{660} A^{610} - \varepsilon_d^{610} A^{660}}{\varepsilon_m^{610} \varepsilon_d^{660} - \varepsilon_m^{660} \varepsilon_d^{610}} \times \frac{1}{D} \qquad (18)$$

$$C_d = \frac{\varepsilon_m^{610} A^{660} - \varepsilon_m^{660} A^{610}}{\varepsilon_m^{610} \varepsilon_d^{660} - \varepsilon_m^{660} \varepsilon_d^{610}} \times \frac{1}{D} \qquad (19)$$

In the case of methylene blue dissolved in water, ε_m^{660}, ε_d^{660}, ε_m^{610}, and ε_d^{610} are 7.18×10^4, 1.54×10^3, 3.88×10^4, and 9.06×10^4 M^{-1} cm^{-1}, respectively [120]. The total concentration of methylene blue ($C_{all} = C_m + 2C_d$) incorporated in the Nafion layer was estimated from the charge consumed in reduction of methylene blue in the Nafion by application of a potential step from 0.5 V to 0 V vs. SCE in 0.5 M H_2SO_4 together with the volume of the Nafion layer (2 cm^2 x 0.50 μm). On the other hand, C_m and C_d were estimated by measuring the A^{660} and A^{610} of methylene blue in the Nafion at 0.5 V vs. SCE and then by using eqs. (3) and (4) together with the molar extinction coefficients of methylene blue dissolved in water. In these estimations, the thickness of the Nafion layer determined by observations with the SEM was employed. Since the Nafion layer must be swollen in electrolyte solutions, the thickness should be determined under wet conditions but no effective means was available for this to do. However, judging from the following results, the incorrectness of the volume estimation of the Nafion layer if any must not bring about any serious errors in the analysis of the dimerization of methylene blue. When

absorption spectra of Nafion-coated electrodes were measured in 0.5 M H_2SO_4 aqueous solution after the incorporation of methylene blue, the obtained spectra were almost the same as those shown in Fig. 39 which was obtained under a dry condition, suggesting that the ratio of the concentration of methylene blue to that of $(MB)_2$ in the Nafion layer was eventually the same between the dry and wet conditions. This result seems to suggest that upon immersion in 0.5 M H_2SO_4, the thickness of the Nafion layer was not so largely increased as to cause any appreciable change in absorption spectrum. If the Nafion layer was swollen to a large extent to result in a decrease in the total concentrations of methylene blue and $(MB)_2$ in the Nafion layer, the concentration of methylene blue relative to that of $(MB)_2$ must be changed, as judged from the concentration dependence of the dimerization constant which will be described as follows (Table 10), and then the absorption spectra should have been changed.

It was found that the C_{all} determined electrochemically was almost equal to the sum of C_m and $2C_d$ determined in this way. For example, in the case of Nafion/Pt immersed in the methylene blue solution for 30 min, the quantity of electricity for the reduction of methylene blue was 4.44 mC which gave C_{all} of 0.230 M, whereas A^{660} and A^{610} of the electrode obtained at 0.5 V vs. SCE were 0.450 and 0.491, from which C_m, C_d, and C_{all} were deduced to be 0.124, 0.053, and 0.230 M, respectively. It was then thought that the molar extinction coefficients of methylene blue and $(MB)_2$ determined in water were useful for methylene blue incorporated in Nafion.

The C_m and C_d in the Nafion layer at various potentials were determined based on the spectra shown in Fig. 40, and the determined C_d is plotted as a function of C_m^2 as shown in Fig. 41. A linear relationship is found, indicating that the ratio of C_d to C_m^2 is not appreciably influenced

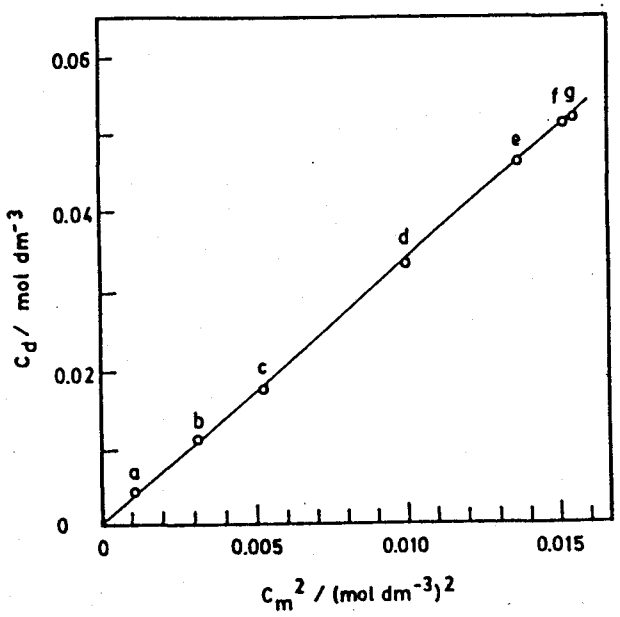

Fig. 41. The relationship between C_d and C_m^2 of MB-incorporated Nafion/ITO electrode polarized at 0.10 (a), 0.26 (b), 0.28 (c), 0.30 (d), 0.32 (e), 0.34 (f), and 0.36 (g) V vs. SCE in 0.5 M H_2SO_4. The MB incorporation was performed in the same manner as described in the captions of Fig. 40.

by the electrode potential. It is well-known that the dimerization constant of methylene blue (K_{eq}) can be determined from the slope of the plots, and then K_{eq} = 3.37 M^{-1} was determined in this case. The same procedures were applied to other concentrations of methylene blue in Nafion which was prepared by changing the immersion time of the Nafion/ITO in the methylene blue solution, and K_{eq} values as listed in Table 10 were determined. The determined K_{eq} values were very small as compared with that determined for methylene blue in aqueous solutions (K_{eq} = 4.67 x 10^3 M^{-1} at 20℃) [120]. The observed differences of K_{eq} values of methylene blue by more than three orders of magnitudes between in the Nafion and aqueous solutions cannot be resulted from the use of incorrect value of

Table. 10 The dimerization constant, the rate constant for dimerization of methylene blue, and the rate constant for release of dimerization in Nafion

immersion time[a] /min	C_{all}[b] /mol dm^{-3}	K_{eq} /mol^{-1} dm^3	k_f /mol^{-1} dm^3 s^{-1}	k_r[c] /s^{-1}
0.25	0.0637	0.661	0.91	1.4
3	0.0966	1.05	1.2	1.1
10	0.150	2.70	1.2	0.44
30	0.230	3.37	1.3	0.39

a) Immersion time of Nafion/ITO in 1.0 x 10^{-3} mol dm^{-3} MB solution.
b) Concentration of MB in Nafion layer determined from the charge consumed in its reduction.
c) $k_r = K_{eq}/k_f$.

the volume of the Nafion layer in the estimation of the concentration of methylene blue and $(MB)_2$, because if the K_{eq} value of methylene blue obtained in aqueous solutions were assumed to be applicable to the Nafion coated electrode, the volume of the Nafion layer should be increased by more than 1000 times by bringing in contact with aqueous solution. It is then concluded that the dimerization of methylene blue is less likely to occur in Nafion due probably to strong electrostatic binding of methylene blue to sulfonate groups of Nafion. The dimerization constant determined in aqueous solution is eventually constant independent of the concentration of methylene blue, but this is not so in Nafion, as Table 10 shows. The dimerization constant becomes small with a decrease in the methylene blue concentration in Nafion. This result seems reasonable if one considers that the electrostatic binding of sulfonate groups of Nafion becomes strong when the number of the incorporated cationic species is decreased.

The estimation of rate constants for dimerization of methylene blue in Nafion. The absorbance at 660 nm and 610 nm of MB-incorporated

Nafion/ITO electrode were monitored under application of a potential pulse between 0 and 0.5 V vs. SCE in 0.5 M H_2SO_4. Figures 42 (a) and (b) show the results obtained by changing the electrode potential from 0 to 0.5 V and from 0.5 to 0 V vs. SCE, respectively, for the Nafion/ITO which was previously immersed in the methylene blue solution for 30 min. In both cases, C_m change more rapidly than C_d. Probably the reaction occurred stepwisely as shown in eq. (20)

$$2(1\text{-MB}) \underset{-4e^-}{\overset{+4e^-}{\rightleftharpoons}} 2MB \underset{k_r}{\overset{k_f}{\rightleftharpoons}} (MB)_2 \qquad (20)$$

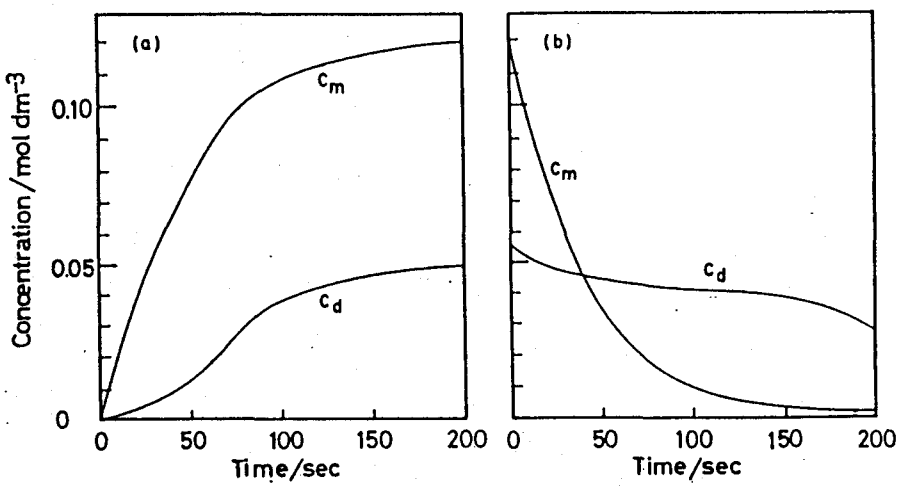

Fig. 42. Changes of C_m and C_d of MB-incorporated Nafion/ITO electrode with time of potential imposition from 0 to 0.5 V vs. SCE (a) and from 0.5 to 0 V vs. SCE (b) in 0.5 M H_2SO_4. The MB incorporation was performed in the same manner as described in the captions of Fig. 40.

where k_f is the rate constant for the dimerization reaction of methylene blue, and k_r is that for the release of the dimerization. The rate of dimerization (V_d) in the course of oxidation of l-MB is then given by

$$V_d = k_f C_m^2 - \frac{k_f}{K_{eq}} C_d \qquad (21)$$

since $K_{eq} = k_f/k_r$.

The validity of eq. (21) was confirmed by comparing experimentally determined V_d with the calculated one. The experimental determination of V_d was performed by determing the change in C_d which was caused by further oxidation for 0.2 s at an arbitrary time of the potential imposition. The calculated V_d was obtained by substituting into eq. (21) C_m and C_d which were determined from A^{660} and A^{610} at the time of potential imposition using eqs. (18) and (19) and by applying variable k_f values. The obtained results are shown in Fig. 43 for the case of the methylene blue incorporation prepared by immersing Nafion/ITO in 1 x 10^{-3} M methylene blue for 30 min. As this figure shows, experimentally determined V_d against time shows fairly good agreement with the calculated one if one uses k_f = 1.3 M^{-1} s^{-1} for the potential imposition time greater than 30 s. Thus it can be concluded that the formation of methylene blue and $(MB)_2$ by the oxidation of l-MB stepwisely progresses with k_f = 1.3 M^{-1} s^{-1}. Judging from the determined K_{eq} value, k_r =0.39 s^{-1} must be valid in that case. The k_f and k_r for other concentrations of methylene blue were determined in the same manner, and the results are also listed in Table 10. The obtained values of k_f and k_r are again apparently very low, as compared with those obtained for methylene blue dissolved in aqueous solution (k_f = 5.1 x 10^8

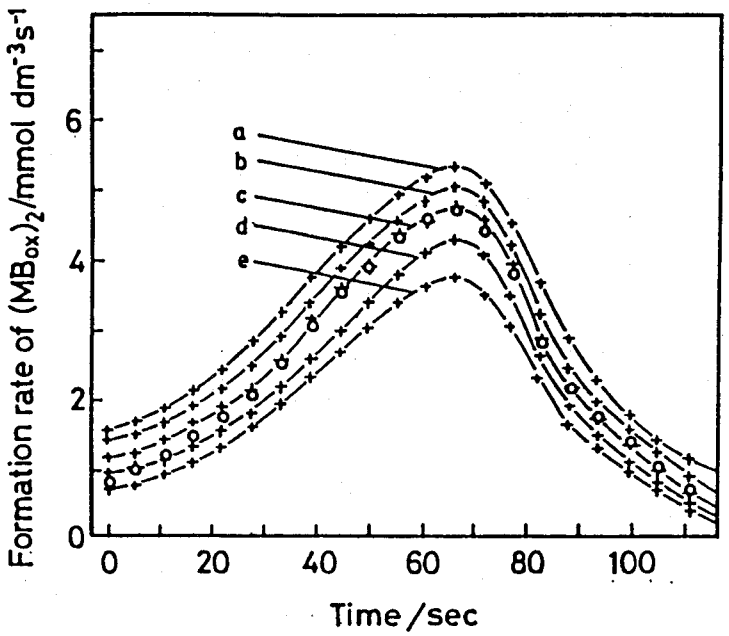

Fig. 43. The rate of dimerization of MB with time of potential imposition of 0.5 V after being reduced at 0 V vs. SCE (O) and that estimated by using eq. (6) (-+-) with k_f = 1.5 (a), 1.4 (b), 1.3 (c), 1.2 (d) , and 1.1 (e) M^{-1} s^{-1}. The MB incorporation was performed in the same manner as described in the captions of Fig. 40.

M^{-1} s^{-1} and k_r = 1.33 x 10^3 s^{-1} at 20℃ C) [120], suggesting again the significant effect of strong electrostatic interaction between methylene blue and the sulfonate groups of the Nafion on the rate of redox reactions of methylene blue.

3-2

Preparation of Polyaniline Films Doped with Methylene Blue-bound Nafion and Electrochromic Properties of the Resulting Films

3-2-1 Introduction

Polyaniline (PAn) films prepared by electrochemical polymerization of aniline exhibit stable redox reactions [17-22], and several applications such as to electrochromic [27-29] and electronic [121,122] devices have been attempted using the redox properties. Recently, modification of electrocatalytic activities of polyaniline by incorporation of cobalt phthalocyanine tetrasulfonates [33] and heteropolyanions [34] has been reported. These functionalizations have successfully been achieved by utilizing the property that electrolyte anions are incorporated into polyaniline films during the course of polymerizations of aniline to compensate positive charges induced in the polymer. However, the procedure for the incorporation of cationic functional molecules into polyaniline films has not yet been devised.

In this section, the preparation of polyaniline films incorporated with cationic methylene blue will be described. The strategy was to polymerize aniline in the presence of methylene blue and Nafion with the latter being in excess. Under such conditions, a fraction of sulfonate groups of Nafion are electrostatically bound with methylene blue, and the rest is free and can work as the charge compensator of positive charges induced in polyaniline. The electrochemical and electrochromic properties of the resulting films will also be described.

3-2-2 Experimental

The anodic polymerization to give polyaniline films doped with methylene blue-bound Nafion, which will be denoted here as PAn/MB-Nafion, was carried out galvanostatically in an one-compartment cell with a Pt counter electrode under N_2 atmosphere. The current density chosen was 40 μA cm^{-2}, and the quantity of electricity used was 12 mC cm^{-2} for electrochemical measurements and 36 mC cm^{-2} for other measurements. The preparation of Nafion-coated Pt electrode containing methylene blue in the Nafion layer (MB-Nafion) was described in the previous section. The incorporation of methylene blue into the Nafion layer in that case was performed by immersing in an 1 mM methylene blue solution for 30 min.

Electrochromic responses of PAn/MB-Nafion and MB-Nafion were investigated by measuring changes in reflectance under applying potential pulses of 0.5 and 0 V vs. SCE. For this purpose, the films coated on Pt plates were irradiated with a 500 W xenon lamp (Ushio Electric UXL-500D-O), and changes in the intensity of reflected light caused by the application of potentials were measured at 660 nm with the use of a monochrometer (JASCO CT-25N) and a PbS detector.

3-2-3 Results and discussion

Electrostatic binding between methylene blue and Nafion. The electrostatic binding of methylene blue with sulfonate groups of Nafion was studied by measuring changes in absorption spectra of methylene blue dissolved in n-propanol with addition of the Aldrich Nafion solution. Results obtained are shown in Fig. 44. The absorption spectrum of

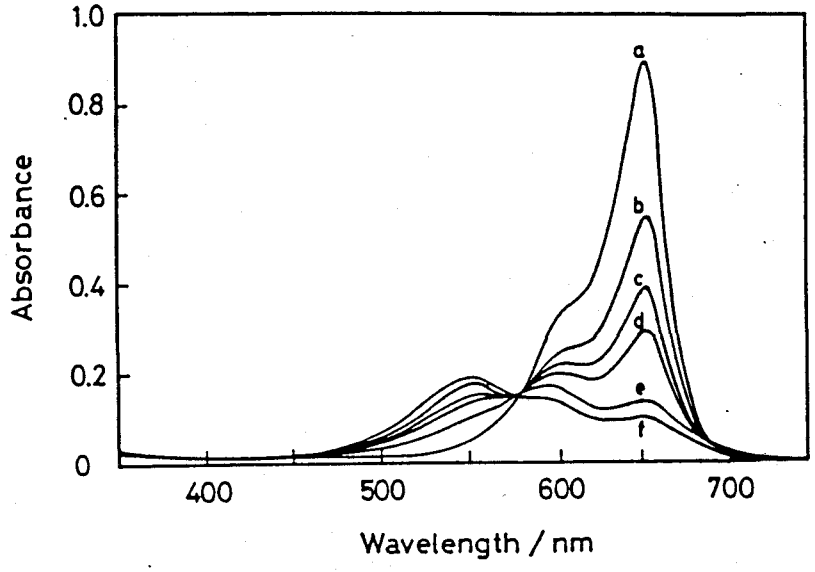

Fig. 44. Changes in absorption spectra of 1.0 x 10^{-5} M methylene blue dissolved in n-propanol with addition of the Nafion solution. The concentration of sulfonate groups of Nafion was 0 (a), 5.0 x 10^{-6} (b), 8.0 x 10^{-6} (c), 1.0 x 10^{-5} (d), 2.0 x 10^{-5} (e), and 5.0 x 10^{-5} (f) M.

methylene blue taken in the absence of Nafion showed a sharp peak at 660 nm and a weak hump at 610 nm which are assigned to the absorption bands of monomeric and dimeric methylene blue, respectively [117,118,120]. The intensity of these bands were definitely decreased with an increase in the concentration of sulfonate groups of Nafion, while a new band assigned to trimeric methylene blue appeared and then increased at 550 nm, and simultaneously the color of the solution was turned from blue to purple. The phenomena observed are regarded as "metachromasia", which was reported for changes in the color of several kinds of cationic dye solutions such as methylene blue, phenosafranine, and pyronine G by addition of anionic polyelectrolytes such as polystyrenesulfonate and polyvinylsulfate [123-127]. The cationic dye molecules were concentrated in the polyelectrolytes

due to electrostatic binding with anionic substituent groups of the polymers, resulting in the formation of dimeric or trimeric dyes.

If binding equilibrium is established between cationic dyes and anionic polyelectrolytes, the ratio (r) of anionic substituent groups of the polyelectrolyte occupied with cationic dyes to all anionic substituent groups is given by eq. (22) [126-128].

$$\frac{1}{r} = \frac{1}{n\ K\ C_{fm}} + \frac{1}{n} \qquad (22)$$

where C_{fm} is the concentration of free cationic dyes dissolved in the solution, and K and n are the intrinsic binding constant and maximum number of cationic dye molecules capable of binding to an anionic substituent group of the polyelectrolyte, respectively. The r in eq. (22) is given by

$$r = \frac{C_m - C_{fm}}{C_s} \qquad (23)$$

where C_m is the total concentration of free and bound methylene blue and C_s is that of methylene blue-bound and -free sulfonate groups of Nafion dissolved in the solution. The concentration of binding-free methylene blue (C_{fm}) can be obtained from apparent molecular absorption coefficient of monomeric methylene blue at 660 nm (ε^{660}) by using eq. (3) [126-128].

$$C_{fm} = \frac{\varepsilon^{660} - \varepsilon_*^{660}}{\varepsilon_o^{660} - \varepsilon_*^{660}} C_m \qquad (24)$$

where ε_*^{660} is the absorption coefficient of monomeric methylene blue obtained when all methylene blue molecules are bound to Nafion, and ε_o^{660} is that in the absence of Nafion. The ε_o^{660} was estimated to be 89800 M^{-1} cm^{-1} from the absorption spectrum shown as curve (a) of Fig. 44. The value of ε_*^{660} was obtained to be 2570 M^{-1} cm^{-1} from the extrapolation of ε^{660} vs. C_m/C_S relation to C_m/C_S = 0 [126,127], as shown in Fig. 45. The values of C_{fm} of methylene blue solutions containing various concentration of Nafion were then obtained from eq. (24) using ε^{660} values deduced from each spectrum shown in Fig. 44, and those of r were determined from eq. (23) using the C_{fm} determined. Figure 46 shows that eq. (22) holds between 1/r and $1/C_{fm}$, indicating the establishment of a binding equilibrium between methylene blue and sulfonate groups of Nafion. The values of n and K were then estimated to be 1.02 and 5.57 x 10^5, respectively. It is

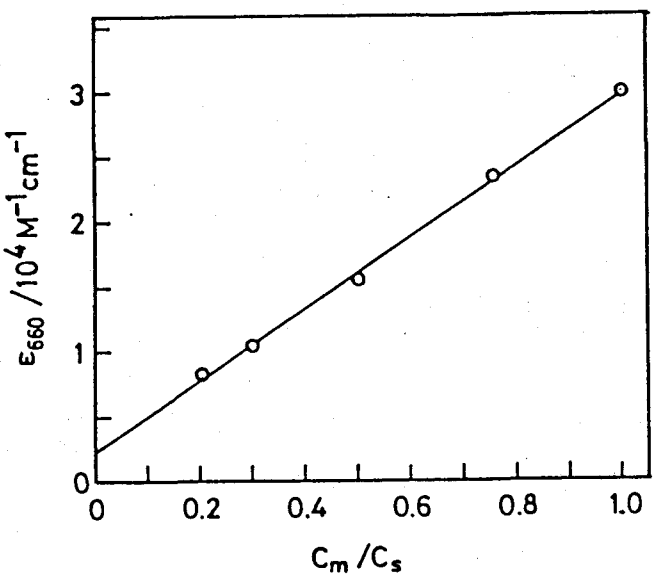

Fig. 45. The relationship between ε_{660} and C_m/C_S of n-propanol containing 1.0 x 10^{-5} M methylene blue and Nafion

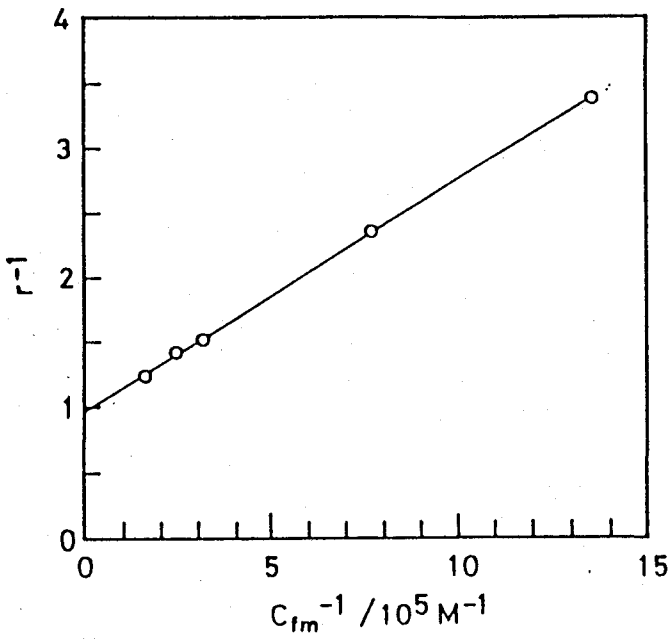

Fig. 46. The relationship between 1/r and $1/C_{fm}$ obtained from ε^{660} of spectra shown in Fig. 44 by using eq. (23) and (24).

recognized from the n value determined that methylene blue molecules are bound to sulfonate groups of Nafion in the ratio of 1:1. The binding constant is then formulated as

$$K = \frac{C_{ms}}{C_{fs}\ C_{fm}} \quad (= 5.57 \times 10^5\ M^{-1}) \qquad (25)$$

where C_{ms} is the concentration of methylene blue-bound sulfonate groups of Nafion in the solution, and C_{fs} is that of methylene blue-free sulfonate groups.

Preparation of polyaniline films doped with methylene blue-bound Nafion. Polyaniline films are prepared by electrooxidation of aniline in high acidic solutions [17,18,129]. It was found that the original Aldrich

Nafion solution had high acidity (pH 1.7) enough to deposit smooth polyaniline films on electrode substrate such as Pt, glassy carbon, and ITO electrodes, as judged from electrolysis results of 5 mM aniline in the Nafion solution. In this case sulfonate groups of Nafion should serve as the charge compensator to positive charges of polyaniline [130]. Polyaniline films were prepared on ITO electrodes from Aldrich Nafion solutions containing 5 mM aniline and 0, 1, 3, and 10 mM methylene blue, and the absorption spectra of the resulting films were obtained as shown in Fig. 47. The spectrum of polyaniline films prepared in the absence of methylene blue (Fig. 47(a)) was almost the same as that of polyaniline films prepared in conventional electrolyte solution such as chloride and perchlorate solutions [17,22,27], whereas polyaniline films prepared in the presence of methylene blue exhibited definite absorptions at 660 and 610 nm

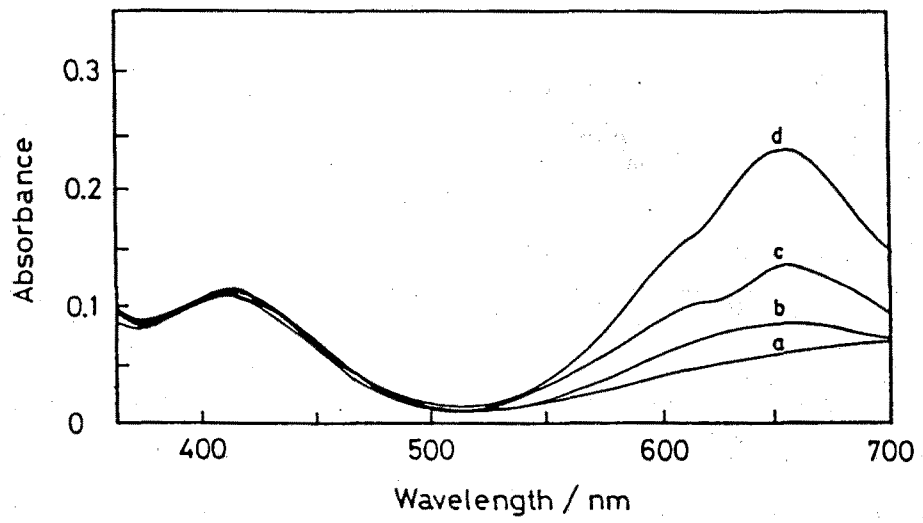

Fig. 47. Absorption spectra of PAn/MB-Nafion films prepared from Nafion solutions containing 5 mM aniline and 0 (a), 1.0 (b), 3.0 (c), and 10.0 (d) mM methylene blue.

which are assigned to monomeric and dimeric methylene blue, respectively. The intensity of these bands increased with increasing the concentration of methylene blue in the deposition bath. As already shown above, methylene blue was bound to sulfonate groups of Nafion, but a fraction of sulfonate groups of Nafion remained free from binding with methylene blue, because the concentration of sulfonate groups was 39.7 mM, being greater than that of methylene blue dissolved. Then it is thought that the observed incorporation of methylene blue in polyaniline films occurs with involvement of methylene blue-free sulfonates of Nafion as the charge compensator. The concentration of monomeric methylene blue (Γ_m) and dimeric methylene blue (Γ_d) in polyaniline films, and the sum of them ($\Gamma_t = \Gamma_m + 2\Gamma_d$) were determined by using eqs. (26) and (27) which were derived from eqs. (18) and (19) in the previous section to estimate the methylene blue concentration incorporated in Nafion modified electrodes.

$$\Gamma_m = \frac{\varepsilon_d^{660} A^{610} - \varepsilon_d^{610} A^{660}}{\varepsilon_m^{610} \varepsilon_d^{660} - \varepsilon_m^{660} \varepsilon_d^{610}} \times 10^{-3} \qquad (26)$$

$$\Gamma_d = \frac{\varepsilon_m^{610} A^{660} - \varepsilon_m^{660} A^{610}}{\varepsilon_m^{610} \varepsilon_d^{660} - \varepsilon_m^{660} \varepsilon_d^{610}} \times 10^{-3} \qquad (27)$$

where A^{610} and A^{660} are absorbance at 610 and 660 nm obtained after correction of the absorbance due to polyaniline. The values of Γ_m, Γ_d, and Γ_t are shown in Table 11 together with C_m/C_s for three different concentrations of methylene blue.

Judging from the electrode potential (ca. 0.5 V vs. SCE) monitored in the course of electropolymerization of aniline, the polyaniline films

Table. 11 The concentration of methylene blue and r value[a] of PAn/MB-Nafion films

C_m/mM	Γ_m/mol cm^{-2}	Γ_d/mol cm^{-2}	Γ_t/mol cm^{-2}	C_m/C_s[b]	r
1.0	1.3×10^{-9}	1.5×10^{-9}	1.6×10^{-9}	0.025	0.021
3.0	4.3×10^{-9}	7.3×10^{-10}	5.8×10^{-9}	0.072	0.076
10.0	1.5×10^{-8}	4.5×10^{-9}	2.4×10^{-8}	0.24	0.252

a) Relative ratio of sulfonate groups bound with MB to all sulfonate groups of Nafion incorporated in PAn/MB-Nafion films, estimated by using eq. (29).
b) C_s = 39.7 mM.

prepared must be emeraldine salt form in which the molar ratio of doped electrolyte anions to aniline units is ca. 0.5 [131-134]. Since the polymerization reaction in that case is given by scheme 2, the concentration of the doped anions in the polymer film (Γ_{A^-}) is given by

$$\Gamma_{A^-} = \frac{Q}{F}\,\frac{0.5n}{2.5n} = 0.2\,\frac{Q}{F} \qquad (28)$$

where F and Q are the Faraday constant and the quantity of electricity consumed in polymerization, respectively. In the present study polyaniline films were prepared using Q = 36 mC cm^{-2}, so that Γ_{A^-} of the sulfonate groups of Nafion must be 7.5×10^{-8} mol cm^{-2}. The total concentration of

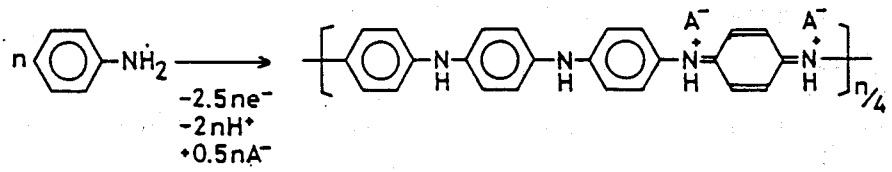

Scheme 2

sulfonate groups of Nafion incorporated in the prepared polyaniline films must be the sum of Γ_{A^-} and Γ_t. Then the ratio of the methylene blue-bound sulfonate groups of Nafion to the total amount of sulfonate groups in polyaniline films is given by

$$r = \frac{\Gamma_t}{\Gamma_{A^-} + \Gamma_t} \qquad (29)$$

The values of r estimated by this equation are given in Table 11. It is noteworthy from the table that the obtained r values were very close to the relative ratio of the concentration of methylene blue to that of sulfonate groups of Nafion (C_m/C_s) in the deposition baths of polyaniline, indicating that almost all methylene blue molecules in the deposition bath were bound to sulfonate groups of Nafion. This is quite natural as judged from very large binding constant ($5.57 \times 10^5\ M^{-1}$) obtained in a relatively dilute concentrations of methylene blue and sulfonate groups of Nafion.

Electrochemical and electrochromic properties of polyaniline films doped with methylene blue-bound Nafion. Cyclic voltammograms of polyaniline films doped with Nafion (PAn/Nafion) and doped with MB-bound Nafion (PAn/MB-Nafion) were taken in 1 M HCl solution. As Fig. 48 shows, a couple of redox waves due to polyaniline alone are observed at the PAn/Nafion, whereas at the PAn/MB-Nafion another couple of anodic and cathodic waves due to redox reactions of methylene blue appeared at 0.27 and 0.23 V vs. SCE, respectively. The peak currents due to this redox reaction increased with an increase in the quantity of methylene blue incorporated in the film, indicating that the redox reactions of methylene

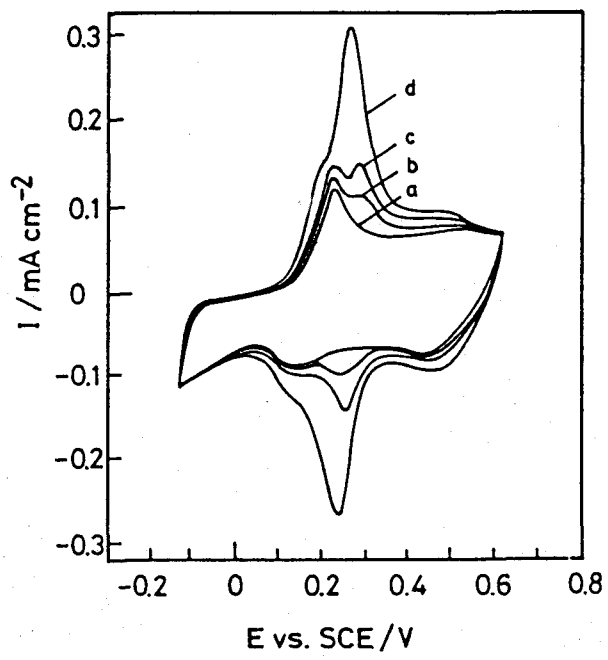

Fig. 48. Cyclic voltammograms of PAn/Nafion (a) and PAn/MB-Nafion (b-d) taken in 1.0 M HCl solution. dE/dt = 100 mV s^{-1}. PAn/MB-Nafion films were prepared from Nafion solutions containing 5 mM aniline and 1.0 (b), 3.0 (c), and 10.0 (d) mM methylene blue.

blue can effectively take place even in the polyaniline films.

The absorption spectra of PAn/MB-Nafion prepared from a deposition bath containing 10 mM methylene blue were measured in-situ under polarization at several potentials in 1 M HCl solution. The results are shown in Fig. 49. The spectrum taken at 0 V vs. SCE where all methylene blue must be reduced to leuco-methylene blue was resembled to that of reduced polyaniline film [17,22,27], and the film was yellow. When the electrode potential was positively shifted, the absorption bands of monomeric and dimeric methylene blue became great, and the color of the film was gradually changed into blue. Figure 50 shows the plots of the potentials applied to the electrode against $\log(\Gamma_{MB}/\Gamma_{LMB})$ where Γ_{MB} and

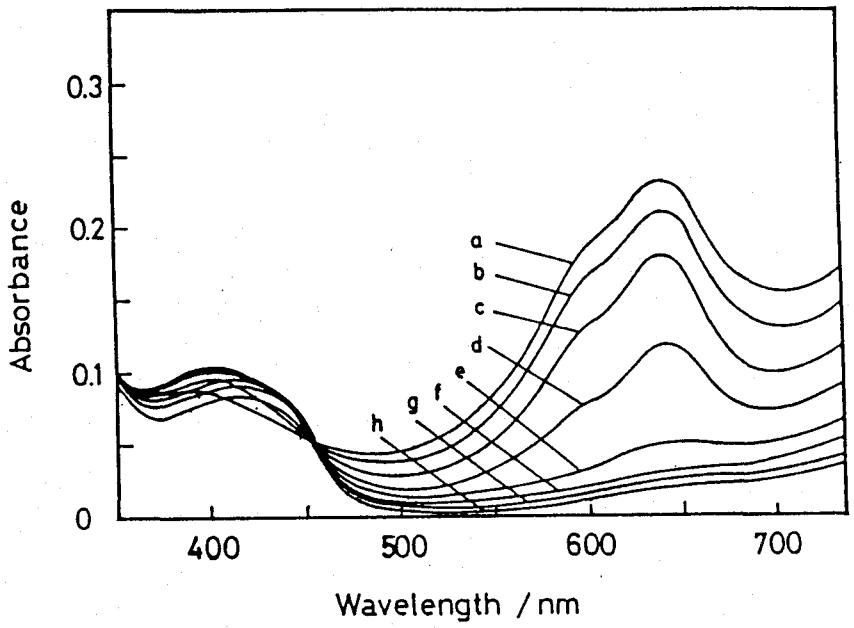

Fig. 49. Absorption spectra of a PAn/MB-Nafion film polarized at 0.5 (a), 0.4 (b), 0.3 (c), 0.25(d), 0.2 (e), 0.15 (f), 0.1 (g), and 0 (h) V vs. SCE in 1.0 M HCl. The PAn/MB-Nafion film was prepared from Nafion solution containing 5 mM aniline and 10 mM methylene blue.

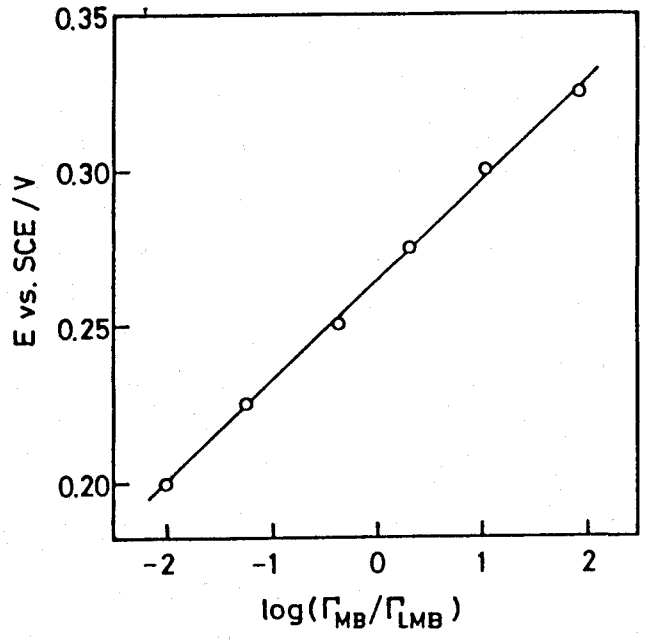

Fig. 50. Relationship between $\log(\Gamma_{MB}/\Gamma_{1\text{-}MB})$ in the PAn/MB-Nafion film and potential applied to the film.

Γ_{LMB} denote the concentration of methylene blue and leuco-methylene blue, respectively. The Γ_{MB} is the sum of Γ_m and $2\Gamma_d$ and was estimated from absorbance at 610 and 660 nm by using eqs. (5) and (6). The A^{610} and A^{660} used in these equations were obtained by subtracting the absorbance at 610 and 660 nm of PAn/Nafion from those of PAn/MB-Nafion which were taken at same potential, while the concentration of leuco-methylene blue was obtained by subtracting Γ_{MB} from Γ_t. Apparently, a linear relationship establishes between the two, and the slope was 30.1 mV, indicating that the Nernstian relation prevails in the methylene blue/leuco-methylene blue couple incorporated in the polyaniline film.

It was shown in the section 3-1 that the methylene blue-incorporated Nafion modified electrodes (MB-Nafion) exhibited electrochromic response due to redox reaction of the incorporated methylene blue. However, the response of color changes in that case was relatively slow; it took more than 3 min to complete the color change. In contrast, the color change completed rather rapidly at the PAn/MB-Nafion. Figure 51 shows electrochromic responses of PAn/MB-Nafion of 0.7 μm thickness and MB-Nafion of 0.5 μm thickness obtained at 660 nm. In the case of PAn/MB-Nafion, the coloring and the bleaching took place within 1 and 2 s, respectively, with the involvement of redox reactions of both polyaniline and the incorporated methylene blue of monomeric and dimeric forms. It is shown that the rate of the electrochromic response was remarkably higher at the PAn/MB-Nafion than at the MB-Nafion. The observed difference of the electrochromic responses does not have resulted from the difference in the film thickness, because the PAn/MB-Nafion was a little thicker than MB-Nafion, but the response rate was higher at the former film. Rather the fast response of the PAn/MB-Nafion must result from that polyaniline

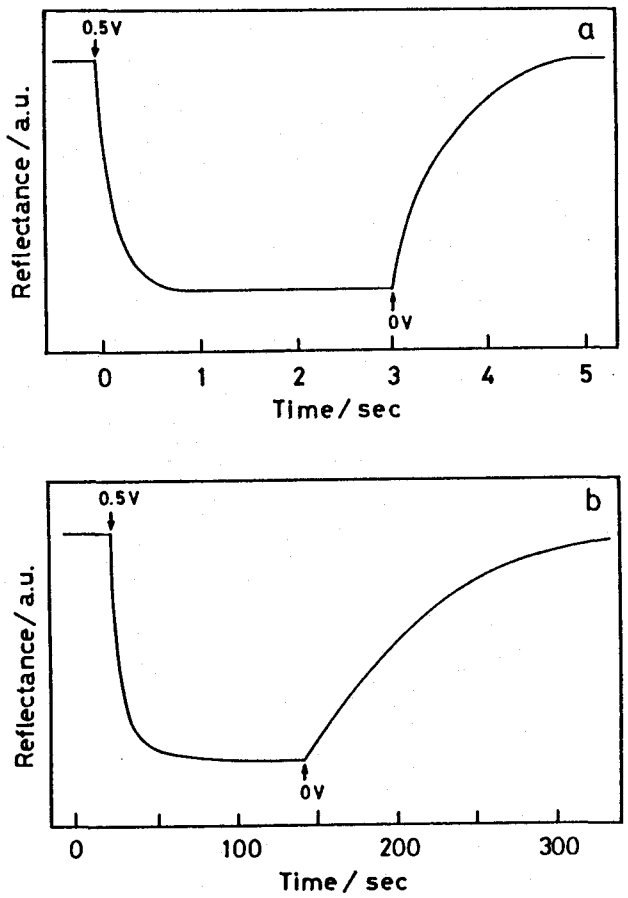

Fig. 51. Response behaviors of reflectance changes at 660 nm of PAn/MB-Nafion (a) and MB-Nafion (b), obtained by a potential pulse imposition of 0.5 and 0 V vs. SCE in 1.0 M HCl. The film thickness of PAn/MB-Nafion was 0.7 μm and that of MB-Nafion was 0.5 μm in dry state, as determined by observations with a scanning electron microscope.

matrices provided conducting networks available for the redox reactions of methylene blue in Nafion. According to the result obtained at PAn/MB-Nafion, the rate of bleaching was lower than that of coloring. This must have resulted from a decrease in the conductivity of the polyaniline matrices by reduction of the film when the bleaching occurred.

Chapter 4

Electrochemical Properties of Electrodes Coated with Polystyrene Films Containing Ionic Surface-active Agents

4-1

Electrodes Coated with Polystyrene Films Containing Surface-active Agents.

4-1-1 Introduction

In last few years, many kinds of polymer-coated electrodes have been reported with the purpose of attaching a variety of functions to the electrodes. The most convenient method of binding chemical species having desired functions to the electrodes is to coat the electrode substrate with polymers containing these species as the constituents. The utility of such approach has been proved in a variety of polymer-coated electrodes [135-140]. In addition, coating the electrode substrates with polyelectrolytes such as polyvinylpyridine [35-38], polystyrenesulfonate [141], and Nafion [39-41] provides another means for binding and concentrating electroactive ionic species to the electrode substrates. In this case, the use of insoluble polymer electrolytes is essential and the insolubility can be achieved by cross-linking soluble ionic polymers [141,142]. Insoluble polyelectrolytes can also be prepared by copolymerization of neutral and ionic monomers [143,144]. The key to obtain these stable polymer-coated electrodes is to synthesize insoluble polymers.

In this section, it ill be described that a new simple method for introducing electroactive ions into the electrode substrates without any

synthetic effort. When conventional surface active agents such as sodium n-dodecylbenzenesulfonate, lauryltrimethylammonium chloride, and laurylpyridinium chloride are blended in films of polystyrene known as one of the most conventional polymers and then applied to electrode substrates, they stably serve as matrixes for binding ionic electroactive species dissolved in electrolyte solutions. The several electrochemical behaviors of these polymer-coated electrodes in aqueous solution containing electroactive ions will be shown.

4-1-2 Experimental

Polystyrene (PSt) (mean molecular weight; 176800), sodium n-dodecylbenzenesulfonate (DBS), lauryltrimethylammonium chloride (LMA), and laurylpyridinium chloride (LPy) were of reagent grade and used without further purification.

Benzene solutions of PSt (6.0×10^{-4} M), DBS (0.01 M), LMA (0.02 M), and LPy (0.02 M) were prepared. Aliquots of the benzene solution of PSt and that of desired species were mixed, and then the resulting benzene solution was dropped onto a glassy carbon electrode (GC) to coat its entire surface. By evaporating the solvent in air, the polymer-coated electrode was prepared. The prepared electrodes will be denoted here by showing components of the coated films in abbreviation, such as PSt-DBS/GC, PSt-LMA/GC, and PSt-LPy/GC.

The supporting electrolyte solution was 0.5 M Na_3PO_4 adjusted to pH = 7.0 with H_3PO_4 into which $Ru(bpy)_3Cl_2$ or $K_3Fe(CN)_6$ was dissolved.

4-1-3 Results and discussion

Incorporation of electroactive cations into glassy carbon electrodes coated with polystyrene containing sodium n-dodecylbenzenesulfonate. The cyclic voltammograms of the GC and the PSt/GC electrodes in 1.0 x 10^{-3} M $Ru(bpy)_3Cl_2$ aqueous solution are shown in Fig. 52 (a) and (b), respectively. A couple of redox waves of $Ru(bpy)_3^{2+/3+}$ which can be observed at the GC are not observed at the PSt/GC electrode, the result indicating that the polystyrene film-coated GC is inactive for the electrochemical reactions. By adding DBS to the PSt film, however, very small anodic and cathodic waves due to the redox reaction of $Ru(bpy)_3^{2+/3+}$ appear at the first potential sweep, and then increase with successive cyclic potential scans until about 60 min, as shown in Fig. 52 (c). The maximum peak currents developed at the PSt-DBS/GC are more than four times as large as those obtained at the bare GC. When the steady voltammogram was obtained, it was very stable to the continuous cyclic potential scans at least for 20 h as shown by a broken line of Fig. 52 (c). If the PSt-DBS/GC was transferred from the 1.0 x 10^{-3} M $Ru(bpy)_3Cl_2$ solution to the supporting electrolyte solution after immersing in the former solution for 60 min, large redox waves comparable to those observed in the $Ru(bpy)_3^{2+/3+}$ solution are seen initially, but gradually decrease with the progress of potential scan as shown in Fig. 53. It is suggested from these behaviors show that sodium dodecylbenzenesulfonate blended in polystyrene is effectively ionized in water to give its anion in the coated layer and then electrostatically binds $Ru(bpy)_3^{2+}$ in solution as in the case of the electrode coated with anionic polyelectrolytes such as Nafion [40]. The DBS in the coated layer seems not to dissolve on ionization in aqueous

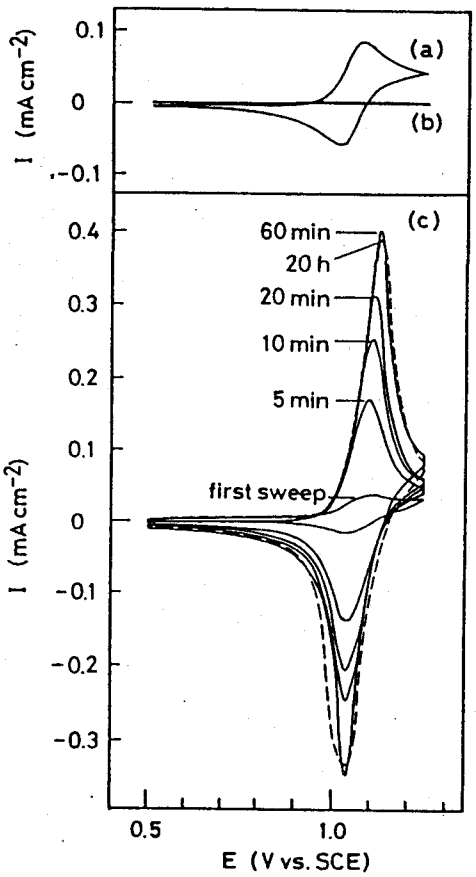

Fig. 52. Cyclic voltammograms of the GC electrode (a), the GC coated with 4.0 x 10^{-10} mol cm^{-2} PSt (b), and the GC coated with a mixture of 4.0 x 10^{-10} mol cm^{-2} PSt and 3.5 x 10^{-7} mol cm^{-2} DBS (c) in 1.0 x 10^{-3} M $Ru(bpy)_3Cl_2$ aqueous solution containing 0.5 M Na_3PO_4 adjusted to pH 7. dE/dt = 100 mV s^{-1}. The time shown in Fig. 52 (c) denotes the time elapsed after the beginning of cyclic potential sweep of the electrode in the electrolyte solution.

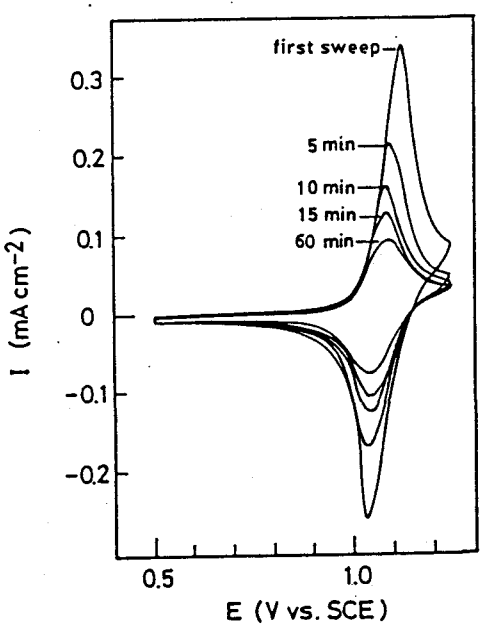

Fig. 53. Cyclic voltammograms of the GC electrode coated with a mixture of 4.0 x 10^{-10} mol cm^{-2} PSt and 3.5 x 10^{-7} mol cm^{-2} DBS, in the supporting electrolyte of 0.5 M Na_3PO_4 adjusted to pH 7 after immersion in 1.0 x 10^{-3} M $Ru(bpy)_3Cl_2$ for 60 min. dE/dt = 100 mV s^{-1}. The time shown denotes the time elapsed after transference of the electrode from $Ru(bpy)_3^{2+}$ solution to the supporting electrolyte solution.

solution, because steady cyclic voltammogram of PSt-DBS/GC in $Ru(bpy)_3Cl_2$ obtained by potential sweeps for 60 min little varied with farther potential sweeps for 20 h. The observed high stability of the blended surface active agent may be indebted to rigid fixation of long alkylchains of DBS in the polymer chains of PSt.

The quantity of $Ru(bpy)_3^{2+}$ incorporated in the polymer layer by 60 min-soaking in several $Ru(bpy)_3^{2+}$ solutions was determined from the charge involved in the anodic peak area of the cyclic voltammograms of the

electrode taken at the initial potential scan at 10 mV s^{-1} in the supporting electrolyte solution. The $Ru(bpy)_3^{2+}$ solutions used were 1, 2, and 3 x 10^{-3} M and the amount of the incorporated $Ru(bpy)_3^{2+}$ was determined as a function of the surface concentration of DBS with fixing the surface concentration of PSt to 2.0 x 10^{-9} mol cm^{-2}. The results are shown in Fig. 54. The quantity of $Ru(bpy)_3^{2+}$ incorporated in the PSt-DBS

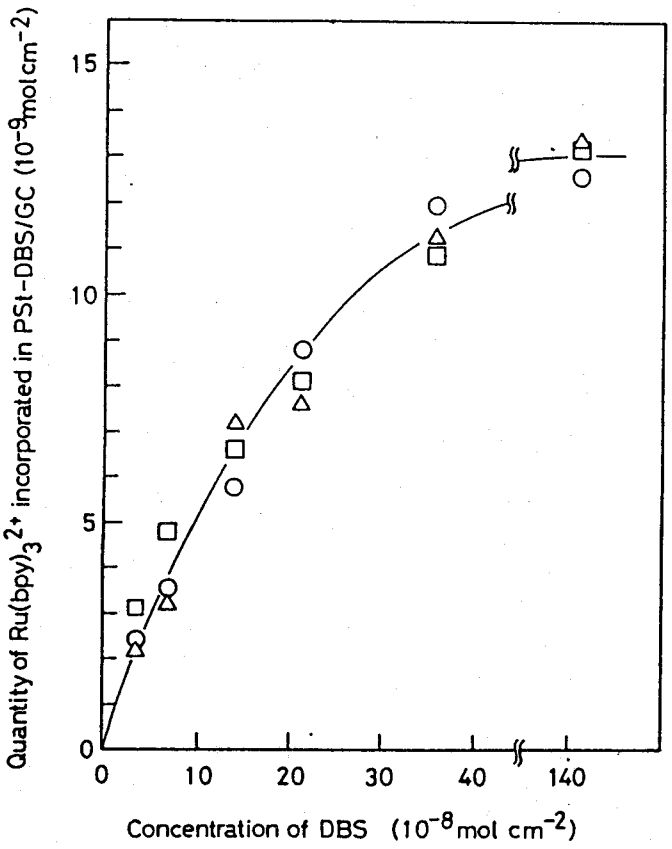

Fig. 54. The quantity of $Ru(bpy)_3^{2+}$ incorporated in the coated layer consisting of 2.0 x 10^{-9} mol cm^{-2} PSt and DBS of various surface concentrations. The $Ru(bpy)_3^{2+}$ incorporation was performed by immersing the electrodes in 1 (○), 2 (△), and 3 (□) x 10^{-3} M $Ru(bpy)_3Cl_2$/0.5 M Na_3PO_4 (pH 7) for 60 min, and the incorporated amount was determined from the quantity of charge involved in the anodic voltammetric waves due to $Ru(bpy)_3^{2+}$ oxidation in the supporting electrolyte solution.

layer increases with increasing the concentration of DBS, but a saturating tendency is noticed above 4 x 10^{-7} mol cm^{-2} DBS. Another noticeable thing is that the concentration of $Ru(bpy)_3Cl_2$ in the solution does not affect the quantity of the incorporated $Ru(bpy)_3^{2+}$. It is then of no doubt that the ability for binding $Ru(bpy)_3^{2+}$ is mainly governed by the concentration of DBS blended in PSt. These results suggest that $Ru(bpy)_3^{2+}$ is incorporated selectively in the PSt-DBS layer, because if the incorporation of $Ru(bpy)_3^{2+}$ and the other cations (Na^+) are competitively occurred, the concentration ratio of both species in the solution should influence the quantity of $Ru(bpy)_3^{2+}$ incorporated in the PSt-DBS layer.

The maximum molar ratio of the incorporated $Ru(bpy)_3^{2+}$ to DBS in the polymer layer was 0.19 which was achieved at 4.0 x 10^{-8} mol cm^{-2} of DBS, and with further increasing the concentration of DBS, the molar ratio of the incorporated $Ru(bpy)_3^{2+}$ decreased. If all the DBS are ionized and electrically compensated by $Ru(bpy)_3^{2+}$, the molar ratio should be 0.5. It is, therefore, suggested that only a part of DBS in the polymer layer work effectively for binding $Ru(bpy)_3^{2+}$. It is thought that there should be free space available for the incorporation of $Ru(bpy)_3^{2+}$ in the PSt-DBS layer. How this is built up is not known, but if the free space is limited, the $Ru(bpy)_3^{2+}$ incorporation would be limited. In addition, the ionization of DBS in the PSt layer may not perfectly occur especially in the PSt-DBS layer containing a high quantity of DBS.

Rotating disk electrode measurements of glassy carbon electrode coated with polystyrene containing sodium n-dodecylbenzenesulfonate. The rate of electron transfer between electroactive species bound in the polyelectrolyte layer and those in the solution can be evaluated by use of

the rotating disk electrode (RDE) technique [105]. This method was applied to the PSt-DBS/GC electrode in $Ru(bpy)_3Cl_2$ solution. Cyclic voltammograms of the rotating PSt-DBS/GC electrode taken in 3.0 x 10^{-3} M $Ru(bpy)_3Cl_2$ solution are shown in Fig. 55. It is seen that in the anodic potential scan, anodic peak currents are followed by the limiting currents (I_{lim}), the magnitude of both being dependent on the electrode rotation rate. In contrast, with increasing the electrode rotation rate the cathodic peak currents decrease. The rate of the decrease in the cathodic peak currents is higher than that of the increase in the anodic ones, and the cathodic currents almost disappear at 2000 r.p.m.. The observed behavior of cathodic currents can be explained in terms of mediation actions of

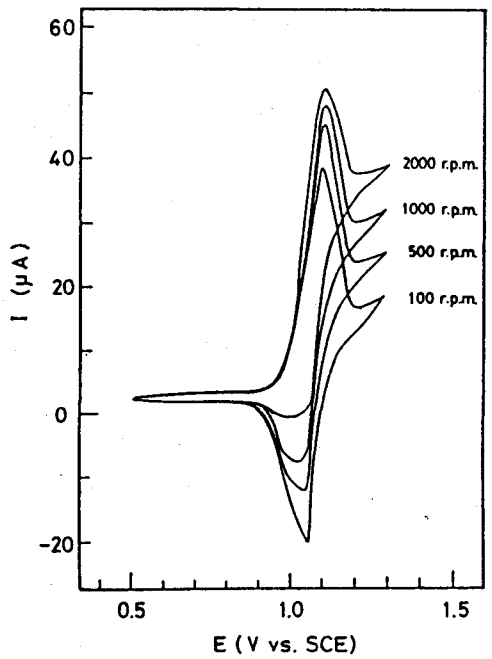

Fig. 55. RDE measurements of the GC electrode coated with a mixture of 5.8 x 10^{-10} mol cm^{-2} PSt and 3.5 x 10^{-7} mol cm^{-2} DBS at several rotation rates in 3.0 x 10^{-3} M $Ru(bpy)_3Cl_2$/0.5 M Na_3PO_4 (pH 7).

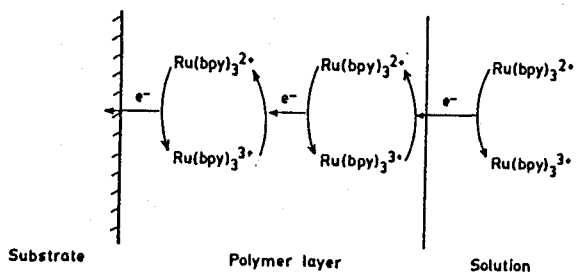

Fig. 56. Schematic representation of electron transfer for oxidation of $Ru(bpy)_3^{2+}$ in the solution at the PSt-DBS/GC electrode.

$Ru(bpy)_3^{2+}$ bound in the coated PSt layer as schematically illustrated in Fig. 56. When $Ru(bpy)_3^{3+}$ is produced at the electrode substrate surface by anodic oxidation, it is reduced by the incorporated $Ru(bpy)_3^{2+}$ in neighborhood. If this rate is assumed to be very rapid, the reduction rate of the $Ru(bpy)_3^{3+}$ in the coated layer is controlled by the supply of $Ru(bpy)_3^{2+}$ from the solution bulk which is affected by the electrode rotation rate. The amount of $Ru(bpy)_3^{3+}$ produced by anodic oxidation in the electrode surface is then decreased by increasing the rotation rate of the electrode as observed. It will be shown below that such interpretation is valid for results obtained at the electrodes used in measurements of Fig. 55.

The Koutecky-Levich plots are made for results obtained under several different experimental conditions. The results give straight lines as shown in Fig. 57 and by extrapolating these lines to $\omega \rightarrow \infty$ ($\omega^{-1/2} \rightarrow 0$), the intercept value of I_{lim} (I_{lim}^{∞}) was obtained. Using the obtained I_{lim}^{∞} and eq. 30 [105], the rate constant of electron transfer (k_{ex}) was

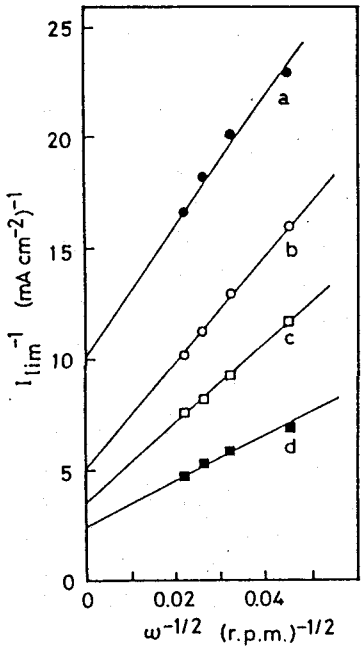

Fig. 57. Koutecky-Levich plots from the RDE measurements of the GC electrode coated with a mixture of 5.8 x 10^{-10} mol cm^{-2} PSt and 7.1 x 10^{-8} mol cm^{-2} DBS (a, b, c) and a mixture of 5.8 x 10^{-10} mol cm^{-2} PSt and 14.1 x 10^{-7} mol cm^{-2} DBS (d) in 1.0 x 10^{-3} (a, d), 2.0 x 10^{-3} (b), and 3.0 x 10^{-3} (c) M $Ru(bpy)_3Cl_2$ solutions. I_{lim} were measured at 1.25 V vs. SCE.

determined.

$$k_{eq} = I_{lim}^{\infty} / (F\Gamma_{Ru}C_{Ru}) \qquad (30)$$

where Γ_{Ru}, C_{Ru}, and F are the concentration of $Ru(bpy)_3^{3+}$ in the coated layer, that of $Ru(bpy)_6^{2+}$ in the solution, and the Faraday constant, respectively. In Fig. 58 the results on the effect of the concentration of DBS in a fixed surface concentration of PSt and that of the quantity of PSt on k_{ex} are given. The surface concentration of DBS up to 3.5 x 10^{-7} mol cm^{-2} in the PSt layer (5.8 x 10^{-10} mol cm^{-2}) does not appreciably affect k_{ex} value and the k_{ex} value of ca. 2.0 x 10^5 mol^{-1} cm^3 s^{-1} is obtained in

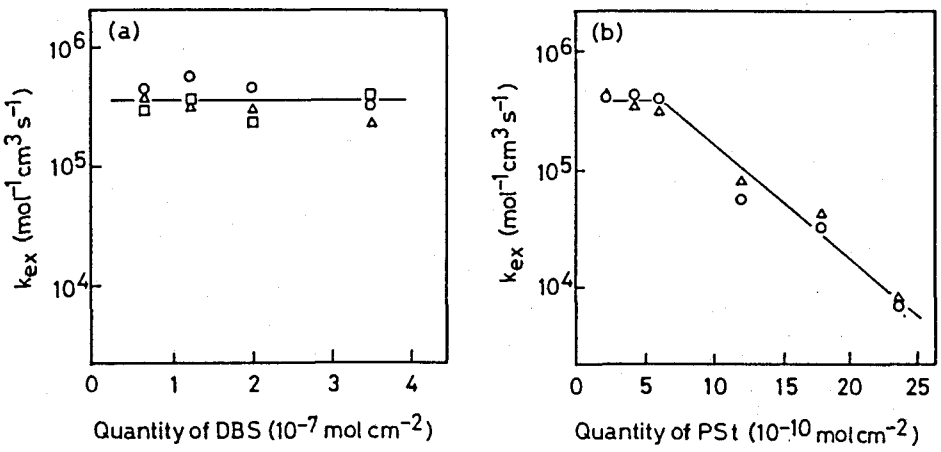

Fig. 58. The effects of the quantity of DBS in PSt (a) and of the quantity of PSt layer on k_{ex} which was determined from RDE measurements in 1.0 x 10^{-3} (○), 2.0 x 10^{-3} (△), 3.0 x 10^{-3} (□) M $Ru(bpy)_3Cl_2$ solutions. In (a) the quantity of PSt was fixed to 5.8 x 10^{-10} mol cm^{-2}, and in (b) the quantity of DBS was 1.02 x 10^{-8} mol cm^{-2} per 1.0 x 10^{-10} mol cm^{-2} PSt.

those cases. It is suggested from the obtained constant k_{ex} that the rate determining step for the electrode reaction in this case is the electron exchange between $Ru(bpy)_3^{3+}$ produced in the polymer layer and $Ru(bpy)_3^{2+}$ in the solution.

As shown in Fig. 58 (b), the quantity of PSt has a great influence on k_{ex}. In those cases, 1.02 x 10^{-8} mol cm^{-2} of DBS was contained in every 1.0 x 10^{-10} mol cm^{-2} of the PSt film. When the quantity of PSt is below 6.0 x 10^{-10} mol cm^{-2}, the quantity of PSt does not significantly affect k_{ex}. However, the increase in the quantity of PSt beyond that value clearly reduce k_{ex}. Since the rate constant changes at this threshold quantity of PSt, the rate determining step must change at this point. Beyond the threshold quantity, electron transport between $Ru(bpy)_3^{2+/3+}$ in the polymer layer may be a rate-determing step. This may be caused at least in part by the increase in the thickness of the coated polymer layer, which

reduces the permeability of electrolyte solutions and thereby reduces the rate of electron transfer through the polymer film.

Incorporation of electroactive anions into glassy carbon electrodes coated with polystyrene containing lauryltrimethylammonium chloride and laurylpyridium chloride. The PSt/GC electrode does not show any remarkable activities in 3.0 x 10^{-3} M $K_3Fe(CN)_6$ solution as shown by the curve (a) of Fig. 59, whereas well-defined redox waves of $Fe(CN)_6^{3-/4-}$ are

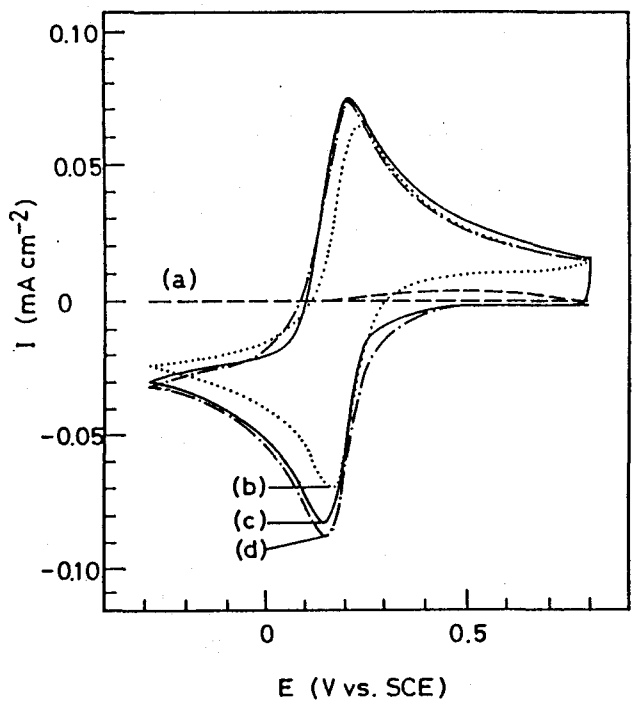

Fig. 59. Cyclic voltammograms in 3.0 x 10^{-3} M $K_3Fe(CN)_6$/0.5 M H_3PO_4 (pH 7) of the GC coated with 4.0 x 10^{-10} mol cm^{-2} PSt (a), the GC electrode (b), the GC coated with a mixture of 4.0 x 10^{-10} mol cm^{-2} PSt and 3.5 x 10^{-7} mol cm^{-2} LMA (c), and the GC coated with a mixture of 4.0 x 10^{-10} mol cm^{-2} PSt and 3.5 x 10^{-7} mol cm^{-2} LPy (d). dE/dt = 50 mV s^{-1}. The curve (c) and (d) were the first potential sweep of the electrodes just soaked in the solution.

seen from the beginning of potential sweep cycles at the PSt-LMA/GC electrode just after being immersed in the $K_3Fe(CN)_6$ solution, as shown by the curve (c) of Fig. 59. Important findings in this case are that the peak currents obtained at the first potential sweep do not largely change for 60 min of potential sweeps and they are almost similar to those taken with the bare GC (the curve (b) of Fig. 59). The same is true for results obtained at PSt-LPy/GC electrode in $K_3Fe(CN)_6$ solution (Fig. 59 (d)). Furthermore, if the PSt-LMA/GC or the PSt-LPy/GC electrode were immersed in the $K_3Fe(CN)_6$ solution for 60 min and then transferred to the supporting electrolyte, the redox waves of $Fe(CN)_6^{3-/4-}$ rapidly decreased to disappear within few minutes of cyclic potential sweeps. These behaviors seem to suggest that the ability of the PSt-LMA and PSt-LPy layers for concentrating electroactive anions is lower than that of the PSt-DBS/GC layer for electroactive cations.

The relationship between the quantity of incorporated $Fe(CN)_6^{3-}$ in the PSt-LMA/GC electrodes and the surface concentration of LMA, obtained by the same manner as the case of PSt-DBS/GC in $Ru(bpy)_3Cl_2$ solutions, is shown in Fig. 60. By comparing Fig. 54 with 60, it is seen that the quantity of $Fe(CN)_6^{3-}$ incorporated in the PSt-LMA/GC is much smaller than that of $Ru(bpy)_3^{2+}$ incorporated in the PSt-DBS/GC when the surface concentration of DBS and LMA blended in PSt is the same. In addition, it is noteworthy that the quantity of $Fe(CN)_6^{3-}$ in the PSt-LMA/GC is influenced not only by the surface concentration of LMA but also by the concentration of $K_3Fe(CN)_6$ in the solution as shown in Fig. 60, the result being in marked contrast to the case of PSt-DBS/GC in $Ru(bpy)_3Cl_2$ solution. Almost the same behaviors were obtained for the case of the incorporation of $Fe(CN)_6^{3-}$ into the PSt-LPy layers.

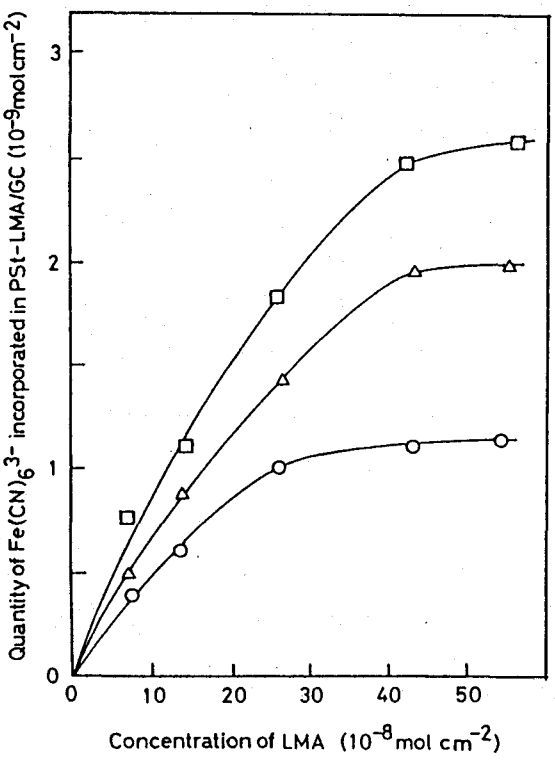

Fig. 60. The quantity of $K_3Fe(CN)_6$ incorporated in the coating layer consisting of 2.0 x 10^{-9} mol cm^{-2} PSt and LMA of various surface concentrations. The $Fe(CN)_6^{3-}$ incorporation was performed by immersing the electrodes in 1 (○), 2 (△), and 3 (□) x 10^{-3} M $K_3Fe(CN)_6$/0.5 M Na_3PO_4 (pH 7) for 60 min, and the incorporated amount was determined from the quantity of charge involved in the anodic voltammetric waves due to $Fe(CN)_6^{3-}$ reduction in the supporting electrolyte solution.

It is suggested from the results obtained at the PSt-LMA/GC and the PSt-LPy/GC that incorporation of anionic species into these coated layers occurs competitively between $Fe(CN)_6^{3-}$ and anionic species of supporting electrolyte such as $H_2PO_4^-$ and HPO_4^{2-} The mobility of $Fe(CN)_6^{3-}$ in the PSt-LMA or PSt-LPy layers seems to be very high, as judged from the result that $Fe(CN)_6^{3-}$ is rapidly incorporated into and eliminated from the PSt-LMA and PSt-LPy layers. As a result, the incorporated $Fe(CN)_6^{3-}$ in

these polymer layers may be easily replaced by other electrolyte anions of high mobilities, and the incorporation of $Fe(CN)_6^{3-}$ occurs competitively with that of the supporting electrolyte anions. If such view is valid, the observed slow incorporation and elimination behaviors of $Ru(bpy)_3^{2+}$ (see Fig. 52 and 53) at the PSt-DBS/GC can be explained in terms of relatively low mobility of $Ru(bpy)_3^{2+}$ in the coated layer. Once $Ru(bpy)_3^{2+}$ is incorporated in the coated layer, it is hardly replaced by electrolyte cations such as Na^+ and then selective concentration of $Ru(bpy)_3^{2+}$ in the coated layer may be accomplished. The difference in the diameter of $Ru(bpy)_3^{2+}$ (8 Å) [145] and $Fe(CN)_6^{3-}$ (5 Å) [146] may provide one probable reason for different mobilities as discussed above.

Regulation of electrode reactivity for cationic or anionic electroactive species by selection of surface-active agents blended in coated polystyrene films. Cyclic voltammograms of the PSt-DBS/GC, the PSt-LMA/GC, and the GC electrodes were measured in a solution containing both $Ru(bpy)_3Cl_2$ and $K_3Fe(CN)_6$. As Fig. 61 (a) shows, two redox waves due to $Ru(bpy)_3^{2+/3+}$ and $Fe(CN)_6^{3-/4-}$ appear in a cyclic voltammogram at the GC electrode, as expected. However, at the PSt-DBS/GC electrode the redox waves of $Ru(bpy)^{2+/3+}$ alone appear, and those of $Fe(CN)_6^{3-/4-}$ are not seen, as Fig. 61 (b) shows. This result is quite reasonable, because the ionized DBS in the PSt layer can attract electrostaically $Ru(bpy)_3^{2+}$ but must repulse $Fe(CN)_6^{3-}$ species, allowing the diffusion of $Ru(bpy)_3^{2+}$ alone into the electrode substrate. Similarly, the repulsion between $Ru(bpy)_3^{2+}$ and the ionized LMA in the PSt layer cannot allow the penetration of the former in the coated PSt layer, and as a result the redox reaction of $Fe(CN)_6^{3-}$ selectively occurs, as shown in Fig. 61 (c). The results presented

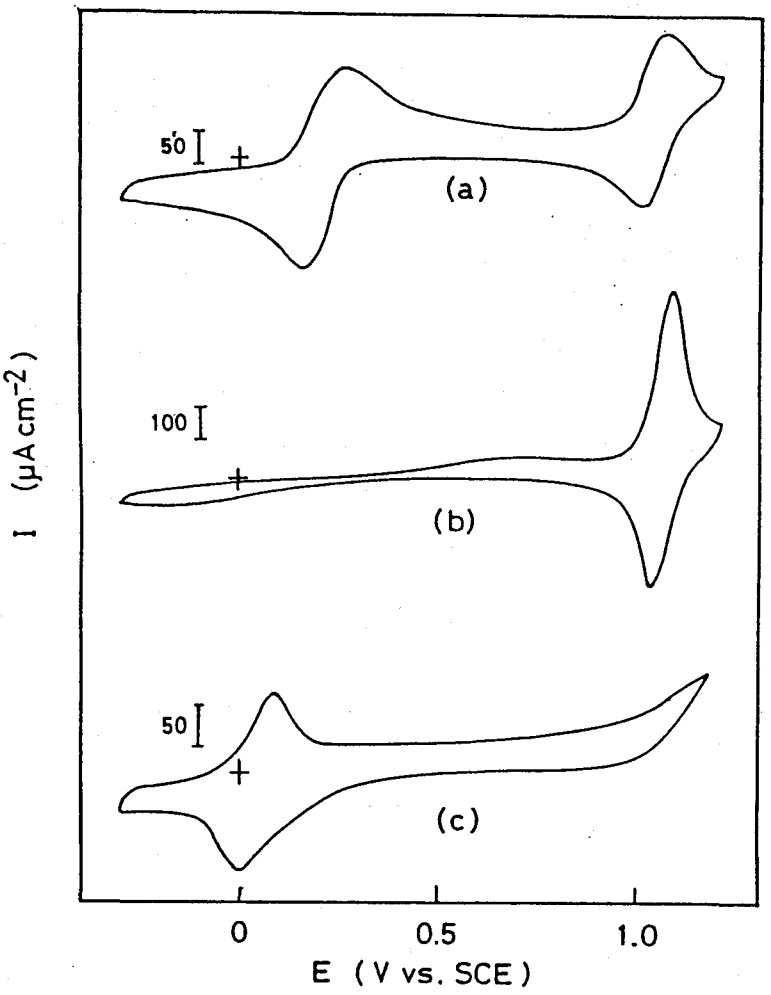

Fig. 61. Cyclic voltammograms of the GC electrode (a), the GC coated with a mixture of 4.0 x 10^{-10} mol cm^{-2} and 3.5 x 10^{-7} mol cm^{-2} DBS (b), and the GC coated with a mixture of 4.0 x 10^{-10} mol cm^{-2} PSt and 3.5 x 10^{-7} mol cm^{-2} LMA (c) in an aqueous solution containing 1.0 x 10^{-3} M $Ru(bpy)_3Cl_2$, 1.0 x 10^{-3} M $K_3Fe(CN)_6$, and 0.5 M Na_3PO_4 (pH 7).

in Fig. 61 demonstrate the merit of the use of surface active-agents as a component of coating materials for electrode substrates in the point that they attach electrodes the reaction selectivities for either cationic or anionic electroactive species.

4-2

Kinetics of Glassy Carbon Electrodes Coated with Polystyrene Films Containing Ferrocene and Ionic Surface-active Agents

4-2-1 Introduction

In the previous section, it has been shown that the coating electrode substrate with a mixture of polystyrene and ionic surface-active agent such as sodium n-dodecylbenzenesulfonate and lauryltrimethylammonium chloride is useful in attaching an ionic electroactive species such as $Ru(bpy)_3^{2+}$ and $Fe(CN)_6^{3-}$ to the electrode substrate. As an extension of the work described in the previous section, it is of interest to investigate the functions of ionic surface-active agent in the polystyrene layer in the redox reactions of electrically neutral redox species such as ferrocene contained in the coated layer. This is the main purpose of the study in this section.

4.2.2 Experimental

Ferrocene (Fc) was purified by sublimation under reduced pressure. Benzene solutions of PSt (6.0×10^{-4} M), Fc (0.1 M), DBS (0.1 M), and LMA (0.1 M) were prepared. Aliquots of the benzene solution of PSt and that of the desired species were mixed, and the polymer-coated electrode was prepared by dropping the resulting benzene solution onto the glassy carbon electrode, followed by evaporating the solvent in air. The prepared electrode will be denoted by the abbreviations of the components of the coated film, such as PSt-Fc/GC, PSt-Fc-DBS/GC, and PSt-Fc-LMA/GC. In order

to determine the concentration of ferrocene in the film under wet conditions, which was required to estimate the apparent diffusion coefficient and the standard rate constant of the charge-transfer reaction of the electrodes, the thickness of the PSt-Fc-DBS and the PSt-Fc-LMA films were prepared on slide glasses and their thickness were determined by observation with an optical microscope (Nikon Model S) after the films were soaked in an electrolyte solution for 1 h.

4.2.3 Results and Discussion

Electrochemical responses of glassy carbon electrodes coated with polystyrene containing ferrocene. Cyclic voltammograms of PSt-Fc/GC, PSt-Fc-LMA/GC, and PST-Fc-DBS/GC electrodes taken in 0.1 M KCl solution at 10 mV s^{-1} are shown in Fig. 62. The PSt-Fc/GC showed no redox waves, although ferrocene was firmly fixed at the surface of the electrode, indicating that the redox reaction of ferrocene does not work in the highly hydrophobic polystyrene film. However when either LMA or DBS was added to the film, definite anodic and cathodic waves due to the redox reaction of ferrocene/ferricinium cation appeared. These waves seemed stable at least for the successive potential sweeps for 3 h, but after then the peak currents decreased gradually with continuation of the potential sweep cycling, resulting in about 10% of decrease in the peak currents after 5 h including the initial 3 h potential cycling. The ionic surface-active agents in the polystyrene film were very stable and no dissolution seemed to occur for the potential sweeps for 20 h, as described in the previous section. The same was true for ferrocene, as judged from the comparison of absorption spectra of it in the polystyrene films before and

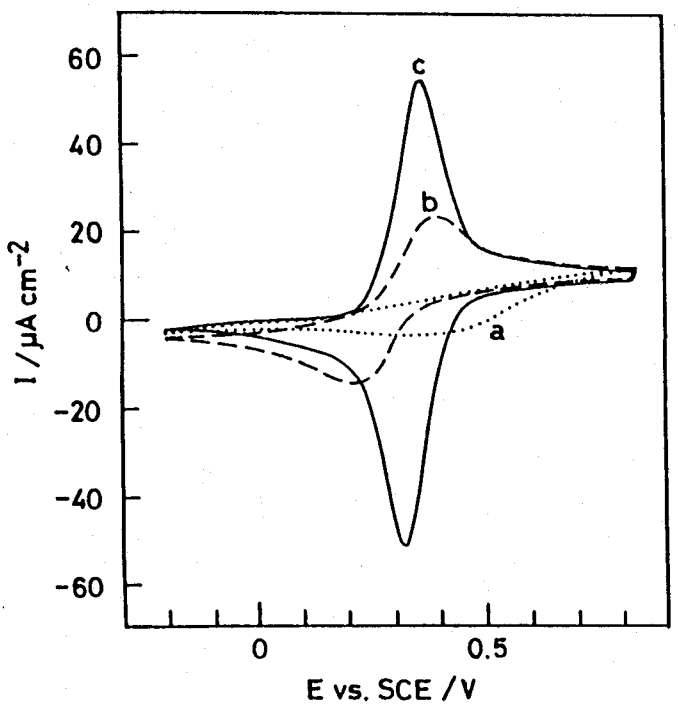

Fig. 62. Cyclic voltammograms of the PSt-Fc/GC (a), the PSt-Fc-LMA/GC (b), and the PSt-Fc-DBS/GC (c) taken in 1.0 M KCl aqueous solution at dE/dt = 10 mV s^{-1}. The amount of PSt coated on the GC electrode was 1.0 x 10^{-9} mol cm^{-2} and that of Fc, LMA, and DBS was 5.0 x 10^{-7} mol cm^{-2} each.

after the potential sweeps for 20 h. The measurements of the absorption spectra in that case was made by stripping the polystyrene films from the electrode substrate. Accordingly, the decrease in the peak currents observed for the potential sweeps for 5 h seemed to result from loosing the adhesion of the coated polystyrene film to the mirror-finished glassy carbon electrode substrate due to the swelling of the polymer.

It is noticed in Fig. 62 that the peak currents obtained at the PSt-Fc-DBS/GC were about 4 times as large as those obtained at the PSt-Fc-LMA/GC, and that the anodic and cathodic peak separation (ΔE_p) of the

former was 18 mV which was smaller than that of the latter (ΔE_p = 170 mV). The peak currents of the cyclic voltammograms of both the PSt-Fc-LMA/GC and the PSt-Fc-DBS/GC were proportional to the potential sweep rate for 1 to 500 mV s^{-1}, indicating that the diffusion of electrons and/or ions in the polymer layer occurs very fast compared to the rate of electron transfer at the polymer/electrode substrate interface for the range of the potential sweep rate chosen [147-151]. The large peak separation observed at the PSt-Fc-LMA/GC is related to a low rate of charge-transfer between the electrode substrate and redox species in the polymer layer [147]. It is then suggested that the electron-transfer between the electrode substrate and the polymer layer can take place more effectively at the PSt-Fc-DBS/GC as compared with that at the PSt-Fc-LMA/GC.

The amount of ferrocene involved in the redox reaction (Γ_{Fc}^{obs}) was evaluated from the charges of the redox waves of the cyclic voltammograms taken at 1 mV s^{-1}. Figure 63 shows the relationship between Γ_{Fc}^{obs} and the quantity of ionic surface-active agents in the film (Γ_{LMA}, Γ_{DBS}) for a fixed amount of ferrocene (Γ_{Fc}) of 5.0 x 10^{-7} mol cm^{-2}. The addition of LMA of 1 x 10^{-7} mol cm^{-2} was effective in activating about 15 % Fc in the polystyrene layer, but further addition did not appreciably increase the utilization of Fc. On the other hand the Γ_{Fc}^{obs} was markedly increased with increasing Γ_{DBS} until 5.0 x 10^{-7} mol cm^{-2} which was same as Γ_{Fc} in the polystyrene layer. The addition of DBS to the polystyrene film attached the film the selective permeability of electrolyte cations due to electrostatic attractions and repulsions between the ionic surface-active agents in the film and electrolyte ions dissolved in solution, as described in the previous section. Similarly, the addition of LMA gives the film selective permeability of electrolyte anions. Thus, the effects of the

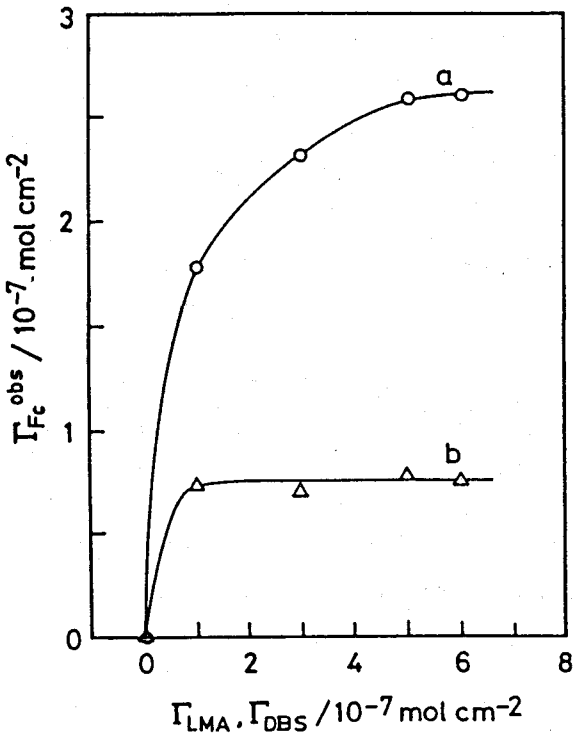

Fig. 63. Plots of Γ_{Fc}^{obs} of the PSt-Fc-DBS/GC (a) and the PSt-Fc-LMA/GC estimated from cyclic voltammograms taken at dE/dt = 1 mV s^{-1} as a function of Γ_{DBS} or Γ_{LMA}. Γ_{Fc} = 5.0 x 10^{-7} mol cm^{-2}, Γ_{PSt} = 1.0 x 10^{-9} mol cm^{-2}.

addition of the ionic surface-active agents were different between the cationic and anionic surfactant. Considering such the behaviors of the polystyrene film containing the ionic surface-active agents, the reaction schemes of the PSt-Fc-LMA/GC and the PSt-Fc-DBS/GC are illustrated as shown in Fig. 64. When the PSt-Fc-LMA/GC and the PSt-Fc-DBS/GC are prepared with the same surface concentration of the surface active agents, the coated films contain the same amount of the counter ions. However, in the course of oxidation of Fc in the PSt-Fc-LMA/GC, Cl^- ions are incorporated into the coated layer to compensate positive charges of the

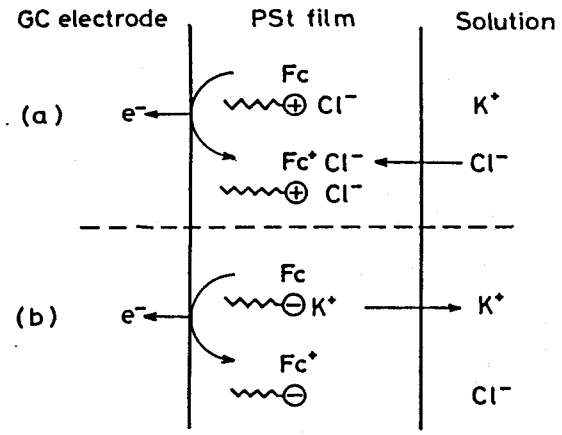

Fig. 64. Schematic representation of compositional changes in polystyrene films of the PSt-Fc-LMA/GC (a) and the PSt-Fc-DBS/GC (b) upon oxidation of ferrocene incorporated in the film.

resulting ferricinium cations (Fc^+). With the similar arguments, cations in the polystyrene layer of the PSt-Fc-DBS are dissolved out into the electrolyte solution on the oxidation of Fc. These differences of the reaction mode seems to bring about the differences of the reactivity of ferrocene between at the PSt-Fc-DBS/GC and the PSt-Fc-LMA/GC, as will be discussed below.

Chronoammperometry of PSt-Fc-DBS/GC and PSt-Fc-LMA/GC In the chronoammperometric experiments, the electrode potential (E_1) was first held in 1.0 M KCl at 0.8 v vs. SCE which is positive enough to oxidize all ferrocene in the film to ferricinium cation ($E^O(Fc/Fc^+)$ = 0.34 V vs. SCE), and then stepped to potentials (E_2) ranged from 0.6 to -0.4 V. Figure 65 shows the time course of cathodic currents at the PSt-Fc-DBS/GC electrode. The apparent diffusion coefficient (D_{app}) can be estimated by using the cottrell equation [151] given by

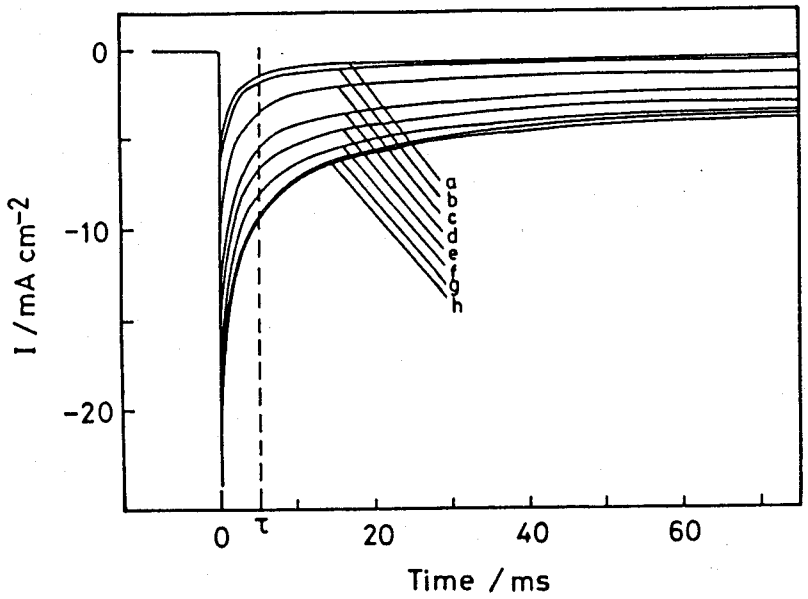

Fig. 65. Response of cathodic currents of the PSt-Fc-DBS/GC obtained by applying potential steps from 0.8 V vs. SCE to 0.6 (a), 0.5 (b), 0.4 (c), 0.2 (e), 0.1 (f), 0 (g), and -0.4 (h) V vs. SCE in 1 M KCl solution. Γ_{PSt} = 1.0 x 10^{-9} mol cm^{-2}, $\Gamma_{Fc} = \Gamma_{DBS}$ = 5.0 x 10^{-7} mol cm^{-2}.

$$i = \frac{n\ F\ D_{app}^{1/2}\ C}{\pi^{1/2}\ t^{1/2}} \qquad (31)$$

where n, F, and C are the number of electron transferred, the Faraday constant, and the concentration of ferrocene incorporated in the film, respectively. The cottrell equation is valid for current transients caused by the imposition of a potential pulse large enough to bring about complete oxidation and reduction of an electroactive species in the coated polymer layers. The potential steps ranged form 0.8 V to -0.4 V vs. SCE satisfies such requirements as evidenced by a linear relationship shown in

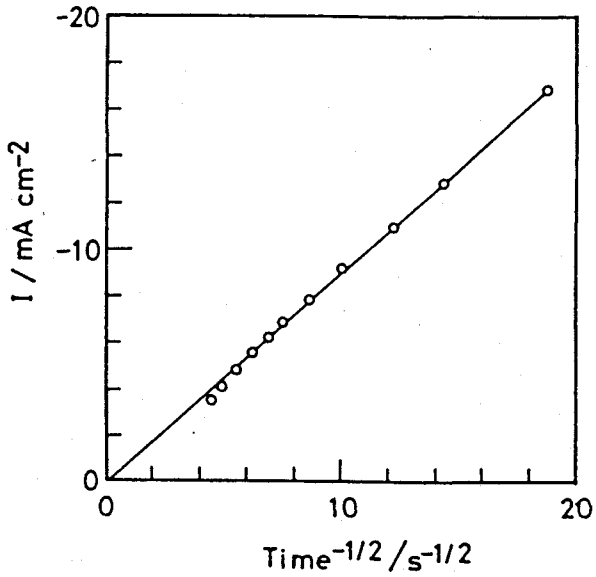

Fig. 66. Cottrell plots of current response of the PSt-Fc-DBS/GC obtained by applying potential step from 0.8 to -0.4 V vs. SCE in 1 M KCl solution. Γ_{PSt} = 1.0 x 10^{-9} mol cm^{-2}, $\Gamma_{Fc} = \Gamma_{DBS}$ = 5.0 x 10^{-7} mol cm^{-2}. The film thickness in wet conditions was 8.5 μm.

Fig. 66. The thickness of the coated the PSt-Fc-DBS film under a wet condition (d_{wet}) was 8.5 μm which showed ca. 20% increase in the film thickness from that of the dry films due to swelling. By using $\Gamma_{Fc}^{obs}/d_{wet}$ as the concentration of ferrocene in the film, D_{app} was determined to be 7.2 x 10^{-9} cm^2 s^{-1} for the experimental conditions given in the figure captions of Fig. 66.

By using all the current-time relations shown in Fig. 65, which were obtained by changing the potential from 0.8 V to different E_2, a normal pulse voltammogram was constructed as shown in Fig. 67 for the sampling time 6 ms which is shown as τ in Fig. 65. It is well-established [106,152-154] that if electron transfer reactions between electroactive species and

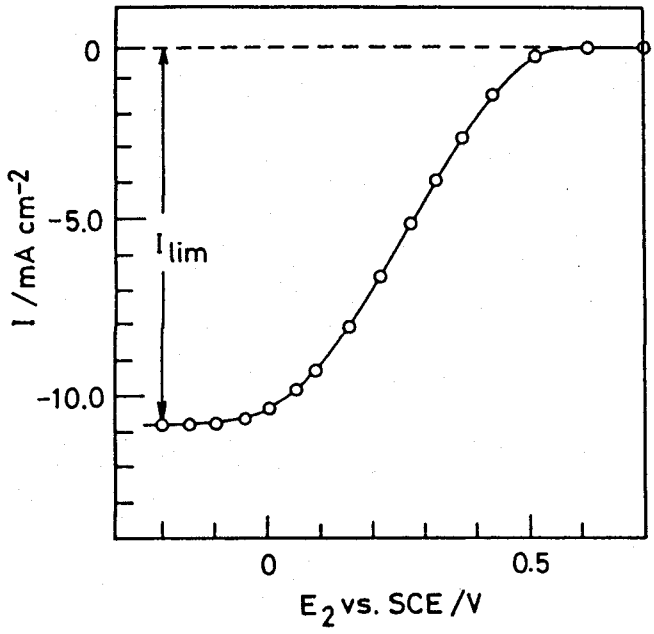

Fig. 67. A normal pulse voltammogram of the PSt-Fc-DBS/GC constructed using data shown in Fig. 65. The sampling time (τ) was 6 ms which is shown in Fig. 4. Γ_{PSt} = 1.0 x 10^{-9} mol cm^{-2}, Γ_{Fc} = Γ_{DBS} = 5.0 x 10^{-7} mol cm^{-2}. Electrolyte solution; 1 M KCl.

an electrode obey the Butler-Volmer equation, a normal pulse voltammogram satisfies the following equation (32).

$$E = E^* \mp \frac{RT}{\alpha nF} \ln\left[x \left(\frac{1.75 + x^2(1 + \exp(\pm\xi))^2}{1 - x(1 + \exp(\pm\xi))} \right)^{1/2} \right] \qquad (32)$$

$$E^* = E_{1/2} \pm \frac{RT}{\alpha nF} \ln\left[\frac{4}{3^{1/2}} \frac{k^o \tau^{1/2}}{D_{app}{}^{1/2}} \right] \qquad (33)$$

$$x = \frac{i}{i_{lim}} \qquad (34)$$

$$\xi = \frac{nF}{RT}(E - E_{1/2}) \qquad (35)$$

where $E_{1/2}$, α, i_{lim}, and k^o are reversible half-wave potential, the charge-transfer coefficient, limiting currents of the normal pulse voltammogram, and the standard rate constant of the charge-transfer reaction, respectively, and R and T have their usual meanings. As the half wave potential, the average of the anodic and the cathodic peak potentials in the cyclic voltammograms (0.34 V vs. SCE) was used in the present study. By applying data shown in Fig. 67 to eq. (32) with setting E_2 in Fig. 67 to

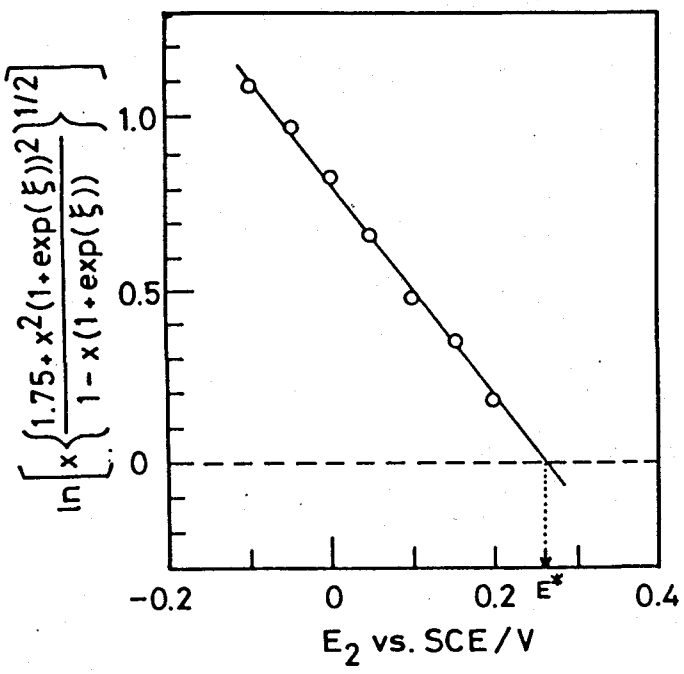

Fig. 68. Plots of log terms of eq. (32) against the second potentials obtained from the normal pulse voltammograms shown in Fig. 67.

E in eq. (32), values in the bracket of the log terms in the right hand of eq. (32) were calculated, and plots of these against E_2 give Fig. 68. The obtained linear relationship shows that the Butler-Volmer equation is applicable to the redox reaction of ferrocene incorporated in the polystyrene layer, and allows the determination of the α value from the slope of the line to be 0.46 $\pm$ 0.08. The E^* given by eq. (33) is obtained to be 0.26 V vs. SCE as shown in Fig. 68, and then k^o can be determined by substituting into eq. (33) the determined values of E^*, α, and D_{app}, and E_2. The same procedures were applied to evaluate k^o in different electrolysis conditions, which will be described in the next section.

The effect of electrolyte cations in the electrolyte solutions on D_{app} and k^o. The values of D_{app} and k^o of the PSt-Fc-DBS/GC and the PSt-Fc-LMA/GC were determined in 1 M KCl, NaCl, LiCl, and HCl aqueous solutions. Figure 69 shows the D_{app} against the diameter of hydrated cations of these electrolyte solutions and the k^o values are shown in Fig. 70. The size of the hydrated cations and H^+ were cited from ref. [66]. The D_{app} value of the PSt-Fc-LMA/GC was not varied with the cation size, but that of the PSt-Fc-DBS/GC was apparently influenced by the size of the hydrated electrolyte cations, and was large for small cations except for H^+ ions. These results correlate well with the reaction scheme given in Fig. 64, where it is shown that electrolyte anions are involved in the redox reaction of Fc in the PSt-Fc-LMA/GC but not so in the PSt-Fc-DBS/GC. The exceptional results obtained for the H^+ ions at the PSt-Fc-DBS/GC is not strange if it is considered that the polystyrene film containing ionic surface-active agent must have high hydrophilicity which allows the proton hopping conduction via the water molecules in the coated layer.

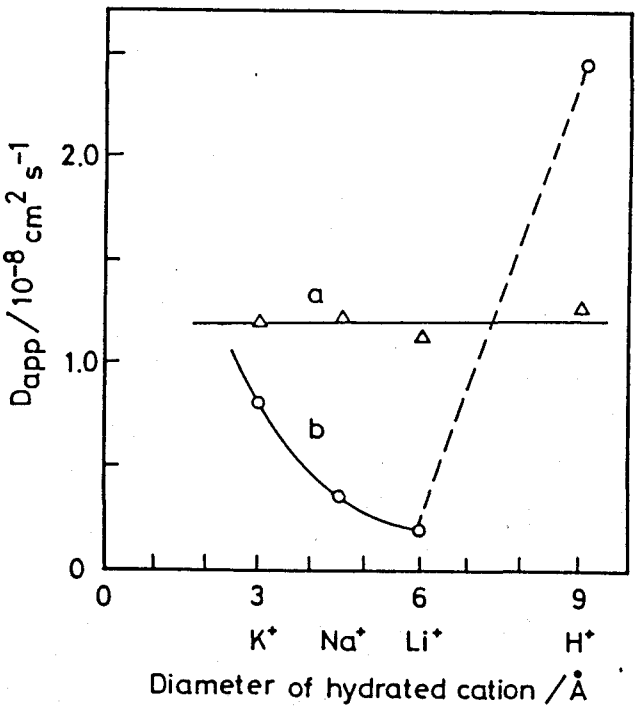

Fig. 69. Relationship between D_{app} of the PSt-Fc-LMA/GC (a) and the PSt-Fc-DBS/GC (b) and the diameter of hydrated cations in the electrolyte solutions. Γ_{PSt} = 1.0 x 10^{-9} mol cm^{-2}, Γ_{Fc} = Γ_{DBS} = Γ_{LMA} = 5.0 x 10^{-7} mol cm^{-2}. The concentration of electrolyte was 1 M. The film thickness of the PSt-Fc-LMA and the PSt-Fc-DBS in wet conditions were 8.1 and 8.5 μm, respectively.

As shown in Fig. 70, the k^o values were unaffected by the kind of the electrolyte cations both for the PSt-Fc-LMA/GC and the PSt-Fc-DBS/GC. The results are in accord with the above-mentioned analysis of the electrode kinetics that the Butler-Volmer equations is applicable to the redox reaction of Fc. The finding that k^o values were greater at the PSt-Fc-DBS/GC than at the PSt-Fc-LMA/GC are correlated with the observation that the peak separation of the cyclic voltammogram was greater at the PSt-Fc-LMA/GC than at the PSt-Fc-DBS/GC.

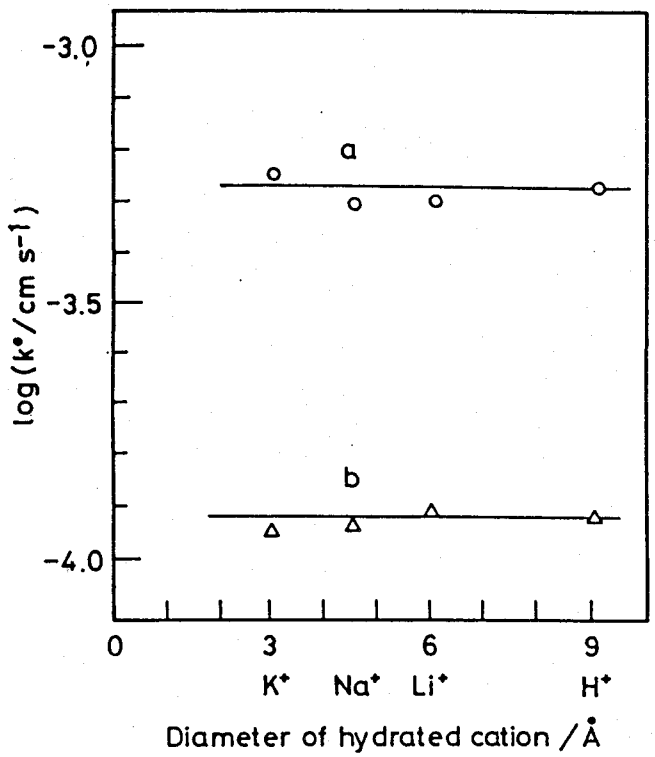

Fig. 70. Relationship between k^o of the he PSt-Fc-DBS/GC (a) and the PSt-Fc-LMA/GC (b) and the diameter of hydrated cations in the electrolyte solutions. Γ_{PSt} = 1.0 x 10^{-9} mol cm^{-2}, Γ_{Fc} = Γ_{DBS} = Γ_{LMA} = 5.0 x 10^{-7} mol cm^{-2}.

The effect of concentration of ferrocene and ionic surface-active agents in polystyrene film. Figure 71 shows the effect of Γ_{DBS} on k^o and D_{app} of the PSt-Fc-DBS/GC which contained 5.0 x 10^{-7} mol cm^{-2} of Γ_{Fc}. The D_{app} was not varied with Γ_{DBS}, while k^o was increased with increasing Γ_{DBS}. In the case of the PSt-Fc-LMA/GC, the k^o and D_{app} values were not influenced by Γ_{LMA} and were almost constant (D_{app} = 1.2 x 10^{-8} cm^2 s^{-1}, k^o = 1.2 x 10^{-4} cm s^{-1}). It is recognized by comparing Figs. 63 and 71 that there is a close relation between k^o values and the reactivity of

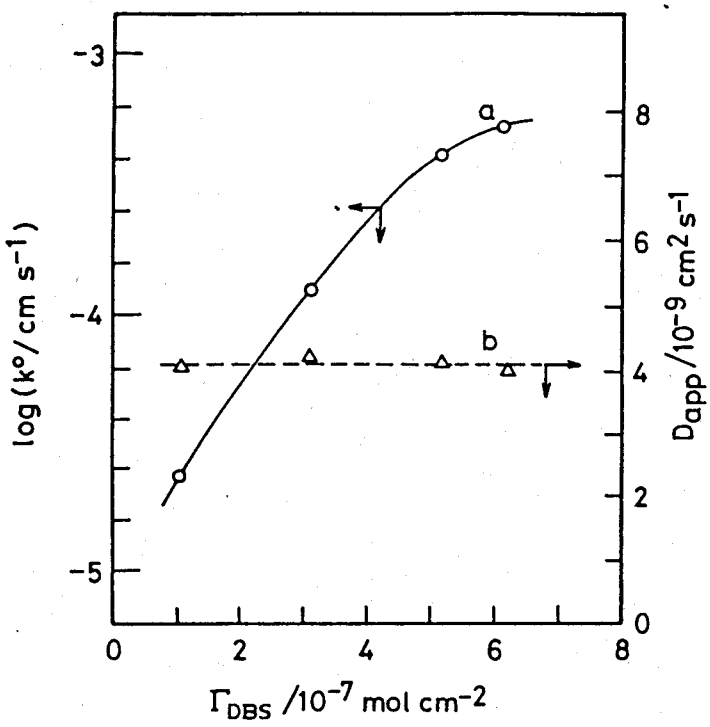

Fig. 71. Plots of log k^o (a) and D_{app} (b) of the PSt-Fc-DBS/GC obtained in 1 M KCl solution as a function of Γ_{DBS}. Γ_{PSt} = 1.0 x 10^{-9} mol cm^{-2}, Γ_{Fc} = 5.0 x 10^{-7} mol cm^{-2}.

ferrocene fixed in the polystyrene film. The rate of the electron-transfer between an electrode and the electroactive species in a solution become high with an increase in the ionic strength of the electrolyte solution because of the enhanced capability of charge compensation in the redox reactions [155]. The observed increase in the k^o of the PSt-Fc-DBS/GC with increasing Γ_{DBS} as shown in Fig. 71 seems to have the same origin. The increase of DBS in the polystyrene film results in the increase of the amount of Na^+ ions around Fc, being favorable for the enhancement in the redox reaction kinetics of Fc. As mentioned above, the polystyrene film containing the ionic surface-active agents was swollen by soaking in the

electrolyte solution. The swelling must result from the hydration of Na^+ to compensate ionized DBS in the film. The oxidation of Fc with release of the Na^+ ions into electrolyte solution occurs rather easily at the swollen film. In the case of the PSt-Fc-LMA/GC, however, a different situation is met in the electrode reaction of Fc. With increasing the amount of LMA in the coated film, Cl^- ions are increased and the coated layer is swollen in proportions to the amount of the incorporated Cl^-. On the oxidation of Fc, further incorporation of Cl^- ions are required. The incorporation of hydrated Cl^- must cause further swelling of the coated layer, which does not easily occur, as judged from the experimental results.

Figure 72 shows the effect of Γ_{Fc} on the D_{app} of the PSt-Fc-DBS/GC in which Γ_{DBS} was fixed to be 5.0×10^{-7} mol cm^{-2}. The k^o value was

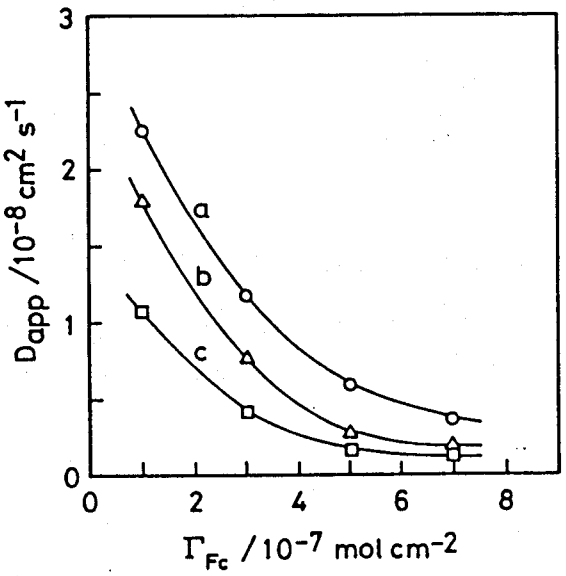

Fig. 72. Plots of D_{app} of the PSt-Fc-DBS/GC obtained in 1 M KCl (a), NaCl (b), and LiCl as a function of Γ_{Fc}. $\Gamma_{PSt} = 1.0 \times 10^{-9}$ mol cm^{-2}, $\Gamma_{DBS} = 5.0 \times 10^{-7}$ mol cm^{-2}.

almost constant (5.2 x 10^{-4} cm s^{-1}) in those conditions but the D_{app} value apparently decreased with increasing Γ_{Fc}. When D_{app} was determined by the chronoamperometry, the diffusion of both electrons and incorporated ions in the polymer layer contribute to the obtained D_{app} value. If the electron diffusion contributes much more than the incorporated ions, the D_{app} should be increased with increasing Γ_{Fc}, because the electron hopping between the fixed redox centers become facile with a decrease in the distances between the redox centers [156-160], being in conflict with the results shown in Fig. 72. Then the D_{app} obtained must be due to the diffusion limitation of the electrolyte cations in the polymer layer. The diffusion of the electrolyte cations must be retarded by an increase in the Γ_{Fc} because free space available for the ion diffusion becomes scarce because of the crowd of Fc in a limited space of the polymer layer.

Conclusion

The main results and conclusions obtained in this study are summarized as follows.

1. Polypyrrole films prepared by anodic polymerization of pyrrole on Pt or SnO_2-coated glass show the redox reactions in aqueous electrolyte solutions containing a supporting electrolyte alone. Transfer of electrolyte anions into and from the film and changes in the film color are involved in the redox reaction. Insertion of divalent anions into the film occurs in two steps but that of monovalent anions in one step. The obtained results indicate that polypyrrole is a promising material for electrochromic display devices.

2. Electrochemical copolymerization of pyrrole and thiophene has been accomplished using an acetonitrile solution containing 0.1 M thiophene and 2.0×10^{-3} M pyrrole. The ratio of pyrrole to thiophene rings in the copolymer can easily be changed by changing oxidation potential, and the electrochemical properties of the resulting copolymers are gradually changed from those of polypyrrole to polythiophene with an increase of the thiophene rings in the copolymers.

3. The conductivity of polypyrrole films doped with various kinds of aromatic sulfonate derivatives is influenced greatly by the number of sulfonate groups of a dopant molecule in such a manner that an increase in the number of sulfonate groups of a dopant made the conductivity decrease. The film conductivity is also varied by more than one order of magnitude by the current density chosen in the film preparation, and the highest conductivity is achieved at moderate current densities such as 0.2 mA cm^{-2}.

4. The electrical conductivity of polypyrrole films doped with various kinds of carboxylate anions decreases with increasing the basicity of the dopant anions. The observed dependence of the conductivity on the basicity can quantitatively be interpreted in terms of association of positive charges in polypyrrole with the dopant anions, the degree of which is different depending on the basicity of dopant anions. The conductivity of polypyrrole films doped with monoanions of dicarboxylic acids such as oxalic acid and maleic acid is decreased by immersing the film in such aqueous solutions as to cause dissociation of the doped monoanions into dianions, and the magnitude of the conductivity change is dependent on the degree of the dissociation of the doped monoanions.

5. The conductivity of polypyrrole films doped with p-phenol sulfonate decreases with increasing pH of aqueous solutions in which the films are immersed. A linear relationship is established between the relative ratio of the conductivity changes and the degree of dissociation of hydroxyl groups of p-phenol sulfonate doped in the film, indicating that the decrease in the conductivity results from an increase in bindings of positive charges of polypyrrole with phenoxide ions produced by dissociation of hydroxyl groups of the dopant. The formation of the phenoxide ions accompanies the incorporation of electrolyte cations into the film to compensate the generated negative charges. The rate of the conductance change caused by changing solution pH is then controlled by the diffusion rate of electrolyte cations in the polypyrrole films and is high for cations of small ionic radius.

6. The dimerization constant of methylene blue in Nafion and the rate of the dimerization were determined by the in-situ spectroelectrochemically investigations of the redox reactions of methylene

blue incorporated in the Nafion film. These values are very small as compared with those obtained for methylene blue dissolved in water, indicating that the dimerization is less likely to occur in Nafion due to a strong electrostatic interaction between methylene blue and sulfonate groups of Nafion.

7. The preparation of polyaniline films incorporated with cationic methylene blue has been accomplished by anodic polymerization of aniline in the presence of dissolved Nafion and methylene blue. The amount of methylene blue in the film can be varied by changing the relative concentration of methylene blue to Nafion in the deposition bath of polyaniline. The incorporation behaviors of methylene blue into polyaniline films can be interpreted in terms of electrostatic binding of methylene blue with sulfonate groups of Nafion in the deposition bath. The resulting films show electrochemical responses of both polyaniline and methylene blue.

8. The glassy carbon electrodes coated with polystyrene films containing sodium n-dodecylbenzenesulfonate as an anionic surface active agent bind $Ru(bpy)_3^{2+}$ in high surface concentrations in aqueous solutions. Rotating disc electrode measurements have clarified that the incorporated $Ru(bpy)_3^{2+}$ in the coated layer mediates the electron transfer reaction of $Ru(bpy)_3^{2+}$ in solution at the electrodes, and the rate constant of the electron transfer is influenced by the quantity of the coated polystyrene. If lauryltrimethylammonium chloride or laurylpyridinium chloride as a cationic surface active agent is blended in the coated polystyrene layers, the resulting electrodes bind $Fe(CN)_6^{3-}$. The electrodes coated with polystyrene films containing surface active agents do not show any electrochemical reactivities for electroactive species having the same polar

charges as the surface-active agents used because electrostatic repulsions are operative between them.

9. Glassy carbon electrodes coated with polystyrene films containing ferrocene show the redox activity when lauryltrimethylammonium chloride as a cationic surface-active agent or sodium n-dodecylbenzenesulfonate as an anionic surface-active agent is blended in the film. Chronoammperometry has revealed that the redox reaction of ferrocene in the polystyrene film containing ferrocene and sodium n-dodecylbenzenesulfonate is accompanied with the diffusion of electrolyte cations in the polymer layer and that ionized n-dodecylbenzenesulfonate works as a charge compensator of ferricinium cations. It is found by the similar analysis that in the case of the polystyrene film containing ferrocene and lauryltrimethylammonium chloride, the incorporation of electrolyte anions is accompanied with the oxidation of ferrocene in the film. The rate of electron-transfer reaction between the electrode substrate and the polymer layer, which is evaluated by normal pulse voltammetry, is greatly influenced by the kind and the amount of the ionic surface-active agents incorporated in the polystyrene film.

Acknowledgment

The work of this thesis was carried out under the guidance of Professor Hiroshi Yoneyama at Department of Applied Chemistry, Faculty of Engineering, Osaka University.

The author would like to express his grateful acknowledgment to Professor Dr. Hiroshi Yoneyama for his continuous guidance and encouragement throughout this work.

The author is also indebted to Professor Dr. Mitsuo Okahara and Professor Dr. Gin-ya Adachi for their valuable comments and suggestions.

The author is so much obliged to Professor Emeritus Dr. Hideo Tamura, Professor Dr. Chiaki Iwakura in University of Osaka Prefecture, Professor Dr. Osamu Ikeda in Kanazawa University, and Assistant Professor Dr. Hiroyuki Uchida in Osaka University for their helpful discussion and encouragement.

Thanks are given to the author's co-workers, Mr. Koichi Okamoto, Mr. Shuji Ito, Mr. Yoichi Maida, Mr. Jiro Nakamura, Mr. Takahiro Hamamoto, Mr. Kazuki Mitsui, and all the other members of Yoneyama Laboratory for their collaboration.

Finally, the author wishes to thank all his friends, his parents, and his wife for their continuous and hearty encouragement.

References

1. J.L. Bredal, J.C. Scott, K. Yakushi and G.B. Street, Phys. Rev. B, 30, 1023 (1984).
2. J.L. Bredas and G.B. Street, Acc. Chem. Res., 18, 3099 (1985).
3. J.C. Scott, P. Pflunger, M.T. Krounbe and G.B. Street, Phys. Rev. B, 28, 2140 (1983).
4. A.F. Diaz and J.I. Castillo, J. Chem. Soc., Chem. Comm., 397 (1980).
5. G.B. Street, T.C. Clarke, M. Krounbe, K.K. Kanazawa, V. Lee, P. Pflunger, J.C. Scott and G. Weiser, Mol. Cryst. Liq. Cryst., 83, 253 (1982).
6. K.K. Kanazawa, A.F. Diaz, R.H. Geniss, W.D. Gill, J.F.Kwak,, J.A. Logan, J.F. Rabolt and G.B. Street, J. Chem. Soc., Chem. Comm., 854 (1979).
7. M. Satoh, K. Kaneto and K. Yoshino, Synth. Met., 14, 2899 (1986).
8. H.S. White, G.P. Kittlesen and M.S. Wrighton, J. Am. Chem. Soc., 106, 5375 (1984).
9. G.P. Kittlesen, H.S. White and M.S. Wrighton, J. Am. Chem. Soc., 106, 7389 (1984).
10. A.F. Diaz and K.K. Kanazawa, J. Chem. Soc., Chem. Comm., 635 (1979).
11. H. Yoneyama, T. Hirai, S. Kuwabata, Chem. Lett., 1243 (1986).
12. S. Hotta, W. Shimotsuma and M. Taketani, Synth. Met., 10, 85 (1984).
13. R.J. Waltman, J. Bargon and A.F. Diaz, J. Phys. Chem., 87, 1459 (1983).
14. S. Panero, P. Prosperi, B. Klaptse and B. Scrosati, Electrochim. Acta., 31, 1597 (1986).
15. G. Tourillon and F. Garnier, J. Electroanal. Chem., 135, 173 (1982).
16. G. Tourillon and F. Garnier, J. Phys. Chem., 87, 2289 (1983).
17. A.F. Diaz and J.A. Logan, J. Electroanal. Chem., 111, 111 (1980).
18. T. Kobayashi, H. Yoneyama and H. Tamura, J. Electroanal. Chem., 177, 281 (1984).
19. A. Kitani, J. Izumi, J. Yano, Y. Hiromoto and K. Sasaki, Bull. Chem. Soc. Jpn., 57, 2254 (1984).
20. E.M. Genies and C. Tsintavis, J. Electroanal. Chem., 195, 109 (1985).
21. E.M. Genies and C. Tsuntavis, J. Electroanal. Chem., 200, 127 (1986).
22. T. Hirai, S. Kuwabata and H. Yoneyama, J. Chem. Soc., Faraday Trans. 1, 85, 969 (1989).

23. A.F. Diaz, J.M.V. Vallejo and A.M. Duran, Ibm J. Res. Develop., 25, 42 (1981).
24. N. Mermilliod, J. Janguy and F. Petiot, J. Electrochem. Soc., 133, 1073 (1986).
25. A. Mohammadi, O. Inganas and I. Lundstrom, J. Electrochem. Soc., 133, 947 (1986).
26. T. Osaka, K. Naoi, S. Ogano and S. Nakamura, Chem. Lett., 1687 (1986).
27. T. Kobayashi, H. Yoneyama and H. Tamura, J. Electroanal. Chem., 161, 419 (1984).
28. A. Kitani, J. Yano and K. Sasaki, J. Electroanal. Chem., 209, 227 (1986).
29. M. Kaneko, H. Nakamura and T. Shimomura, Makromol. Chem. Rapid. Comm., 8, 179 (1987).
30. R.A. Bull, F.R. Fan and A.J. Bard, J. Electrochem. Soc., 130, 1636 (1983).
31. F. Bedioui, C. Bongars and J. Devynck, J. Electroanal. Chem., 207, 87 (1986).
32. M.V. Rosenthal, T.A. Skotheim and C.A. Linkous, Synth. Met., 15, 219 (1986).
33. R. Jiang and S. Dong, J. Electroanal. Chem., 246, 101 (1988).
34. G. Bidan, E.M. Genies and M. Lapkowski, J. Chem. Soc., Chem. Comm., 533 (1988).
35. N. Oyama and F.C. Anson, J. Electrochem. Soc., 127, 247 (1980).
36. N. Oyama and F.C. Anson, Anal. Chem., 52, 1192 (1980).
37. H.R. Zumbrunnen and F.C. Anson, J. Electroanal. Chem., 152, 111 (1983).
38. M. Sharp, D.D. Montgomery and F.C. Anson, J. Electroanal. Chem., 194, 247 (1985).
39. I. Rubinstein and A.J. Bard, J. Am. Chem. Soc., 102, 6641 (1980).
40. C.R. Martin, I. Rubinstein and A.J. Bard, J. Am. Chem. Soc., 104, 4817 (1982).
41. C.M. Lieber and N.S. Lewis, J. Am. Chem. Soc., 107, 7190 (1985).
42. R. McNell, R. Siudak, J.H. Wardlaw and D.E. Weiss, Aust. J. Chem., 16, 1056 (1963).
43. B.A. Bolto and D.E. Weiss, Aust. J. Chem., 16, 1076 (1963).
44. B.A. Bolto, R. Mcnell and D.E. Weiss, Aust. J. Chem., 16, 1090 (1963).
45. A.F. Diaz, J.I. Castillo, J.A. Logan and W.Y. Lee, J. Electroanal. Chem., 129, 115 (1981).

46. A.F. Diaz, A. Martinez and K.K. Kanazawa, J. Electroanal. Chem., 130, 181 (1981).
47. R. Noufi, D. Tench and L.F. Warren, J. Electrochem. Soc., 127, 2310 (1980).
48. A.J. Noufi R. Frank and A.J. Nozik, J. Am. Chem. Soc., 103, 1849 (1981).
49. R. Noufi, D. Tench and L.F. Warren, J. Electroanal. Chem., 128, 2596 (1981).
50. T. Skotheim and I. Lundstrom, Appl. Phys. Lett., 40, 281 (1982).
51. T. Skotheim, L.G. Petersson, O. Inganos and I. Lundstrom, J. Electrochem. Soc., 129, 1737 (1982).
52. A.J. Frank and K. Honda, J. Phys. Chem., 86, 1933 (1982).
53. G. Cooper, R. Noufi, A.J. Frank and A.J. Nozik, Nature, 295, 578 (1982).
54. R.A. Bull, F.R.F. Fan and A.J. Bard, J. Electrochem. Soc., 129, 1009 (1982).
55. T. Inoue and T. Yamase, Bull. Chem. Soc. Jpn., 56, 985 (1983).
56. S.K. Deb, Appl. Opt. Suppl., 3, 192 (1969).
57. M. Green and D. Richman, Thin Solid Films, 24, 545 (1974).
58. H.N. Hersh, W.E. Kramer and J.H. McGee, Appl. Phys. Lett., 27, 464 (1975).
59. S.K. Mohapatra, J. Electrochem. Soc., 125, 284 (1978).
60. R.J. Colton, A.M. Guzman and J.W. Rabalais, J. Appl. Phys., 49, 409 (1978).
61. M.M. Nicholson, J. Electrochem. Soc., 126, 1490 (1979).
62. F. Garnier and G. Tourillon, J. Electroanal. Chem., 148, 299 (1983).
63. B. Valdes, Proc. Ire, 42, 420 (1954).
64. H. Kim and H.A. Laitinen, J. Am. Che. Soc., 58, 23 (1975).
65. A.J. Bard and L.R. Faulkner, "Electrochemical Method", John Woley and Sons, Inc., New York (1980), p. 522.
66. J. Kielland, J. Am. Chem. Soc., 59, 1675 (1937).
67. S. Naitoh, K. Sanui and N. Ogata, J. Chem. Soc., Chem. Comm., 1348 (1986).
68. K.K. Kanazawa, A.F. Diaz, M.T. Krounbi and G.B. Street, Synth. Met., 4, 119 (1981).
69. N. Kumar, B.D. Malhotra and S. Chandra, J. Polym. Sci. Polym. Lett. Ed., 23, 57 (1985).
70. O. Ingnas, B. Liedberg and W. Chang-Ru, Synth. Met., 11, 239 (1985).

71. R. Danieli, P. Ostoja, M. Tiecco, R. Zamboni and C. Taliani, J. Chem. Soc., Chem. Comm., 1437 (1986).
72. J.C. Scott, J.L. Bredas, K. Yakushi, P. Pflunger and G.B. Street, Synth. Met., 9, 165 (1984).
73. H.S. Nalwa, J.G. Robe, W.F. Schmidt and L.R. Dalton, Makromol. Chem. Rapid Comm., 7, 553 (1986).
74. J.L. Bredas, J.C. Scott, K. Yakushi and G.B. Street, Phys. Rev. Sect. B, 30, 1023 (1984).
75. K. Yakushi, J. Sauchlan, T.C. Clarke and G.B. Street, J. Chem. Phys., 79, 4774 (1983).
76. M. Salmon, A.F. Diaz, A.J. Logan, M. Krounbe and J. Bargon, Mol. Cryst. Liq. Cryst., 83, 265 (1982).
77. J.P. Trvers, P. Audebert and G. Bidan, Mol. Cryst. Liq. Cryst., 118, 149 (1985).
78. T. Skotheim, Rosenthal and Linkous, C.A., J. Chem. Soc., Chem. Comm., 612 (1985).
79. M. Ogasawara, K. Funahashi, T. Demura, T. Hagiwara and K. Iwata, Synth. Met., 14, 61 (1986).
80. W. Werenet, M. Monkenbusch and G. Wegner, Makromol. Chem. Rapid. Comm., 5, 157 (1984).
81. L.E. Alexander, "X-ray Diffraction Methods In Polymer", Wiley Interscience, New York, 1969 p. 137.
82. L.F. Warren and D.P. Anderson, J. Electrochem. Soc., 134, 101 (1987).
83. T. Shimidzu, A. Ohtani, T. Iyoda and K. Honda, J. Chem. Soc., Chem. Comm., 1415 (1986).
84. M. Szwarc, in "Ions And Ion Pairs in Organic Reactions", Vol. 1, M. Szwarc, Editor, John Wiley and Sons, Inc., New York 1972, p6.
85. D.P.N. Satchell, Trans. Faraday Soc., 61, 1132 (1965).
86. A. Mohammad and D.P.N. Satchell, J. Chem. Soc. B, 331 (1968).
87. D.P.N. Satchell and R.S. Satchell, Chem. Rev., 69, 251 (1969).
88. W.B. Jesen, Chem. Rev., 78, 1 (1978).
89. D.A. Deakin M.R. Bittru, Anal. Chem., 61, 1147A (1989).
90. D. Orata and D.A. Buttry, J. Am. Chem. Soc., 109, 3574 (1987).
91. C.K. Baker and J.R. Reynolds, J. Electroanal. Chem., 251, 307 (1988).
92. J.H. Kaufamn, K.K. Kanazawa and G.B. Street, Phys. Rev. Lett., 53, 2461

(1984).
93. D.D. Perlmutter and B. Scrosati, Solid State Ionics, 27, 115 (1988).
94. J.B. Schlenoff and C.W. Chien, J. Am. Chem. Soc., 109, 6269 (1987).
95. E.M. Genies, G. Bidan and A.F. Diaz, J. Electroanal. Chem., 149, 101 (1983).
96. H. Shinohara, M. Aizawa and H. Shirakawa, J. Chem. Soc., Chem. Comm., 87 (1986).
97. N. Oyama and F.C. Anson, J. Electroanal. Chem., 127, 640 (1980).
98. N. Oyama, T. Shimomura, K. Shigehara and F.C. Anson, J. Electroanal. Chem., 112, 271 (1980).
99. N. Oyama, S. Yamaguchi, Y. Nishiki, K. Tokuda, H. Matsuda and F.C. Anson, J. Electroanal. Chem., 139, 371 (1982).
100. D.D. Montgomery and F.C. Anson, J. Am. Chem. Soc., 107, 3431 (1985).
101. T.P. Henning and A.J. Bard, J. Electrochem. Soc., 130, 613 (1983).
102. J. Leddy and A.J. Bard, J. Electroanal. Chem., 189, 203 (1985).
103. I. Rubinstein, J. Electroanal. Chem., 176, 359 (1984).
104. K. Shigehara, E. Tsuchida and F.C. Anson, J. Electroanal. Chem., 175, 291 (1984).
105. K. Shigehara, N. Oyama and F.C. Anson, Inorg. Chem., 20, 518 (1981).
106. N. Oyama, T. Ohsaka, M. Kaneko, K. Sato and H. Matsuda, J. Am. Chem. Soc., 105, 6003 (1983).
107. B. Lindholm and M. Sharp, J. Electroanal. Chem., 215, 385 (1986).
108. H.S. White, J. Am. Chem. Soc., 104, 4811 (1982).
109. M. Sharp, J. Electroanal. Chem., 230, 109 (1987).
110. D.A. Battry, J.M. Saveant and F.C. Anson, J. Phys. Chem., 88, 3086 (1984).
111. C.P. Andrieux and J.M. Saveant, J. Electroanal. Chem., 142, 1 (1982).
112. C.M. Lieber, M.H. Schmidt and N.S. Lewis, J. Am. Chem. Soc., 108, 6103 (1986).
113. L. Michaelis and S. Granick, J. Am. Chem. Soc., 63, 1636 (1941).
114. C.Y. Tzung, Anal. Chem., 67, 390 (1967).
115. R.H. Wopshall and I. Shain, Anal. Chem., 39, 1527 (1967).
116. K.J. Vetter and J. Bardeleben, Z. Electrochem., 61, 135 (1957).
117. C.N. Lewis, O. Goldschmid and J. Bigeleisen, J. Am. Chem. Soc., 65, 1150 (1943).
118. D.R. Lemin and T. Vickerstaff, Trans. Faraday Soc., 43, 491 (1947).

119. M. Schubert and A. Levine, J. Am. Chem. Soc., 77, 4197 (1955).
120. W. Spencer and J.R. Sutter, J. Phys. Chem., 83, 1573 (1979).
121. E.W. Paul, A.J. Ricco and M.S. Wrighton, J. Phys. Chem., 89, 1441 (1985).
122. S. Chao and M.S. Wrighton, J. Am. Chem. Soc., 109, 6627 (1987).
123. J.S. Moore, G.O. Phillips and D.M. Power, J. Chem. Soc. A, 1155 (1970).
124. P.J. Baugh, J.B. Lawton and G.O. Phillips, J. Phys. Chem., 76, 688 (1972).
125. M. Shirai and M. Tanaka, J. Polym. Sci., Polym. Chem. Ed., 14, 343 (1976).
126. M. Shirai, T. Nagatsuka and M. Tanaka, Makromol. Chem., 178, 37 (1977).
127. M. Shirai, Y. Murakami and M. Tanaka, Makromol. Chem., 178, 2141 (1977).
128. I.M. Klotz, F.M. Walker and R.B. Pivan, J. Am. Chem. Soc., 68, 1486 (1946).
129. E.M. Genies and M. Lapkowski, J. Electroanal. Chem., 236, 189 (1987).
130. T. Hirai, S. Kuwabata and H. Yoneyama, J. Electroanal. Chem., 135, 1132 (1988).
131. A.G. MacDiarmid, J.C. Chiang, A.F. Richter and A.J. Epstein, Synth. Met., 18, 285 (1987).
132. W.S. Huang, Humphrey and MacDiarmid, J. Chem. Soc., Faraday Trans. 1, 82, 2385 (1986).
133. R.J. Cushman, P.M. McManus and S.C. Yang, J. Electroanal. Chem., 291, 335 (1986).
134. R.J. Cushman, P.M. McManus and S.C. Yang, Makromol. Chem. Rapid Comm., 8, 69 (1987).
135. A. Merz and A.J. Bard, J. Am. Chem. Soc., 100, 3222 (1978).
136. P. Daum and R.W. Murray, J. Electroanal. Chem., 103, 389 (1979).
137. P.J. Peerce and A.F. Bard, J. Electroanal. Chem., 114, 89 (1981).
138. S. Nakahara and R.W. Murray, J. Electroanal. Chem., 158, 303 (1979).
139. C. Degrand and L.L. Miller, J. Electroanal. Chem., 117, 267 (1981).
140. L. Roullier, E. Waldner and E. Laviron, J. Electroanal. Chem., 139, 199 (1982).
141. B.R. Shaw, G.P. Haight and L.R. Faulkner, J. Electroanal. Chem., 140, 147 (1982).
142. B. Lindholm and M. Sharp, J. Electroanal. Chem., 198, 37 (1986).
143. P.R. Montgomery, K. Shigehara, E. Tsuchida and F.C. Anson, J. Am. Chem. Soc., 106, 7991 (1984).
144. J. Facci and R.W. Murray, J. Phys. Chem., 85, 2870 (1981).
145. Kielland, J. Am. Chem. Soc., 59, 1675 (1973).

146. W. Rudzinski and A.J. Bard, J. Electroanal. Chem., 199, 323 (1986).
147. E. Laviron, J. Electroanal. Chem., 100, 263 (1979).
148. E. Laviron, J. Electroanal. Chem., 101, 19 (1979).
149. E. Laviron, J. Electroanal. Chem., 52, 395 (1974).
150. E. Laviron, J. Electroanal. Chem., 112, 1 (1980).
151. F.G. Cottrell, Z. Phys. Chem., 42, 385 (1903).
152. H. Matsuda, Bull. Chem. Soc. Jpn., 53, 3439 (1980).
153. T. Ohsaka, N. Oyama, K. Sato and H. Matsuda, J. Electrochem. Soc., 132, 1871 (1985).
154. N. Oyama, T. Ohsaka, H. Yamamoto and M. Kaneko, J. Phys. Chem., 90, 3850 (1986).
155. L.M. Peter, W. Durr, P. Bindra and H. Gerischer, J. Electroanal. Chem., 71, 31 (1976).
156. H.S. White, J. Leddy and A.J. Bard, J. Electroanal. Chem., 114, 89 (1980).
157. D.A. Buttry and F.C. Anson, J. Am. Chem. Soc., 105, 685 (1983).
158. H. Dahms, J. Phys. Chem., 72, 362 (1968).
159. I. Ruff and V. Friedrich, J. Phys. Chem., 75, 3297 (1971).
160. I. Ruff, V. Friedrich and K. Csillag, J. Phys. Chem., 75, 3303 (1971).